R. & M. No. 2630
(11,770)
A.R.C. Technical Report

MINISTRY OF SUPPLY

AERONAUTICAL RESEARCH COUNCIL
REPORTS AND MEMORANDA

Regenerator Heat Exchangers for Gas-Turbines

By

J. E. JOHNSON, M.SC.TECH., A.M.I.MECH.E.

LONDON: HER MAJESTY'S STATIONERY OFFICE
1952

PRICE 19s 0d NET

Regenerator Heat Exchangers for Gas-Turbines

By

J. E. JOHNSON, M.SC.TECH., A.M.I.MECH.E.

COMMUNICATED BY THE PRINCIPAL DIRECTOR OF SCIENTIFIC RESEARCH (AIR),
MINISTRY OF SUPPLY

Reports and Memoranda No. 2630*
May, 1948

Summary.—Information was required from which the performance of regenerators suitable for heat exchangers for gas-turbines could readily be estimated. A series of tables and curves have been prepared from which the efficiency of a regenerator can be calculated if the operating conditions and heat transfer coefficients are known. The tables and curves cover a range of lengths and blow times appropriate to gas-turbine conditions.

Measurements of heat transfer and pressure drop coefficients have been made on several examples of matrix of both the gauze and flame trap type in conditions similar to those in a gas turbine. A number of examples have been worked out from the experimental results to show the relative importance of the different variables on the performance of typical regenerators.

A gauze matrix of fine wire and open mesh has a much lower weight and only slightly higher pressure drop than a flame-trap matrix for the same efficiency. The recommended size of gauze is a wire diameter of 0·002 in. to 0·004 in. and a mesh of 20 to 40 wires per inch, the material should be stainless steel. Further design study is necessary to determine whether this advantage can be maintained in a complete regenerator.

1. *Introduction*.—The possibility of adapting the regenerative type of heat exchanger, which has been used in various forms for many years in blast furnace and boiler practice, to the gas turbine has been proposed by Ritz during the war[1]. Very remarkable claims to high cycle efficiencies and low weights were made in his report, but there was little experimental evidence for the heat transfer coefficients assumed and the derivation of the method of estimating the thermal ratios was not given. A preliminary survey of the possibilities of this type of heat exchanger for gas turbine work was made[2]. This showed that there was no information available on the heat transfer and pressure drop of small passages at the low Reynolds numbers it was proposed to use, but that if the anticipated values were realised and the considerable practical difficulties of sealing the rotating matrix were overcome, the regenerator heat exchanger could make a substantial improvement in turbine cycle efficiencies with a reasonable increase in weight and bulk. This preliminary report also showed that the existing methods of calculation of regenerator performance[3,4] were not sufficiently far advanced and simplified to be readily used by designers.

The present report extends the earlier work of Hausen[3,4] in the ranges which it is thought will be required for turbine work and the results of numerous calculations have been plotted so that designers can easily estimate the efficiency of a wide range of regenerators. Previous calculations have only considered the case where the high- and low-pressure portions of the regenerator were of equal size. In order to distribute the pressure losses in the high- and low-pressure parts of the cycle to get the least effect on the cycle efficiency it is desirable to divide

* R.A.E. Report Aero. 2266, S.D.27, received 15th September, 1948.

the regenerator into two unequal portions. The calculations have been extended to cover all practical ratios between the two portions. The report also describes the results of tests made on a simple rig designed to measure heat transfer coefficients of suitable matrices in conditions approximating closely to operating conditions in a gas turbine. The method of calculating heat transfer coefficients from rig tests is fully described and all the necessary curves are given.

The problems of mechanical design and sealing of the rotating matrix and the choice of matrix materials and construction methods have not been considered. The results are expressed in such a form that they are applicable to matrices of any material provided the arrangement is geometrically similar to those tested.

2. *The Calculation of Regenerator Efficiency.*—One of the major problems to be solved before the possibilities of the regenerator can be fully assessed is to find a method by which the thermal ratio given by a regenerator can be calculated from the heat transfer properties and dimensions of a suitable matrix. There appears to be no general analytical solution to this problem which can be put in a form suitable for easy solution of particular examples. The method described in this report is an extension of the approximate method suggested by Hausen[4]. The method can only be used with high accuracy over a limited range of conditions, these limitations are given in detail later.

2.1. *The Assumptions made for the Calculations.*—It is necessary to make a number of assumptions about the matrix properties and the operating condition to enable the problem to be put in a soluble form, these are :—

1. The thermal conductivity of the matrix material is infinitely large in a direction across the flow and infinitely small in a direction along the flow. This condition is closely approximated to in practice by making the walls of the matrix very thin relative to the passage length so that the interior of the material soon reaches the same temperature as the walls, and the rate of heat flow along the passages is relatively negligibly small.

2. The gas and air enter the regenerator at uniform and constant temperatures.

3. The hot and cold blow periods are of equal length and equal quantities of gas and air of equal specific heat flow through the regenerator at the same rate. Also the heat transfer coefficient between gas and matrix is constant over the length of the matrix and equal to that between matrix and air.

4. The blow time is long compared with the time required for an element of gas to pass through the matrix.

2.2. *The Differential Equations in Non-dimensional Form.*—With the above assumptions the differential equations giving the matrix and gas temperatures may be reduced to the simple non-dimensional form given below. The gas temperature at any time and position in the matrix is given by

$$\left(\frac{\partial \vartheta}{\partial \xi}\right)_{\eta} = t - \vartheta \qquad (1)$$

and the matrix temperature at any time and position is given by

$$\left(\frac{\partial t}{\partial \eta}\right)_{\xi} = \vartheta - t \qquad (2)$$

where
- ϑ gas temperature
- t matrix temperature
- α heat transfer coefficient
- H heating surface area per unit length of matrix

C heat capacity of matrix per unit length

V volume flow of gas per unit time

c_p specific heat of gas (per unit volume)

x distance from front of matrix

Z time from beginning of blow period

ξ distance from front of matrix (non-dimensional)

$$\xi = \frac{\alpha H}{V c_p} x$$

η time from beginning of blow period (non-dimensional)

$$\eta = \frac{\alpha H}{C} Z$$

The whole length and blow time of the regenerator may also be expressed in the same non-dimensional form giving,

non-dimensional length of regenerator $\Lambda = \dfrac{\alpha H}{V c_p} L$ .. .. (3)

non-dimensional blow time $\Pi = \dfrac{\alpha H}{C} Z$ .. .. (4)

where L length of regenerator matrix,

Z blow time.

When the regenerator has attained steady conditions, it is required that the gas and matrix temperatures at any position and time during one cycle shall be the same after a further complete cycle (one hot and one cold blow). The temperature scale may be chosen so that the cold gas enters from the left at temperature $\vartheta = 0$ and the hot gas from the right at $\vartheta = \theta$, the length of the matrix extends from $\xi = 0$ to $\xi = \Lambda$ and the blow time from $\eta = 0$ to $\eta = \Pi$. For reversibility, the matrix temperature at each point must be the same at the end of a cold blow as it is at the beginning of a hot blow. The boundary conditions required for solution of equations (1) and (2) are then given by

$$\vartheta = 0 \text{ when } \xi = 0 \text{ from time } \eta = 0 \text{ to } \eta = \Pi,$$
$$\vartheta = \theta \text{ when } \xi = \Lambda \text{ from time } \eta = \Pi \text{ to } \eta = 2\Pi.$$

Assuming values of Λ and Π for both hot and cold blows and a contraflow arrangement, the remaining reversal condition is

$$t(\xi, \Pi) = \theta - t(\Lambda - \xi, 0)$$

where $t(\xi, \Pi)$ and $\theta - t(\Lambda - \xi, 0)$ are the matrix temperatures at the end of the cold blow and beginning of the hot blow respectively. Parallel flow is not considered as it can be shown that the limiting thermal ratio is then only 0·5.

2.3. *Solution of the Differential Equations.*—The problem now is to find a solution of the differential equations (1) and (2) for the conditions obtaining after a large number of reversals. Hausen[3] has produced an approximate analytical solution and has worked out a few examples but the method is very laborious to use and considerable effort would be required to work out sufficient examples to cover the required range of conditions.

A more suitable approach seems to lie in the development of a solution on the lines of Hausen's approximate method[4]. This method starts from a solution to the problem of the initial cooling of a uniformly heated matrix by a steady flow of cooling air. Hausen uses a solution due to Anzelius[3] but an alternative method suggested by R.A. Fairthorne was found to be easier and more accurate to use. A solution to the final regenerator problem is then built up from the initial cooling solution in which the regenerator matrix is assumed to be split up into a number of small elements throughout which the temperature is considered to be uniform and varying continuously with time only. This method gives reasonably accurate results in most cases with a fairly small number of elements.

The required boundary conditions for reversal appear as a number of simultaneous equations, the number being equal to the number of elements into which the matrix is divided for the case of equal hot and cold blow times and double that number for unequal blow times. The solution of these equations is laborious ; but, by a combination of the use of the Mallock electrical calculating machine at Cambridge (which solved up to 8 equations), one check solution of 20 equations by the National Physical Laboratory, and the solution of a number of groups of 5 equations by direct computation, the useful field for gas-turbine applications has been well covered for equal blow times to an accuracy of about 1 per cent on thermal ratio. A higher accuracy is not justified owing to the probable errors in the heat transfer coefficients assumed for design purposes and to the fact that the initial assumptions of section 2.1 will not be fulfilled completely in practice. These results are combined in Figs. 7, 8 and Table 10 and are recommended for general use in regenerator design. Full details of the methods used and the solutions obtained are given in Appendix II.

For the limiting case when the blow time $\Pi = 0$ it can be shown that the efficiency of the regenerator (thermal ratio) is given by

$$\eta_{reg} = \frac{\Lambda}{2 + \Lambda} \qquad \ldots \quad (6)$$

and that this is also the thermal ratio of a contraflow recuperator of the same dimensions. The curve of equation (6) forms a very useful boundary curve for Fig. 7.

The method of calculating regenerator efficiencies described in Appendix II can also be applied to the case where the blow times are of unequal length on the hot and cold sides. As mentioned in section 1, this is usually necessary for gas-turbine applications to equalise the air and gas pressure drops and reduce their combined effect on the turbine cycle efficiency. Such a regenerator may be described as being unbalanced. Details of the method of calculation of efficiency of an unbalanced regenerator and the results of a number of calculations are given in Appendix III. It is found that a close approximation to the efficiency of an unbalanced regenerator can be reached by taking the arithmetic mean of the efficiencies obtained by considering each portion separately as half of a balanced regenerator and applying the following small correction factors.

Ratio $\frac{\Lambda a}{\Lambda g}$	Error $\eta_{mean} - \eta_{true}$
$^1/_2$	0·004
$^1/_3$	0·008
$^1/_4$	0·013
$^1/_5$	0·014

The efficiencies of a wide range of unbalanced regenerators are shown on Figs. 9 to 16 and have been calculated from Figs. 7, 8 using the above correction factors. The efficiency of an unbalanced regenerator of any intermediate ratio between 1 and 5 can be calculated from Figs. 7, 8 and the correction factor curve on Fig. 17.

3. *The Measurement of Heat Transfer Coefficients on Regenerator Matrices.*—In a recuperator where the two fluids flow continuously and are separated by a surface, it is a comparatively simple matter to measure the amount of heat transferred and the resistance to flow in the passages. It is more difficult to measure the heat transfer coefficient between one fluid and the intervening surface as then the temperature of the surface has to be deduced from known results or measured experimentally. The measurement of heat transfer coefficients in a regenerator matrix presents a much more difficult problem as there is only one set of passages and the fluid flow, heat transfer, surface and fluid temperatures are not continuous and all vary rapidly with time. It is, therefore, impossible to use a direct method of measurement and the heat transfer coefficient must be deduced by comparing the experimental variation of gas outlet temperature with time with similar theoretical curves calculated from assumed heat transfer coefficients. The method described in the following sections is similar to that used by Saunders and Ford[6] which is based on the theoretical calculations of Schumann[7].

3.1. *The Calculation of Heat Transfer Coefficients from Initial Heating or Cooling Curves.*—If a regenerator matrix is cooled for a comparatively long period, so that it is all at a known temperature, and then a stream of hot gas at a constant temperature and constant rate of flow is passed through it, it is possible to measure experimentally the variation with time of the outlet gas temperature from the time when the hot gas flow commences to the time when the outlet temperature reaches its maximum value. It was shown in section 2.2 and Appendix I that the variation of gas and matrix temperature could be expressed in terms of ξ and η where

$$\xi = \text{non-dimensional length} = \frac{\alpha H}{V c_p} L$$

and

$$\eta = \text{non-dimensional time} = \frac{\alpha H}{C} Z\,.$$

For the experiment under discussion, the only unknown quantity, is the heat transfer coefficient α, therefore for a given matrix the quantity $\eta/\xi = (Vc_p/C)Z$ is known. The experimental curve of actual gas temperature against time can, therefore, be transformed into a curve of ϑ against η/ξ where

$$\vartheta = \frac{T_{go} - T_m}{T_g - T_m}$$

and T_{go} gas outlet temperature

T_g gas inlet temperature

T_m initial matrix temperature.

Figs. 2, 3 show calculated values of ϑ against η for a range of values of ξ for initial cooling, these can be converted to the case of initial heating as in the experiments by reversing the scale of ϑ. Curves of ϑ against ξ for fixed values of η/ξ can be plotted from these curves. Such curves are shown in Figs. 18, 19. The method of using them is to read off the experimental curve values of ϑ at decimal values of η/ξ and then to read off from Fig. 18 or 19 the corresponding values of ξ. From these the values of α are calculated. If the conditions assumed in the theory were realised completely in the experiment, the same value of ξ would be obtained for all values of η/ξ, except when $\vartheta = 0$ or 1 or $\eta/\xi = 1{\cdot}0$, where the values of ξ become indeterminate. In practice the variations of ξ became large in these regions, but sensibly constant values of ξ were obtained over the range of $\eta/\xi = 0{\cdot}5$ to $0{\cdot}8$. Further values of ξ could have been obtained from the upper portions of the experimental curves where $\eta/\xi - 1{\cdot}0$ but these were rejected as unreliable because of larger heat losses from the thermocouples and matrix to the casing.

For quick comparison of experimental and theoretical results it is preferable to compare curves of ϑ vs. η/ξ for fixed values of ξ as in Figs. 23, 25, 27. From such comparisons it is easy to investigate the cause of errors in the experimental curves as described in Appendix IV.

3.2. *Test Rig for Measuring Heat Transfer Coefficients.*—From the foregoing section the requirements of the test rig are seen to be :—

(a) A supply of hot air or gas at constant temperature and pressure.

(b) Provision for starting and stopping the gas supply instantaneously without upsetting the temperature or pressure appreciably.

(c) Provision for measuring the mass flow of gas through the matrix.

(d) Provision for measuring accurately the variation of inlet and outlet gas temperatures with time after commencement of the hot gas flow.

(e) Provision for measuring the pressure drop across the matrix during the blow period.

(f) Provision for cooling the matrix uniformly to a constant low temperature after each heating.

The size of the test matrix was kept to a minimum so that test samples of unusual materials or difficult construction could be provided more readily. When heat transfer measurements only are required, a lower temperature, to reduce heat losses, and a large size to reduce the relative weights of casing and insulation, would improve the accuracy considerably.

3.21. *Hot gas and cold air circuits.*—Fig. 20 shows the arrangement of the test rig in its final form. Hot gas was supplied from a typical gas turbine combustion chamber so that the mixture of gas, amount of soot and the temperature corresponded closely to those encountered in practice.

3.22. *Measurement of temperature and time.*—Due to the rapid changes of temperature of the gas, of the order of 30 deg C per second, thermocouples having a very quick response, but sufficiently robust to stand up to the gas loads, were necessary. These requirements were met by using Chromel-Alumel couples of 30 S.W.G. The wires were bent in a direction parallel to the gas flow for a distance of about $\frac{3}{4}$ in. to minimise conduction along the wires. The wires entered the duct and were supported across the flow in ceramic tubes about $\frac{3}{32}$ in. diameter, each wire being in a separate tube. The wires were electrically welded together to form a junction.

It was also necessary for the voltage recording instrument to have a negligible time lag and to be accurate over a wide range of temperature. The possibility of using a high speed galvanometer and photographing its movements on a film was considered but no such instrument was available and would have taken too long to develop. The only instrument available was a Negretti and Zambra quick reading potentiometer which can be read to 0·02 millivolts (about $\frac{1}{2}$ deg C) the galvanometer of which responds very rapidly. The only way to co-ordinate time and temperature accurately was to set the potentiometer to a suitable voltage and measure the time taken from the start of the hot gas flow to the instant when the galvanometer showed that the potentiometer was balanced. The cycle of cooling and heating was then repeated with the potentiometer set to a different voltage. In this way the complete time-temperature curve of the gas at the matrix outlet was built up. An electrically operated stop clock was fitted and arranged to be operated by the rise in voltage of the inlet thermo-couple. The circuit diagram is shown in Fig. 21. Time and temperature curves were taken in this way for each of the three thermocouples (1, 2, 3). The variation of pressure drop across the orifice and across the matrix during a heating period were also recorded at intervals of 5 sec, and readings were taken of the three temperatures, gas inlet pressure and pressure drop and orifice inlet pressure and pressure drop when the matrix has reached steady conditions after heating for at least 5 min. Provided that care was taken to maintain the temperature in the combustion chamber at a constant value during the whole test no difficulty was experienced in obtaining consistent and repeatable results.

3.3. *The installation of the Matrix in the Test Rig.*—The arrangement of matrix container is shown in Fig. 24. The container was 3 in. diameter made from 0·006 in. beryllium-copper foil of a length appreciably greater than the matrix and insulated with crumpled 'Alfol,' The matrix was made accurately circular and a tight push fit in the container. A typical heating curve obtained with this arrangement is shown on Fig. 25 with the corresponding theoretical curve for comparison.

3.4. *Condensation Effects in the Matrix.*—During the winter it was found that considerable distortion of the heating curve was being caused by condensation of the moisture in the hot gas during the initial stages of the heating cycle. Fig. 26 shows the distortion due to this effect. The effect was easily overcome when the cooling air flow was altered so as to be in the same direction as the gas flow when the leakage of hot gas through the sluice valve was sufficient to raise the cooling air temperature to about 40 deg C which was above the dew point of the moisture in the hot gas. The heating curves then obtained agreed very well with the theoretical ones as shown on Fig. 27.

4. *Details of Matrices and Results Obtained.*—The most essential characteristic of a regenerator matrix of minimum weight is a large surface/volume ratio which can be obtained by very fine subdivision of the material. Two types of matrix have been considered, firstly one with long smooth passages to give minimum pressure drop and secondly one with flow over the outside of wires or rods to give maximum heat transfer coefficients. For the first type, flame-trap material of alternate layers of plain and corrugated cupro-nickel sheets were used and for the second type packs of wire gauze were used. A few tests were also made with random packings of glass and steel wool. Details of the matrices tested are given in Table 12.

4.1. *Materials for Matrices.*—The flame-trap material was made from 70/30 cupro-nickel in strips of 0·002 in. thickness and the wire gauzes were of brass, mild steel, stainless steel and copper. With the exception of the copper none of these materials showed any deterioration or corrosion after tests in the heat transfer rig with gas at temperatures of about 500 deg C. As might be expected the copper gauze oxidised and disintegrated fairly rapidly. One matrix was made from a loose pack of glass wool and another from a similar pack of mild steel wool as these would give a much finer subdivision of surface than is possible with gauzes. Examples of the surface areas obtainable with steel wool are given in Table 12.

In practice, however, it was found that the glass wool disintegrated and a large proportion of it disappeared during the first test. The steel wool exploded immediately the hot gas was admitted.

4.2. *Details of Matrices.*—4.21. *Flame-trap matrices.*—Flame-trap material consists of alternate layers of plain and corrugated strip $\frac{7}{8}$ in. wide and 0·002 in. thick. Two sizes of corrugation, 0·03 in. and 0·02 in. high, were used. Detailed shapes are shown on Figs. 28, 29. Details of dimensions, surface areas and weights of all the arrangements tested are given in Table 12. Only those matrices in a round container gave satisfactory test results, they are listed below :—

Height of corrugation (in.)	Number of layers used	Total passage length (ft)	Remarks
0·03	1	0·073	
0·03	2	0·146	
0·03	4	0·292	
0·03	1	0·073	Slitted*
0·02	1	0·073	
0·02	4	0·292	

* Material slitted at $\frac{3}{16}$ in. pitch to reduced longitudinal conduction, *see* section 4.40.

4.22. *Gauze matrices.*—Measurements have been made on packs of both standard and special gauzes. Standard meshes of gauze have too close a mesh relative to the size of wire and so have rather a small throughway area for use as a matrix. Table 12 shows that for a given matrix volume the flame traps and standard gauzes have about the same surface area, but the flame trap has twice the throughway area. For this reason various special gauzes having roughly twice the wire spacing of a standard gauze were made. All details of the various gauze matrices tested are given in Table 12.

Those arrangements for which satisfactory test results were obtained are listed below :—

	Number of wires per inch	Wire diameter (in.)	Number of layers used
(1)	30	0·0105	100
(2)	30	0·0105	150
(3)	20	0·009	100
(4)	40	0·0045	98

Gauzes (1) and (2) provide a check on the independence of the heat transfer coefficient on the number of layers used. Gauzes (3) and (4) are roughly geometrically similar. It will be seen from Table 12 that the fine gauze (4) has a much larger surface area and lower weight per unit volume than the other gauzes.

4.3. *Choking and Fouling of the Matrices.*—No trouble was experienced with appreciable choking of the matrices during tests. When the combustion chamber was in need of cleaning, loose particles of carbon would collect on the face of the matrix but were easily removed. There was no sign of any building up of soot inside the passages in the matrices. As mentioned in section 3.2, above, too much weight must not be given to this result.

4.4. *Test Results—Heat Transfer Coefficients.*—The results of the heat transfer measurements are shown on Figs. 30, 31, 32 and Table 13. The method of obtaining heat transfer coefficients from the experimental heating curves has been described in section 3.1. The results given are the mean of the values calculated for η/ξ values of 0·1, 0·2, 0·3 . . . . . . 0·9 excluding all points where $\vartheta = 0$. The viscosity and density of the gas were taken to be the average value of the mean between the inlet and outlet gas temperatures in the matrix. The minimum throughway area has been used for calculating the mass velocity in conformity with the general practice for heat transfer from banks of tubes.

The heat transfer coefficient $k_H = \alpha/G_{\max} c_p$ is plotted on a log scale against Reynolds number on Fig. 30 ; for gauzes $R_p = G_{\max} \pi D/\mu$ was used and for flame-trap matrices $R_p = G_{\max} \Delta L \; \Delta t/\mu A_a$. The use of wire perimeter for Reynolds number was suggested by Norris and Spofford[8] for correlating heat transfer results on interrupted fin surfaces. The recommended line from their results is shown on Fig. 30. The results for gauzes were also correlated on a basis of Reynolds number using hydraulic diameter, but better agreement between the results for different gauzes was obtained by using wire perimeter.

It will be seen that the results from tests on gauzes lie on straight lines parallel to and substantially below Norris and Spofford's lines. The equation for the line through the 20-mesh results is

$$k_H = 0{\cdot}81 R_p^{-0{\cdot}50} \qquad (40)$$

for the 30-mesh results

$$k_H = 0{\cdot}66 R_p^{-0{\cdot}50} \quad \ldots \quad (41)$$

and for the 40-mesh results

$$k_H = 0{\cdot}60 R_p^{-0{\cdot}50}. \quad \ldots \quad (42)$$

As the 20- and 40-mesh gauzes are approximately geometrically similar it might have been expected that the relationship between k_H and Reynolds number would have been the same for both gauzes. The results show however that the larger gauze tends to have a higher heat transfer coefficient than the smaller one. The reason for this is not clear though there are several reasons why some such discrepancy might exist. There may not be complete geometrical similarity, and the Reynolds similarity does not cover effects of conductivity, heat soakage or non-uniform wire surface temperature.

On Fig. 31 the results of the 20-, 30- and 40-mesh gauze heat transfer tests are plotted on log scales in the form of Nusselt number $N_u = \alpha D/k$ against Reynolds number $R_d = G_{max} D/\mu$ where D is the wire diameter. For comparison the curve for heat transfer from single wires given by McAdams[10] is also shown. The results of the tests on gauzes lie on lines almost parallel to that for a single wire and some 50 per cent below it, giving the following equations for the heat transfer of gauzes

$$\left.\begin{aligned} &\text{20-mesh gauze } \frac{\alpha D}{k} = 0{\cdot}33\left(\frac{G_{max} D}{\mu}\right)^{0{\cdot}50} \\ &\text{30-mesh gauze } \frac{\alpha D}{k} = 0{\cdot}27\left(\frac{G_{max} D}{\mu}\right)^{0{\cdot}50} \\ &\text{40-mesh gauze } \frac{\alpha D}{k} = 0{\cdot}24\left(\frac{G_{max} D}{\mu}\right)^{0{\cdot}50}. \end{aligned}\right\} \quad \ldots \quad (43)$$

It was to be expected that the heat transfer coefficient k_H of the flame-trap matrices would be inversely proportional to the Reynolds number (based on hydraulic diameter). In practice this was found to be approximately true for Reynolds numbers above about 60 but at lower flows there is no further increase and some evidence of a reduction of heat transfer coefficient as shown by the lower group of curves on Fig. 30. It was also to be expected that with laminar flow the heat transfer coefficient would be lower for longer passages, though the fact that the long passages were made up of several $\frac{7}{8}$ in. lengths in series might reduce this effect. The results show that there is an appreciable effect of length, the heat transfer coefficient for four elements being lower than for 2 elements. It was not possible to test single elements at Reynolds numbers above the critical value owing to their low heat capacity. The small size of corrugation having larger values of l/d has a lower heat transfer coefficient than the large size at the same Reynolds number.

The equations of the straight portions of the curves are

$$\left.\begin{aligned} &\text{for 2-element large corrugation } k_H = 2{\cdot}7R^{-1{\cdot}0} \\ &\text{for 4-} \quad ,, \quad ,, \quad ,, \quad k_H = 0{\cdot}845R^{-0{\cdot}81} \\ &\text{for 4-} \quad ,, \quad \text{small} \quad ,, \quad k_H = 0{\cdot}205R^{-0{\cdot}55}. \end{aligned}\right\} \quad \ldots \quad (44)$$

The flame-trap results are also plotted on Fig. 31. It will be seen that at low Reynolds numbers the Nusselt number is nearly proportional to the Reynolds number but above the critical region the Nusselt number tends to become constant as would be expected for laminar flow in a smooth tube. The results obtained by Glaser[11] are also shown on Fig. 31 for comparison. His results are approximately in agreement with the present results at low flows but he did not show any tendency for the Nusselt number to become constant at high flows. This may be attributed to the fact that he used diagonal corrugated strip without any intermediate flat strip, the resulting passage then has some resemblance to the passage through a gauze matrix. The mean steady values for flame-trap matrices are

2-element large corrugation $N_u = 1{\cdot}9$,

4- ,, ,, ,, $N_u = 1{\cdot}6$,

4- ,, ,, ,, $N_u = 1{\cdot}5$.

It has been suggested that thermal conduction along the walls of flame-trap material might adversely affect the performance ; to check this a single round element was constructed from plain and corrugated material which had been perforated along its length so that the $\frac{7}{8}$ in. width of material had four slits about $\frac{3}{16}$ in. apart. The performance of this element was compared with that of an otherwise identical unslitted element. Figs. 30, 31 show that there was a slight advantage for the slitted element at low flows only. As there was only a single element of slitted material available it was not possible to get results at higher flows. The difference measured is less than the limits of accuracy of the tests and cannot be relied upon.

4.41. *Pressure-drop results and the relation between heat transfer and pressure drop.*—The results of static-pressure drop measurements taken during the heat transfer tests and averaged in the same way are also shown on Fig. 30 and Table 13, the dotted lines showing the half friction factors $C_f/2$ calculated from the pressure-drop results. It will be seen that the results lie on straight lines parallel to and considerably above the heat transfer results indicating that the ratio $k_H/C_f/2$ is approximately constant over the range of Reynolds numbers but that the value of the ratio is much less than the value of unity derived from Reynolds analogy for friction and heat transfer for flow inside a round tube. Values of the ratio $k_H/C_f/2$, which may be regarded as a measure of heat transfer efficiency, for both gauzes and flame-traps are tabulated in Table 13 and plotted against Reynolds number on Fig. 32. It was thought that the ratio would be higher for flame-trap material than for gauzes as the passages are much smoother and the flow more truly laminar, but there is actually no appreciable difference at Reynolds numbers above about 60, but at lower flows the ratio $k_H/C_f/2$ for flame-traps is lower than for gauzes because the heat transfer coefficient of flame-traps decreases while the friction factor continues to increase as the flow is reduced. The results of friction factor measurements on flame-traps lie approximately parallel to and slightly below the usual line for laminar pipe flow

$$C_f/2 = 8R^{-1\cdot0}. \qquad \ldots \qquad (45)$$

The equation of the line through the results for the larger flame-traps is

$$C_f/2 = 2{\cdot}21R^{-0\cdot78} \qquad \ldots \qquad (46)$$

and for the small flame traps

$$C_f/2 = 3{\cdot}73R^{-0\cdot87}. \qquad \ldots \qquad (47)$$

The reason for the higher friction factor for the small flame-traps may be the relatively greater thickness of material used, giving higher end losses.

The average values of the heat transfer efficiency of the various matrices are

20-mesh gauze $k_H/C_f/2 = 0{\cdot}35$

30- ,, ,, $= 0{\cdot}45$

40- ,, ,, $= 0{\cdot}27$

2-element flame-trap (large) $= 0{\cdot}38$

4- ,, ,, ,, ,, $= 0{\cdot}35$

4- ,, ,, ,, (small) $= 0{\cdot}26$

5. *Examples of Regenerator Performance.*—In the following sections a number of examples have been worked out to show the effect of the main variables of matrix type, blow time, flow rate and ratio of air to gas blow time on the weight, pressure drop and efficiency of a regenerator. The examples are all based on a typical gas-turbine cycle in which the following operating conditions are assumed :—

Mass flow rate of gas	= 20 lb/sec
Mass flow rate of air	= 20 lb/sec
Mean density of gas	= 0·033 lb/cu ft
Mean density of air	= 0·184 lb/cu ft
Mean viscosity of gas and air	= $2{\cdot}25 \times 10^{-5}$ lb/ft sec

In most of the examples a flow rate of 1 lb/sec/sq ft of frontal area of matrix has been assumed. This gives a total frontal area for the matrix of 40 sq ft which would probably have to be folded in some way to reduce the dimensions to reasonable values.

When designing regenerators to work to a fixed efficiency it will be found more convenient to use the curves on Fig. 33 or 34 which show the variation of efficiency with length and utilisation factor Π/Λ instead of Figs. 7 and 8. Utilisation factor is independent of the heat transfer coefficient and depends on the matrix dimensions, heat capacity, gas or air flow and blow time. For working out a number of regenerators with the same efficiency it is useful to plot Λ against (Π/Λ) for the particular efficiency as for example, on Fig. 35.

6. *Conclusions.*—Hausen's heat pole method gives a comparatively simple solution to the problem of calculating the efficiency of a regenerator. The method is accurate over a limited range of conditions only, but sufficient reliable results have been obtained to give the efficiency over most of the range required for gas turbines. The results are given in the form of curves from which intermediate values can easily be obtained. The accuracy is estimated to be within 1 per cent of thermal ratio. For a regenerator with unequal blow times curves giving the efficiency for inequalities up to 5/1 are given, though it seems unlikely that ratio much greater than about 2/1 will be encountered in practice owing to the variation of heat transfer with flow rate. The arithmetic mean of the separate efficiencies of the two halves of the cycle gives a close approximation to the true efficiency and correction factors are given to obtain the true efficiency, the correction is of the order of 1 per cent.

The method described of measuring the heat transfer coefficient of a finely divided matrix from the heating or cooling curves is the most practical way when the passages are too small to allow of direct measurement. The accuracy is not high (about $\pm$ 20 per cent) but the test rig is simple and tests can be made under operating conditions. It was found that a round matrix was the only construction which could be made to withstand high temperature conditions and retain its shape and yet have a sufficiently low weight and heat loss to have a negligible influence on the test results. None of the matrices tested showed any deterioriation or tendency to soot up during the tests with the exception of the copper gauze, glass wool and steel wool, which were quite unsuitable for high temperature conditions. It is recommended that future test rigs should be designed for matrices not less than about 6 in. in diameter, so as to keep the heat losses and heat capacity of the casing small relative to the heat capacity of the matrix.

The heat transfer coefficient of gauze matrices are two or three times those of flame-traps but with a corresponding increase in pressure drop. The heat transfer coefficients of the gauze matrices all lie on lines parallel to and appreciably below, the published results for interrupted finned surfaces. This may be attributed to shielding of part of the surface of the wire in the meshes. Thick wires tend to have slightly higher coefficients than thin wires, at a given Reynolds number. Further work is required to establish the effects of spacers between the layers and of compressing the layers tightly together. The heat transfer efficiency $k_H/C_f/2$ has a value of about 0·3 for gauzes and is independent of Reynolds number. The number of layers does not affect the heat transfer coefficient.

With flame-trap matrices, the heat transfer only conforms to laminar laws for Reynolds number greater than about 60, below this point the heat transfer decreases rapidly, following closely the relationship between Nusselt number and Reynolds number found by Glaser. The friction factor remains inversely proportional to the Reynolds number over the whole range so that the heat transfer efficiency only remains constant and approximately equal to that for gauzes at Reynolds numbers above 60, below which it decreases rapidly. There is a small decrease in heat transfer coefficient at the same Reynolds number as the number of elements in series is increased. The heat transfer coefficients of the small (0·02 in.) flame-traps is lower for the same length and Reynolds number than for the large (0·03 in.) elements.

The lowest weight for a given performance is obtained for a fine wire gauze matrix, but the pressure drop is higher than for a smooth flame-trap passage. The saving in weight is more marked than the increase in pressure drop. For a gauze matrix the weight is approximately proportional to the wire diameter and nearly independent of the mesh of the gauze. A gauze of 40 wires per inch, 0·0045 in. diameter, is a good compromise for low weight and moderate pressure drop. Some reduction of pressure drop at the expense of increased bulk could be obtained by using 20 wires per inch. Stainless steel is the best material to use for wires because of its high specific heat and heat resisting properties. The weights given are for the matrix only; when total weights are considered the advantage gained by using gauzes may be reduced. A detailed study of possible framework designs is necessary to determine the net saving.

The effect of speed of rotation of the matrix on the performance is not large provided the speed is not too low. Too high a speed leads to excessive leakage and let down losses. A matrix material of high specific heat is an advantage in that lower speeds are required for the same performance.

A substantial reduction of gas pressure drop can be obtained at the expense of some increase in air pressure drop and a small increase in weight by dividing the matrix unequally between gas and air. A division which gives a gas blow time two or three times the air blow time will probably be found most satisfactory. The best ratio to use depends on a large number of factors and no precise general answer can be given.

List of Symbols

A	Frontal area of matrix	sq ft
A_t	Minimum throughway area of matrix	sq ft
A_a	Surface area of matrix	sq ft
C	Heat capacity of matrix per unit length	C.H.U./deg C ft
c_p	Specific heat of gas	C.H.U./lb deg C or C.H.U./cu ft deg C
$C_f/2$	Half friction factor $= \rho \Delta_p g(1/G_{\max}{}^2)(A_t/A_a)$ (non-dimensional)	
D	Wire diameter	ft
d	Hydraulic diameter $= 4LA_t/A_a$	ft
G	Minimum mass velocity $= W/A$	lb/sec sq ft
$G_{\max}$	Maximum mass velocity $= W/A_t$	lb/sec sq ft
H	Heating surface per unit length of matrix $= A_a/L$	ft
J_0	Bessel function zero order	
J_1	Bessel function first order	
k	Thermal conductivity of gas	C.H.U./sec sq ft deg C per ft
k_H	Heat transfer coefficient (non-dimensional) $= \alpha/G_{\max}\, c_p$	
L	Total length of regenerator passage	ft
M	Weight of matrix (excluding frame etc.)	lb

M_c	Weight of matrix container	lb
N	Number of strips or layers in matrix	
N_u	Nusselt number, non-dimensional heat transfer coefficient $= \alpha D/k$ or $\alpha d/k$	
Q	Amount of heat transferred in actual regenerator per blow period	C.H.U.
Q_{id}	Amount of heat transferred in ideal regenerator per blow period	C.H.U.
R	Reynolds number based on hydraulic diameter $= G_{\max}\, d/\mu$	
R_d	Reynolds number based on wire diameter $= G_{\max}\, D/\mu$	
R_p	Reynolds number based on wire perimeter $= G_{\max}\, \pi D/\mu$	
t	Matrix temperature	
t_n	Final temperature at end of blow period in nth strip of matrix	
T_{go}	Gas outlet temperature	
T_g	Gas inlet temperature	
T_m	Matrix temperature at start of heating	
U	Utilisation factor $= \Pi/\Lambda$	
v	Velocity of gas	ft/sec
V	Volume flow of gas per unit time	cu ft/sec
V_o	Volume of gas flowing in one blow period	cu ft
V_L	Volume of matrix $= AL$	cu ft
w	Volume flow of gas during time, Z	cu ft
W	Mass flow rate of gas or air	lb/sec
x	Distance from entrance to matrix passage	ft
z	Time from start of blow	sec
Z	Blow time	sec
α	Heat transfer coefficient	C.H.U./sec sq ft deg C
Δ_{yn}	Heat-pole function for nth strip of matrix	
Δ_p	Pressure drop	lb/sq in.
ρ	Density of gas or air	lb/cu ft
ξ	Distance from front of regenerator $= (\alpha H/Vc_p)x$ (non-dimensional)	
η	Time from beginning of blow $= (\alpha H/VC)w$ (non-dimensional)	
η_{reg}	Regenerator efficiency $= Q/Q_{id}$ (Thermal Ratio)	
η_{rec}	Recuperator efficiency $= \Lambda/(2 + \Lambda)$ (Thermal Ratio)	
Λ	Length of whole regenerator $= (\alpha H/Vc_p)L$ (non-dimensional)	
Π	Blow time $= (\alpha H/C)Z$ (non-dimensional)	
μ	Viscosity of gas or air	lb/ft sec
ϑ	Gas temperature	

REFERENCES

No.	Author	Title, etc.
1	L. Ritz	Summary of the Theory and Construction of a Rational Gas Turbine. A.V.A. Gottingen R. & T. 1. July, 1945.
2	L. F. Nicholson and J. E. Johnson ..	Heat Exchangers for Gas Turbines. A.R.C. 954. February, 1946. (Unpublished.)
3	H. Hausen	On the Theory of Heat Exchange in Regenerators. *Z.A.M.M.* Vol. 9, p. 173. June, 1929. (R.A.E. Library Translation No. 126.)
4	H. Hausen	An Approximate Method of Dimensioning Regenerative Heat Exchangers. *Z.A.M.M.* Vol. 11, p. 105, 1931. (R.A.E. Library Translation No. 98.)
5	A. Anzelius	Über Erwärmung Vermittels Durchströmender Medien. *Z.A.M.M.* Vol. 6, p. 291. 1926.
6	O. A. Saunders and H. Ford	Heat Transfer in the Flow of Gas Through a Bed of Solid Particles. *J. of Iron and Steel Inst.* No. 1. 1940.
7	T. E. W. Schumann	Heat Transfer to a Liquid Flowing Through a Porous Prism. *J. of the Franklin Institute.* Vol. 208, p. 405. 1929.
8	R. H. Norris and W. A. Spofford ..	High Performance Fins for Heat Transfer. Am. Soc. of Mech. Engineers. Advance Paper. New York. December, 1941.
9	Physics Division, N.P.L.	*Physical Properties of a Series of Steels—Part II.* Iron and Steel Institute. 1946.
10	W. H. McAdams	*Heat Transmission.* Second Edition, 1942. McGraw-Hill Book Company, Inc.
11	H. Glaser	Heat Transfer in Regenerators. *Z.V.D.I.*—Beiheft Verfahrungstechnik, 1938, p. 122.

APPENDIX I

1. It is required to find a solution of the differential equations (1) and (2) for the boundary conditions obtaining after a large number of reversals with steady gas and air temperatures when the matrix has reached a constant temperature at a given time in the cycle. The temperature scale may be chosen so that the cold gas enters from the left at temperature $\vartheta = 0$ and the hot gas from the right at temperature $\vartheta = \theta$, the length of the matrix extends from $\xi = 0$ to $\xi = \Lambda$ and the blow time from $\eta = 0$ to $\eta = \Pi$. For reversal, the matrix temperature at each point must be the same at the end of a cold blow as it is at the beginning of a hot blow. The boundary conditions are then

$$\vartheta = 0 \text{ when } \xi = 0 \text{ from time } \eta = 0 \text{ to } \eta = \Pi$$

$$\vartheta = \theta \text{ when } \xi = \Lambda \text{ from time } \eta = \Pi \text{ to } \eta = 2\Pi \text{ (or 0 to } \Pi).$$

Assuming equal values of Λ and Π for both hot and cold blows and a contraflow arrangement the remaining reversal condition is

$$t(\xi, \Pi) = \theta - t(\Lambda - \xi, 0) \quad \ldots \quad (1)$$

where $t(\xi, \Pi)$ is the temperature at the end of a cold blow and $\theta - t(\Lambda - \xi, 0)$ is the temperature at the beginning of a hot blow.

Hausen has suggested a possible analytical method of solution[3] but it is very laborious to use and he has only worked out a few examples covering a very wide range. Fig. 13 of Ref. 3 shows his results in the form of regenerator efficiency for lengths up to 50 and times of 0, 10, 20, 30, 40, 50. The most useful range for turbines is for lengths up to 40 and times up to 10 ; therefore, an alternative solution on the lines of Hausen's second paper[4] has been developed as follows.

2. *Solution of the Equations for the Initial Blow Period.*—Anzelius[5] has shown that if the gas flows from the left at temperature $\vartheta = 0$ and the matrix is initially at a uniform temperature $t = 1$ then during the first cooling period the solution of the differential equations is

$$t - \vartheta = e^{-(\xi + \eta)} J_0(2i\sqrt{(\xi\eta)}) \quad \ldots \quad (2)$$

hence

$$\left(\frac{\partial t}{\partial \xi}\right)_\eta = e^{-(\xi+\eta)} \left(\frac{\eta}{\xi}\right)^{1/2} . \, i.J_1(2i\sqrt{(\xi\eta)}) . \quad \ldots \quad (3)$$

Equation (3) cannot be integrated in a closed form. Values of t can be found by plotting values of $(\partial t/\partial \xi)_\eta$ for a suitable range of values of ξ and η and integrating the resulting curves graphically. Tables of Bessel functions are available for low values of $\xi\eta$ and there are approximation formulæ available for higher values. This method was tried and found to be laborious and not very accurate. Alternatively Hausen suggests finding a cubic equation to fit the curve of $(\partial t/\partial \xi)_\eta$ sufficiently accurately over the required range and then integrating the cubic equation.

A more direct method suggested by R. A. Fairthorne has been used extensively in this report. Equations (1) and (2) can be represented in the form of a matrix or mesh of points by

$$(1 + h)x_{m,n} = x_{m-1,n} + x_{m,n-1} - (1 - h)x_{m-1,n-1} \quad \ldots \quad (4)$$

where $x_{m,n} \equiv \vartheta_{mh,nh}$ or $t_{mh,nh}$ and h is the size of mesh

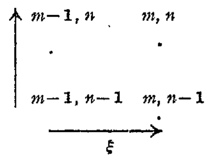

so that this equation can be used for finding either t or ϑ by substituting the appropriate starting values for t or ϑ when $\xi = 0$, $\eta = 0$. The need for using a very fine mesh can be avoided by using Richardson's 'deferred approach to the limit.' That is, find the values at the required points using an interval h_1 and then using a smaller interval h_2 and extrapolate to the values when $h = 0$. It is convenient to make $h_2 = \frac{1}{2}h$, then if ϕ_1 is the value found with h_1 and $\phi_{1/2}$ the value with $h_1/2$ then the better approximation is

$$\phi = \phi_{1/2} + \tfrac{1}{3}(\phi_{1/2} - \phi_1). \quad \ldots \quad (5)$$

It was found that except at low values of η and ξ very accurate results could be obtained by using $h_1 = 1$ and $h_2 = 0{\cdot}5$. For low values $h_1 = 0{\cdot}5$ and $h_2 = 0{\cdot}25$ was used. The starting values for matrix temperatures during initial cooling are given by $t = e^{-\eta}$ when $\xi = 0$ and $t = 1$ when $\eta = 0$ for all values of ξ. For gas temperatures during initial cooling $\vartheta = 0$ when $\xi = 0$ for all values of η and $\vartheta = 1 - e^{-\xi}$ when $\eta = 0$. Table I shows values of matrix temperatures (t) during initial cooling calculated by this method for values of $\xi = 0, 0{\cdot}5, 1, 1{\cdot}5 \ldots\ldots 7{\cdot}5, 8, 9, \ldots\ldots 20$ and $\eta = 0, 0{\cdot}5, 1, 1{\cdot}5, 2 \ldots\ldots 4$ and for $\xi = 0, 1, 2, \ldots\ldots 20$ for $\eta = 4, 5, 6 \ldots\ldots 10$. Similarly Table II shows values of gas temperature (ϑ) during initial cooling for values of $\xi = 0, 1, 2, 3 \ldots\ldots 80$ and $\eta = 0, 1, 2, 3 \ldots\ldots 80$. These results are plotted on Fig. 1 for matrix temperatures and Figs. 2 and 3 for gas temperatures.

3. *Solution of the Reversal Condition by the Heat Pole Method.*—It has been shown in the preceding section that from an initial uniform condition the final matrix temperature distribution can be found. In Ref. 4 Hausen gives a method which he calls the 'heat pole' method by which this information can be used to find the final matrix temperature distribution from any initial temperature distribution and hence find the distribution required for the reversal condition.

Briefly, the matrix is divided up into a number of narrow strips and initially the temperature distribution is assumed to be as shown in Fig. 4, that is $t = 0$ at all points except in one section where $t = 1$. If gas then flows through at a temperature $\vartheta = 0$ after a time η the heat will be given up to the succeeding sections of the matrix and the hot section will be cooled down as shown by the curve on Fig. 4. This is called the heat pole function Δ_y and is obtained from the curves of Fig. 1 by subtracting the average value of the appropriate curve over the width of one heat pole from the average value in the succeeding section. It is now assumed that the matrix has an initial temperature distribution such that the average values of the matrix temperature in each section is $f_1, f_2, f_3 \ldots\ldots f_n$ then the effect of f_1 on each section after a time η will be

$$f_1\Delta_{y1}, f_1\Delta_{y2}, f_1\Delta_{y3} \ldots\ldots f_1\Delta_{yn}$$

and similarly for all except the first section the effect of f_2 will be

$$f_2\Delta_{y1}, f_2\Delta_{y2}, f_2\Delta_{y3}, \ldots\ldots f_2\Delta_{y\,n-1}$$

and so on.

Owing to the linear characteristics of the differential equations it is permissible to add up the effects in each section so that the total temperature in the sections after a time η is

$$\left.\begin{array}{lll} \text{1st section} & & t_1 = f_1\Delta_{y1} \\ \text{2nd} & ,, & t_2 = f_1\Delta_{y2} + f_2\Delta_{y1} \\ \text{3rd} & ,, & t_3 = f_1\Delta_{y3} + f_2\Delta_{y2} + f_3\Delta_{y1} \\ \text{4th} & ,, & t_4 = f_1\Delta_{y4} + f_2\Delta_{y3} + f_3\Delta_{y2} + f_4\Delta_{y1} \\ n\text{th} & ,, & t_n = f_1\Delta_{yn} + f_2\Delta_{y\,n-1} + f_3\Delta_{y\,n-2} + \ldots\ldots + f_n\Delta_{y1}. \end{array}\right\} \quad \ldots \quad (6)$$

All that is now required to satisfy the reversal condition is to choose values of $f_1, f_2, f_3 \ldots f_n$ such that the final distribution after a cooling and an equal and opposite heating is the same as $f_1, f_2, f_3 \ldots f_n$. It was first thought that this could best be done by starting from a uniform distribution of $f_{1\text{ to }n} = 1$ and applying the heat pole functions alternately in each direction until a balance was obtained. The example chosen was $\Lambda = 20$, $\Pi = 3$ but it was found that after several reversals the required condition was very far from being reached. To speed things up a fresh start was made with the initial distribution assumed diagonal and after a few reversals a condition was reached which appeared to be very close to the required balanced condition, but when the efficiency was calculated from these results it was appreciably below the known true result. A more accurate value of efficiency could be obtained by taking an average of the initial and final distribution curves but when this average was used for a further reversal it did not fulfil the reversal condition. This process was found to be very laborious and of doubtful accuracy and was therefore abandoned.

The exact values of $f_1, f_2 \ldots f_n$ required to meet the reversal conditions can be found by expressing the problem in the form of simultaneous equations. If the hot gas and cold gas temperature are 1 and 0 respectively then for the reversal condition and equal flow times the initial and final temperature distribution curves must be symmetrical at opposite ends of the diagonal line when the hot gas and cold gas are in contraflow, that is,

$$\left.\begin{array}{l} t_1 = 1 - f_n \\ t_2 = 1 - f_{n-1} \\ t_3 = 1 - f_{n-2} \\ \vdots \\ t_n = 1 - f_1 \end{array}\right\} \quad \ldots \quad \ldots \quad \ldots \quad \ldots \quad \ldots \quad \ldots \quad \ldots \quad (7)$$

where $f_1, f_2, f_3 \ldots f_n$ are the mean temperatures in the matrix sections at the beginning of the cold blow and $t_1, t_2 \ldots t_n$ are the corresponding temperatures at the end of the cold blow. Substituting the equation (6) in (7) gives,

$$\left.\begin{array}{ll} \Delta_{y1}f_1 \qquad\qquad\qquad\qquad\qquad\qquad + f_n & = 1 \\ \Delta_{y2}f_1 + \Delta_{y1}f_2 \qquad\qquad\qquad\qquad + f_{n-1} & = 1 \\ \Delta_{y3}f_1 + \Delta_{y2}f_2 + \Delta_{y1}f_3 \qquad\qquad + f_{n-2} & = 1 \\ \vdots & \\ \Delta_{yn}f_1 + \Delta_{y\,n-1}f_2 + \Delta_{y\,n-2}f_3 \ldots\ldots \Delta_{y1}f_n + f_1 & = 1. \end{array}\right\} \quad \ldots \quad \ldots \quad (8)$$

If values of the heat pole functions $\Delta_{y1} \ldots \Delta_{yn}$ are chosen for the blow time required then solving the simultaneous equations (8) gives the initial temperature distribution $f_1, f_2 \ldots f_n$ required to meet the reversal conditions. This is quite a simple method provided that the simultaneous equations can be solved readily. Unfortunately there is no quick method of solving equations of more than a very few unknowns and the accuracy of the solution is bound to decrease as the width of the heat poles is increased. In practice it was found that equations of more than 5 unknowns were very cumbersome to solve by ordinary methods, though a number of solutions for 8 unknowns were obtained on the Mallock calculating machine at Cambridge. This machine is very quick but not very accurate. Electronic calculating machines now being built will extend the practicable range of this method considerably. A trial set of 20 equations was solved by the relaxation method by the N.P.L. and, as will be discussed later, gave a very accurate result.

4. *Heat Pole Functions.*—Tables 3 to 7 give the heat pole functions for blow times between 1·5 and 10 and for heat poles of width 1 to 5. These were obtained from Table 1 or Fig. 1, by subtracting the average value of matrix temperature over the required width from the average value in the next section. Originally the arithmetic mean value over each section was used but it was found that for the shorter blow times this caused appreciable errors and so the true average was generally used. Widths greater than 5 are not likely to be sufficiently accurate except for very long blow times which are not of great interest for gas-turbine applications.

5. *The Calculation of Regenerator Efficiency by the Heat Pole Method.*—If an ideal regenerator is defined as one which heats the cold gas up to the same temperature as the hot gas (that is from $\vartheta = 0$ to $\vartheta = 1$) then the heat transferred during the blow time Z would be

$$Q_{id} = Vc_pZ \times 1. \quad \ldots \quad \ldots \quad \ldots \quad \ldots \quad \ldots \quad \ldots \quad \ldots \quad (9)$$

The regenerator efficiency or thermal ratio η_{reg} may be defined as the ratio of the amount of heat actually transferred during one blow time to that of an ideal regenerator (Q_{id}). Consider an actual regenerator divided into N strips with starting temperatures for the cold blow $f_1, f_2, f_3 \ldots f_N$ then the final temperature in the nth strip for contraflow will be

$$t_n = 1 - f_{N-(n-1)} \quad \ldots \quad \ldots \quad \ldots \quad \ldots \quad \ldots \quad \ldots \quad \ldots \quad (10)$$

and during the cold blow the nth strip will give up a quantity of heat to the gas

$$\Delta Q = C\frac{L}{N}(f_n - t_n)$$

$$= C\frac{L}{N}\left[f_n - 1 + f_{N-(n-1)}\right] \quad \ldots \quad \ldots \quad \ldots \quad \ldots \quad \ldots \quad (11)$$

where C is the heat capacity per unit length of matrix and L the length of matrix.

The heat given up by the whole matrix during one blow period would then be

$$Q = \sum_1^N \Delta Q = CL\left[\frac{L}{N}\sum_1^N f_n - 1\right] \times 1. \quad \ldots \quad (12)$$

Then the regenerator efficiency will be given by

$$\eta_{\text{reg}} = \frac{Q}{Q_{id}} = \frac{CL\left[\frac{2}{N}\sum_1^N f_n - 1\right]}{V c_p Z} \quad \ldots \quad (13)$$

which becomes

$$\eta_{\text{reg}} = \frac{\Lambda}{\Pi}\left[\frac{2}{N}\sum_1^N f_n - 1\right]. \quad \ldots \quad (14)$$

In Ref. 3 Hausen shows that the limiting value of η_{reg} when the blow time becomes zero is given by

$$\lim_{\Pi=0} \; (\eta_{\text{reg}}) = \frac{\Lambda}{2+\Lambda}. \quad \ldots \quad (15)$$

This is also the efficiency of the corresponding recuperator for if Δ is the uniform temperature difference between the two fluids then the heat transmitted through the metal wall in a time Z will be

$$Q = \alpha HLZ\frac{\Delta}{2} \quad \ldots \quad (16)$$

and one fluid is heated through a temperature range of $(1 - \Delta)$ so that also

$$Q = \; VZc_p\,(1 - \Delta) \quad \ldots \quad (17)$$

eliminating Δ from equation (16) and (17) gives

$$Q = \frac{\Lambda}{2+\Lambda}\; VZc_p$$

as before $\quad Q_{id} = VZc_p\,.$

Therefore $$\eta_{\text{rec}} = \frac{Q}{Q_{id}} = \frac{\Lambda}{2+\Lambda}. \quad \ldots \quad (18)$$

This means that the efficiency of a regenerator with very frequent reversals closely approaches that of a recuperator. Equation (15) is also very useful when checking the accuracy of calculations of η_{reg} for very short blow times as it forms an easily calculated boundary within which all results must lie.

6. *Results of Calculations of Regenerator Efficiency.*—In section 4 it was mentioned that a number of sets of simultaneous equations (8) were solved using the Mallock machine with up to 8 unknowns. The efficiencies η_{reg} were calculated from the solutions using equation (14). The examples chosen and the results obtained are given in Table 8. Inspection of these results showed that although the machine had calculated the correct solutions to the equations, the resulting efficiency was not correct. This is shown clearly in Fig. 5 where the difference between the corresponding value of η_{rec} and the calculated η_{reg} is plotted against blow time Π. From equations (15) and (18) it can be seen that the lines of constant Λ should all approach zero as Π approaches zero ; the directions which the curves should take are indicated by the dotted lines. The error introduced by the heat pole method is seen to vary with the blow time, the length or number of heat poles taken and the width of the heat poles, the error increasing rapidly as

Π approaches zero. Taking as the required standard accuracy an error of -1 per cent in η_{reg} it is then possible to fix limits within which the heat pole method is sufficiently accurate. This limit is marked on Table 8. A more detailed examination of the errors gives the following recommended limitations for the heat pole method.

Heat pole width	Minimum value of Π
1	1·5
2	3·5
3	5
4	6
5	8

The increase of error with length is in most cases small and there is some evidence to show that it may reach a maximum and then decrease with increasing length or number of steps. With the possible exception of $\Pi = 1{\cdot}5$ for width 1 any number of steps from 5 to at least 20 should be satisfactory. For $\Pi = 1{\cdot}5$ width 1, the error appears to be increasing rapidly for more than 5 steps, it is 1 per cent for 5 and nearly $1\frac{1}{2}$ per cent for 6 but it may not go above 2 per cent and may decrease again above 10 steps and in any case the true answer for such a short blow time must be within 1 per cent of η_{rec} for all lengths likely to be used.

A few additional solutions by the heat pole method have been worked out by direct solution of the simultaneous equations. These are all for 5 steps and for heat poles of width 1 to 5. The values of η_{reg} calculated from these results are shown on Table 9.

By combining all the reliable results from the Mallock machine and those of Table 9 along with a few read as accurately as possible from Hausen's results, the curves shown on Fig. 5 have been obtained and from these the curves of Figs. 7, 8 have been constructed and give the recommended values of η_{reg} for a wide range of values of Λ and Π. The results are also given in Table 10.

APPENDIX II

Efficiency of Unbalanced Regenerators

When a regenerator is applied to a gas-turbine some account must be taken of the large difference in density between the charge air and the exhaust gas. This difference may be up to 5/1 or even more depending on the operating temperatures and the compression ratio. As the mass flow of the charge air and exhaust gas are approximately equal it follows that if the regenerator matrix is divided equally between the two fluids the pressure drop on the gas side will be higher than that on the charge side in approximately the inverse ratio of the densities. It is desirable from the point of view of efficiency of the turbine cycle to have the pressure drops at least equal or preferably lower on the gas side than on the air side. This can only be done with a rotating matrix by dividing the circle of rotation unequally between the gas and air so that a given portion of the matrix is heated by the gas for a longer time than it is cooled by the air. In non-dimensional terms this means that, assuming the heat transfer coefficient and mass flows are equal on both sides, then the ratio Λ/Π must be equal on both sides and that the ratio of the reduced lengths is the same as that of the reduced times.

By choosing heat poles of suitable widths the solutions for unbalanced regenerators can be found. The width of heat pole on each side must be chosen so that there are the same number of sections on each side. For example, if the air side has a length $\Lambda_a = 5$ and the matrix is to be divided in the ratio of 1/5, then 5 heat poles of width 1 are taken for the air side and the length on the gas side $\Lambda_g = 25$ is divided into 5 heat poles of width 5. Equation (7) of Appendix I then becomes

$$\left.\begin{aligned} t_{a1} &= 1 - f_{g5} & t_{g1} &= 1 - f_{a5} \\ t_{a2} &= 1 - f_{g4} & t_{g2} &= 1 - f_{a4} \\ t_{a3} &= 1 - f_{g3} & t_{g3} &= 1 - f_{a3} \\ t_{a4} &= 1 - f_{g2} & t_{g4} &= 1 - f_{a2} \\ t_{a5} &= 1 - f_{g1} & t_{g5} &= 1 - f_{a1} \end{aligned}\right\} \quad \ldots \quad \ldots \quad \ldots \quad \ldots \qquad (1)$$

where $f_{a1}, f_{a2}, \ldots f_{a5}$ are the mean temperatures in the matrix sections at the beginning of the cold blow and $t_{a1}, t_{a2}, \ldots t_{a1}$ are the corresponding temperatures at the end of the cold blow. Similarly $f_{g1}, f_{g2} \ldots f_{g5}$ and $t_{g1}, t_{g2}, \ldots t_{g5}$ are the temperatures at the beginning and end of the hot blow. Equation (8) then becomes

$$\left.\begin{aligned} &\Delta_{ya1} f_{a1} && + f_{g5} = 1 \\ &\Delta_{ya2} f_{a1} + \Delta_{ya1} f_{a2} && + f_{g4} = 1 \\ &\Delta_{ya3} f_{a1} + \Delta_{ya2} f_{a2} + \Delta_{ya1} f_{a3} && + f_{g3} = 1 \\ &\Delta_{ya4} f_{a1} + \Delta_{ya2} f_{a3} + \Delta_{ya2} f_{a3} + \Delta_{ya1} f_{a4} && + f_{g2} = 1 \\ &\Delta_{ya5} f_{a1} + \Delta_{ya4} f_{a2} + \Delta_{ya3} f_{a3} + \Delta_{ya2} f_{a4} + \Delta_{ya1} f_{a5} && + f_{g1} = 1 \\ \\ &\Delta_{yg1} f_{g1} && + f_{a5} = 1 \\ &\Delta_{yg2} f_{g1} + \Delta_{yg1} f_{g2} && + f_{a4} = 1 \\ &\Delta_{yg3} f_{g1} + \Delta_{yg2} f_{g2} + \Delta_{yg1} f_{g3} && + f_{a3} = 1 \\ &\Delta_{yg4} f_{g1} + \Delta_{yg3} f_{g2} + \Delta_{yg2} f_{g3} + \Delta_{yg1} f_{g4} && + f_{a2} = 1 \\ &\Delta_{yg5} f_{g1} + \Delta_{yg4} f_{g2} + \Delta_{yg3} f_{g3} + \Delta_{yg2} f_{g4} + \Delta_{yg1} f_{g5} && + f_{a1} = 1 \end{aligned}\right\} \quad \ldots \qquad (2)$$

These simultaneous equations can then be solved to get values of f_a and f_g. From these η_{reg} can be calculated as before, equation (14) of Appendix I becomes

$$\eta_{reg} = \frac{\Lambda_a}{\Pi_a} \cdot \frac{1}{N} \left[\Sigma f_a - \Sigma(1 - f_g) \right]. \quad \ldots \quad \ldots \quad \ldots \quad \ldots \quad \ldots \qquad (3)$$

A number of values of η_{reg} have been calculated by this method for unbalanced regenerators divided into five sections and with ratios of air/gas of 1/2, 1/3, 1/4 and 1/5. The number of examples for which accurate answers can be obtained by this method with only 5 sections is rather limited but sufficient results have been obtained to determine the magnitude of error involved by using the arithmetic mean efficiency given by the two sides of the regenerator independently. Table 11 shows the results obtained and the difference between the calculated values of efficiency and the mean values. The mean values are calculated from the curves on Figs. 6, 7. It is probable that some of the difference between calculated and mean values may be due to the heat pole method and not to the out-of-balance of the regenerator. From Table 9 it was possible to deduce the errors introduced by the heat-pole method for regenerators divided into 5 sections over the range of lengths and times used for the unbalanced regenerators, these errors were then subtracted from the efficiencies given for each side in Table 11 and new mean efficiencies obtained. The difference between the calculated efficiencies and these new efficiencies should then be a measure of the error introduced by taking the mean efficiency instead of the calculated value. It was found that the error was fairly constant for a given ratio of unbalance over a wide range of blow times and for two different lengths but that it increased with the ratio of unbalance. For the present purpose it is sufficiently accurate to take the mean of all the values for each ratio of unbalance. This gives the following mean errors :—

Ratio $\frac{A_a}{A_g}$	Error $(\eta_{mean} - \eta_T)$
1/2	0·004
1/3	0·008
1/4	0·013
1/5	0·014

From Figs. 7, 8, the mean efficiencies of a wide range of unbalanced regenerators have been found and these have been corrected using the above correction factors. The results were given on Figs. 9 to 16 which show the effect of length and time on the efficiencies of unbalanced regenerators with ratios of A_a/A_g of 1/2, 1/3, 1/4, 1/5. The values calculated by the heat pole method are also shown without any correction factors. The results given by the curves are thought to be accurate to within less than 1 per cent. The efficiency of a regenerator with any ratio of unbalance up to 5 can be calculated from the mean efficiency obtained from the curves on Figs. 7, 8 and the correction factor which is plotted on Fig. 17.

In Ref. 3, Hausen states that the efficiency of an unbalanced regenerator is given approximately by the efficiency of a balanced regenerator of a length and blow time equal to the mean values on the two sides. The efficiencies given by this method are given on Table 11 for comparison with the values obtained by the other methods. They are from 0·015 to 0·083 higher than those given by the heat pole method and therefore it is concluded that the first method of taking the mean of the efficiencies of the two sides is preferable as it gives values much closer to the calculated ones.

TABLE 1

Matrix Temperatures during Initial Cooling

η	ξ = 0	0·5	1·0	1·5	2·0	2·5	3·0	3·5	4·0
0	1·0	1·0	1·0	1·0	1·0	1·0	1·0	1·0	1·0
0·5	0·6065	0·7328	0·8192	0·8781	0·9181	0·9451	0·9633	0·9755	0·9837
1·0	0·3679	0·5301	0·6542	0·7478	0·8174	0·8687	0·9061	0·9333	0·9528
1·5	0·2231	0·3793	0·5120	0·6215	0·7097	0·7796	0·8341	0·8761	0·9081
2·0	0·1353	0·2690	0·3943	0·5064	0·6035	0·6854	0·7530	0·8079	0·8519
2·5	0·0821	0·1893	0·2995	0·4059	0·5041	0·5918	0·6680	0·7329	0·7872
3·0	0·0498	0·1323	0·2250	0·3209	0·4147	0·5029	0·5833	0·6548	0·7169
3·5	0·0302	0·0919	0·1673	0·2506	0·3366	0·4215	0·5022	0·5769	0·6443
4·0	0·0183	0·0635	0·1234	0·1936	0·2700	0·3489	0·4269	0·5018	0·5717
5·0	0·0067		0·0658		0·1689		0·2987		0·4358
6·0	0·0025		0·0341		0·1019		0·2007		0·3184
7·0	0·0009		0·0173		0·0597		0·1304		0·2247
8·0	0·0003		0·0087		0·0342		0·0824		0·1537
9·0	0·0001		0·0043		0·0192		0·0508		0·1024
10·0	0		0·0021		0·0107		0·0307		0·0666

η	ξ = 4·5	5·0	5·5	6·0	6·5	7·0	7·5	8·0	9·0
0	1·0	1·0	1·0	1·0	1·0	1·0	1·0	1·0	1·0
0·5	0·9892	0·9928	0·9953	0·9969	0·9979	0·9986	0·9991		
1·0	0·9667	0·9767	0·9837	0·9886	0·9921	0·9944	0·9962	0·9975	0·9988
1·5	0·9323	0·9504	0·9638	0·9737	0·9810	0·9861	0·9902		
2·0	0·8868	0·9140	0·9351	0·9513	0·9636	0·9730	0·9800	0·9855	0·9922
2·5	0·8319	0·8683	0·8976	0·9208	0·9392	0·9536	0·9647		
3·0	0·7702	0·8150	0·8522	0·8828	0·9077	0·9278	0·9438	0·9569	0·9746
3·5	0·7039	0·7558	0·8004	0·8380	0·8695	0·8956	0·9170		
4·0	0·6356	0·6930	0·7436	0·7876	0·8254	0·8575	0·8845	0·9075	0·9410
5·0		0·5648		0·6766		0·7672		0·8372	0·8890
6·0		0·4417		0·5591		0·6630		0·7499	0·8194
7·0		0·3333		0·4462		0·5546		0·6522	0·7357
8·0		0·2437		0·3451		0·4498		0·5510	0·6433
9·0		0·1732		0·2592		0·3546		0·4582	0·5480
10·0		0·1199		0·1897		0·2722		0·3626	0·4553

η	ξ = 10·0	11·0	12·0	13·0	14·0	15·0	16·0	17·0	18·0	19·0	20·0
0	1·0	1·0	1·0	1·0	1·0	1·0	1·0	1·0	1·0	1·0	1·0
0·5											
1·0	0·9994	0·9997	0·9999	0·9999	1·0	1·0	1·0	1·0	1·0	1·0	1·0
1·5											
2·0	0·9959	0·9979	0·9989	0·9994	0·9997	0·9999	0·9999	1·0	1·0	1·0	1·0
2·5											
3·0	0·9853	0·9919	0·9953	0·9974	0·9986	0·9992	0·9996	0·9998	0·9999	0·9999	1·0
3·5											
4·0	0·9632	0·9774	0·9864	0·9919	0·9953	0·9973	0·9984	0·9991	0·9995	0·9997	0·9998
5·0	0·9261	0·9517	0·9691	0·9805	0·9879	0·9926	0·9955	0·9973	0·9984	0·9991	0·9995
6·0	0·8726	0·9121	0·9406	0·9605	0·9473	0·9834	0·9895	0·9934	0·9959	0·9975	0·9985
7·0	0·8041	0·8580	0·8993	0·9299	0·9521	0·9678	0·9876	0·9861	0·9910	0·9943	0·9964
8·0	0·7236	0·7907	0·8449	0·8874	0·9197	0·9437	0·9612	0·9736	0·9823	0·9883	0·9924
9·0	0·6358	0·7131	0·7790	0·8331	0·8764	0·9100	0·9356	0·9546	0·9685	0·9784	0·9854
10·0	0·5455	0·6293	0·7041	0·7686	0·8224	0·8662	0·9009	0·9277	0·9481	0·9633	0·9743

TABLE 2

Gas Temperature during Initial Cooling

η	ξ								
	0	1·0	2·0	3·0	4·0	5·0	6·0	7·0	8·0
0	0	0·6321	0·8647	0·9502	0·9817	0·9933	0·9975	0·9991	0·9997
1	0	0·3469	0·6057	0·7748	0·8764	0·9342	0·9658	0·9825	0·9911
2	0	0·1905	0·3966	0·5851	0·7297	0·8311	0·8979	0·9401	0·9654
3	0	0·0935	0·2467	0·4164	0·5727	0·7014	0·7992	0·8693	0·9171
4	0	0·0468	0·1477	0·2827	0·4279	0·5645	0·6815	0·7750	0·8459
5	0	0·0231	0·0857	0·1847	0·3066	0·4356	0·5584	0·6664	0·7560
6	0	0·0112	0·0484	0·1167	0·2119	0·3238	0·4413	0·5537	0·6546
7	0	0·0054	0·0268	0·0717	0·1419	0·2330	0·3371	0·4453	0·5499
8	0	0·0026	0·0145	0·0429	0·0927	0·1629	0·2500	0·3478	0·4488
9	0	0·0013	0·0078	0·0252	0·0589	0·1108	0·1804	0·2642	0·3564
10	0	0·0006	0·0041	0·0146	0·0361	0·0733	0·1269	0·1957	0·2760
11	0	0·0003	0·0022	0·0084	0·0221	0·0477	0·0873	0·1415	0·2087
12	0	0·0001	0·0013	0·0048	0·0134	0·0304	0·0587	0·1001	0·1544
13	0	0	0·0006	0·0027	0·0081	0·0190	0·0389	0·0693	0·1119
14	0	0	0·0002	0·0014	0·0047	0·0117	0·0253	0·0473	0·0796
15	0	0	0	0·0007	0·0027	0·0072	0·0162	0·0317	0·0555
16	0	0	0	0·0003	0·0016	0·0042	0·0101	0·0208	0·0380
17	0	0	0	0	0·0007	0·0024	0·0062	0·0134	0·0255
18	0	0	0	0	0·0002	0·0013	0·0037	0·0084	0·0168
19	0	0	0	0	0	0·0006	0·0021	0·0052	0·0110
20	0	0	0	0	0	0·0002	0·0012	0·0030	0·0069
21	0	0	0	0	0	0·0003	0·0010	0·0023	0·0050
22	0	0	0	0	0	0·0001	0·0005	0·0014	0·0032
23	0	0	0	0	0	0	0·0002	0·0008	0·0020
24	0	0	0	0	0	0	0·0001	0·0005	0·0013
25	0	0	0	0	0	0	0	0·0002	0·0008
26	0	0	0	0	0	0	0	0·0001	0·0005
27	0	0	0	0	0	0	0	0	0·0003
28	0	0	0	0	0	0	0	0	0·0001
29	0	0	0	0	0	0	0	0	0
30	0	0	0	0	0	0	0	0	0
31	0	0	0	0	0	0	0	0	0
32	0	0	0	0	0	0	0	0	0
33	0	0	0	0	0	0	0	0	0
34	0	0	0	0	0	0	0	0	0
35	0	0	0	0	0	0	0	0	0
36	0	0	0	0	0	0	0	0	0
37	0	0	0	0	0	0	0	0	0
38	0	0	0	0	0	0	0	0	0
39	0	0	0	0	0	0	0	0	0
40	0	0	0	0	0	0	0	0	0

TABLE 2—*continued*

η	ξ								
	9·0	10·0	11·0	12·0	13·0	14·0	15·0	16·0	17·0
0	0·9999	1·0	1·0	1·0	1·0	1·0	1·0	1·0	1·0
1	0·9956	0·9978	0·9989	0·9995	0·9998	0·9999	0·9999	1·0	1·0
2	0·9804	0·9892	0·9940	0·9967	0·9982	0·9988	0·9993	0·9998	0·9999
3	0·9486	0·9688	0·9815	0·9891	0·9937	0·9962	0·9977	0·9990	0·9995
4	0·8972	0·9329	0·9572	0·9732	0·9833	0·9898	0·9937	0·9966	0·9981
5	0·8262	0·8794	0·9181	0·9456	0·9644	0·9771	0·9853	0·9912	0·9947
6	0·7403	0·8097	0·8638	0·9045	0·9345	0·9557	0·9704	0·9811	0·9879
7	0·6449	0·7270	0·7952	0·8497	0·8919	0·9239	0·9470	0·9643	0·9761
8	0·5468	0·6368	0·7158	0·7825	0·8369	0·8805	0·9135	0·9391	0·9576
9	0·4515	0·5441	0·6298	0·7058	0·7711	0·8259	0·8696	0·9043	0·9310
10	0·3637	0·4539	0·5418	0·6235	0·6971	0·7614	0·8155	0·8596	0·8593
11	0·2862	0·3699	0·4557	0·5395	0·6181	0·6897	0·7525	0·8054	0·8504
12	0·2202	0·2950	0·3754	0·4574	0·5378	0·6139	0·6831	0·7432	0·7968
13	0·1660	0·2304	0·3029	0·3801	0·4591	0·5365	0·6097	0·6750	0·7359
14	0·1227	0·1765	0·2398	0·3101	0·3845	0·4604	0·5351	0·6033	0·6696
15	0·0890	0·1328	0·1864	0·2482	0·3164	0·3882	0·4617	0·5305	0·6001
16	0·0634	0·0981	0·1423	0·1952	0·2558	0·3219	0·3920	0·4591	0·5296
17	0·0444	0·0713	0·1068	0·1509	0·2032	0·2626	0·3275	0·3912	0·4604
18	0·0305	0·0509	0·0789	0·1149	0·1588	0·2108	0·2693	0·3283	0·3944
19	0·0206	0·0358	0·0573	0·0860	0·1224	0·1665	0·2179	0·2715	0·3330
20	0·0136	0·0246	0·0408	0·0633	0·0928	0·1296	0·1737	0·2214	0·2772
21	0·0097	0·0173	0·0290	0·0458	0·0687	0·0982	0·1347	0·1781	0·2277
22	0·0065	0·0119	0·0205	0·0332	0·0510	0·0746	0·1047	0·1414	0·1846
23	0·0043	0·0081	0·0143	0·0238	0·0374	0·0560	0·0804	0·1109	0·1478
24	0·0028	0·0055	0·0099	0·0169	0·0272	0·0416	0·0610	0·0860	0·1169
25	0·0018	0·0037	0·0068	0·0119	0·0196	0·0306	0·0458	0·0659	0·0914
26	0·0012	0·0025	0·0047	0·0083	0·0140	0·0223	0·0341	0·0500	0·0707
27	0·0008	0·0017	0·0032	0·0058	0·0099	0·0161	0·0251	0·0376	0·0542
28	0·0005	0·0011	0·0022	0·0040	0·0070	0·0116	0·0184	0·0280	0·0411
29	0·0003	0·0007	0·0014	0·0027	0·0049	0·0083	0·0134	0·0207	0·0309
30	0·0001	0·0004	0·0009	0·0018	0·0034	0·0059	0·0097	0·0152	0·0231
31	0	0·0002	0·0006	0·0012	0·0023	0·0041	0·0069	0·0111	0·0171
32	0	0·0001	0·0003	0·0008	0·0016	0·0029	0·0049	0·0080	0·0126
33	0	0	0·0001	0·0004	0·0010	0·0020	0·0035	0·0058	0·0092
34	0	0	0	0·0002	0·0006	0·0013	0·0024	0·0041	0·0067
35	0	0	0	0·0001	0·0004	0·0009	0·0017	0·0029	0·0048
36	0	0	0	0	0·0002	0·0006	0·0012	0·0021	0·0035
37	0	0	0	0	0·0001	0·0004	0·0008	0·0015	0·0025
38	0	0	0	0	0	0·0002	0·0005	0·0010	0·0018
39	0	0	0	0	0	0·0001	0·0003	0·0007	0·0013
40	0	0	0	0	0	0	0·0001	0·0004	0·0008

TABLE 2—*continued*

η	ξ 18·0	19·0	20·0	21·0	22·0	23·0	24·0	25·0	26·0
0	1·0	1·0	1·0	1·0	1·0	1·0	1·0	1·0	1·0
1	1·0	1·0	1·0	1·0	1·0	1·0	1·0	1·0	1·0
2	1·0	1·0	1·0	1·0	1·0	1·0	1·0	1·0	1·0
3	0·9998	0·9999	1·0	1·0	1·0	1·0	1·0	1·0	1·0
4	0·9990	0·9995	0·9998	0·9999	1·0	1·0	1·0	1·0	1·0
5	0·9969	0·9982	0·9990	0·9995	0·9998	0·9999	1·0	1·0	1·0
6	0·9924	0·9953	0·9972	0·9994	0·9991	0·9995	0·9998	0·9999	1·0
7	0·9843	0·9898	0·9935	0·9960	0·9976	0·9986	0·9992	0·9996	0·9998
8	0·9709	0·9804	0·9869	0·9915	0·9946	0·9966	0·9979	0·9988	0·9993
9	0·9510	0·9657	0·9763	0·9839	0·9893	0·9930	0·9955	0·9972	0·9983
10	0·9232	0·9445	0·9604	0·9722	0·9808	0·9869	0·9912	0·9942	0·9963
11	0·8868	0·9157	0·9381	0·9552	0·9680	0·9775	0·9844	0·9893	0·9928
12	0·8418	0·8788	0·9085	0·9319	0·9499	0·9637	0·9741	0·9817	0·9873
13	0·7889	0·8339	0·8712	0·9016	0·9258	0·9448	0·9595	0·9706	0·9790
14	0·7293	0·7816	0·8264	0·8640	0·8949	0·9199	0·9397	0·9552	0·9671
15	0·6647	·07232	0·7748	0·8194	0·8572	0·8886	0·9142	0·9347	0·9509
16	0·5972	0·6602	0·7175	0·7685	0·8129	0·8508	0·8825	0·9086	0·9298
17	0·5288	0·5945	0·6560	0·7123	0·7626	0·8067	0·8446	0·8766	0·9032
18	0·4616	0·5281	0·5921	0·6522	0·7074	0·7571	0·8009	0·8388	0·8710
19	0·3973	0·4627	0·5274	0·5898	0·6486	0·7029	0·7519	0·7954	0·8332
20	0·3373	0·4000	0·4637	0·5268	0·5877	0·6453	0·6986	0·7470	0·7901
21	0·2825	0·3413	0·4025	0·4647	0·5262	0·5858	0·6422	0·6946	0·7424
22	0·2336	0·2875	0·3450	0·4049	0·4656	0·5257	0·5839	0·6393	0·6909
23	0·1907	0·2391	0·2921	0·3485	0·4071	0·4664	0·5252	0·5823	0·6366
24	0·1538	0·1965	0·2443	0·2964	0·3518	0·4091	0·4672	0·5248	0·5807
25	0·1226	0·1596	0·2020	0·2492	0·3005	0·3548	0·4110	0·4679	0·5243
26	0·0967	0·1282	0·1651	0·2072	0·2539	0·3044	0·3577	0·4128	0·4686
27	0·0755	0·1019	0·1335	0·1704	0·2122	0·2583	0·3080	0·3604	0·4145
28	0·0583	0·0801	0·1068	0·1368	0·1754	0·2169	0·2625	0·3115	0·3630
29	0·0446	0·0624	0·0846	0·1116	0·1435	0·1802	0·2214	0·2665	0·3148
30	0·0339	0·0482	0·0664	0·0890	0·1163	0·1483	0·1849	0·2257	0·2703
31	0·0255	0·0369	0·0517	0·0704	0·0934	0·1209	0·1529	0·1893	0·2298
32	0·0191	0·0280	0·0399	0·0552	0·0743	0·0976	0·1253	0·1573	0·1936
33	0·0142	0·0211	0·0305	0·0429	0·0586	0·0781	0·1017	0·1295	0·1616
34	0·0104	0·0158	0·0232	0·0331	0·0459	0·0620	0·0819	0·0157	0·1337
35	0·0076	0·0117	0·0175	0·0253	0·0356	0·0488	0·0654	0·0856	0·1097
36	0·0056	0·0087	0·0131	0·0192	0·0274	0·0381	0·0518	0·0687	0·0892
37	0·0041	0·0064	0·0098	0·0145	0·0210	0·0296	0·0407	0·0547	0·0719
38	0·0030	0·0047	0·0073	0·0109	0·0159	0·0228	0·0318	0·0433	0·0576
39	0·0022	0·0035	0·0054	0·0082	0·0121	0·0175	0·0247	0·0340	0·0458
40	0·0015	0·0025	0·0040	0·0061	0·0091	0·0133	0·0190	0·0265	0·0362

TABLE 2—*continued*

η	ξ								
	27·0	28·0	29·0	30·0	31·0	32·0	33·0	34·0	35·0
0	1·0	1·0	1·0	1·0	1·0	1·0	1·0	1·0	1·0
1	1·0	1·0	1·0	1·0	1·0	1·0	1·0	1·0	1·0
2	1·0	1·0	1·0	1·0	1·0	1·0	1·0	1·0	1·0
3	1·0	1·0	1·0	1·0	1·0	1·0	1·0	1·0	1·0
4	1·0	1·0	1·0	1·0	1·0	1·0	1·0	1·0	1·0
5	1·0	1·0	1·0	1·0	1·0	1·0	1·0	1·0	1·0
6	1·0	1·0	1·0	1·0	1·0	1·0	1·0	1·0	1·0
7	0·9999	1·0	1·0	1·0	1·0	1·0	1·0	1·0	1·0
8	0·9996	0·9998	0·9999	1·0	1·0	1·0	1·0	1·0	1·0
9	0·9990	0·9994	0·9997	0·9999	1·0	1·0	1·0	1·0	1·0
10	0·9977	0·9986	0·9992	0·9996	0·9998	0·9999	1·0	1·0	1·0
11	0·9953	0·9970	0·9981	0·9989	0·9994	0·9997	0·9999	1·0	1·0
12	0·9913	0·9942	0·9962	0·9976	0·9985	0·9991	0·9995	0·9998	0·9999
13	0·9852	0·9897	0·9930	0·9953	0·9969	0·9980	0·9988	0·9993	0·9996
14	0·9762	0·9830	0·9880	0·9917	0·9943	0·9962	0·9975	0·9984	0·9990
15	0·9636	0·9733	0·9807	0·9862	0†9903	0·9933	0·9954	0·9969	0·9980
16	0·9467	0·9600	0·9704	0·9783	0·9843	0·9888	0·9921	0·9945	0·9963
17	0·9250	0·9425	0·9565	0·9674	0·9759	0·9824	0·9873	0·9909	0·9936
18	0·8930	0·9203	0·9384	0·9529	0·9644	0·9734	0·9804	0·9857	0·9897
19	0·8656	0·8930	0·9157	0·9343	0·9494	0·9614	0·9709	0·9783	0·9840
20	0·8279	0·8605	0·8881	0·9112	0·9303	0·9459	0·9584	0·9684	0·9762
21	0·7852	0·8229	0·8555	0·8834	0·9069	0·9264	0·9424	0·9554	0·9658
22	0·7381	0·7805	0·8180	0·8507	0·8788	0·9026	0·9225	0·9390	0·9524
23	0·6874	0·7339	0·7760	0·8134	0·8461	0·8744	0·8985	0·9188	0·9356
24	0·6341	0·6840	0·7300	0·7717	0·8089	0·8417	0·8701	0·8945	0·9151
25	0·5972	0·6316	0·6808	0·7263	0·7676	0·8047	0·8374	0·8660	0·8906
26	0·5239	0·5778	0·6293	0·6778	0·7227	0·7637	0·8006	0·8333	0·8620
27	0·4692	0·5235	0·5764	0·6271	0·6749	0·7193	0·7599	0·7966	0·8293
28	0·4161	0·4698	0·5231	0·5751	0·6250	0·6722	0·7161	0·7564	0·7929
29	0·3655	0·4177	0·4704	0·5228	0·5739	0·6231	0·6696	0·7130	0·7530
30	0·3179	0·3678	0·4191	0·4710	0·5225	0·5728	0·6212	0·6671	0·7101
31	0·2739	0·3209	0·3700	0·4205	0·4715	0·5222	0·5717	0·6194	0·6648
32	0·2338	0·2774	0·3237	0·3721	0·4218	0·4720	0·5219	0·5707	0·6178
33	0·1977	0·2376	0·2807	0·3264	0·3741	0·4231	0·4725	0·5216	0·5697
34	0·1657	0·2017	0·2412	0·2838	0·3290	0·3761	0·4243	0·4730	0·5214
35	0·1377	0·1697	0·2055	0·2447	0·2869	0·3315	0·3779	0·4255	0·4735
36	0·1135	0·1416	0·1736	0·2092	0·2481	0·2898	0·3339	0·3797	0·4266
37	0·0927	0·1172	0·1454	0·1773	0·2127	0·2513	0·2926	0·3362	0·3814
38	0·0752	0·0962	0·1208	0·1491	0·1809	0·2161	0·2544	0·2953	0·3384
39	0·0605	0·0784	0·0996	0·1244	0·1527	0·1844	0·2194	0·2574	0·2979
40	0·0484	0·0634	0·0815	0·1030	0·1279	0.1562	0·1878	0·2226	0·2603

TABLE 2—*continued*

η	ξ 36·0	37·0	38·0	39·0	40·0	41·0	42·0	43·0	44·0
0	1·0	1·0	1·0	1·0	1·0	1·0	1·0	1·0	1·0
1	1·0	1·0	1·0	1·0	1·0	1·0	1·0	1·0	1·0
2	1·0	1·0	1·0	1·0	1·0	1·0	1·0	1·0	1·0
3	1·0	1·0	1·0	1·0	1·0	1·0	1·0	1·0	1·0
4	1·0	1·0	1·0	1·0	1·0	1·0	1·0	1·0	1·0
5	1·0	1·0	1·0	1·0	1·0	1·0	1·0	1·0	1·0
6	1·0	1·0	1·0	1·0	1·0	1·0	1·0	1·0	1·0
7	1·0	1·0	1·0	1·0	1·0	1·0	1·0	1·0	1·0
8	1·0	1·0	1·0	1·0	1·0	1·0	1·0	1·0	1·0
9	1·0	1·0	1·0	1·0	1·0	1·0	1·0	1·0	1·0
10	1·0	1·0	1·0	1·0	1·0	1·0	1·0	1·0	1·0
11	1·0	1·0	1·0	1·0	1·0	1·0	1·0	1·0	1·0
12	1·0	1·0	1·0	1·0	1·0	1·0	1·0	1·0	1·0
13	0·9998	0·9999	1·0	1·0	1·0	1·0	1·0	1·0	1·0
14	0·9994	0·9997	0·9999	1·0	1·0	1·0	1·0	1·0	1·0
15	0·9987	0·9992	0·9996	0·9998	0·9999	1·0	1·0	1·0	1·0
16	0·9975	0·9984	0·9990	0·9994	0·9997	0·9999	1·0	1·0	1·0
17	0·9956	0·9970	0·9980	0·9987	0·9992	0·9996	0·9998	0·9999	1·0
18	0·9927	0·9949	0·9965	0·9976	0·9984	0·9980	0·9994	0·9997	0·9999
19	0·9884	0·9917	0·9941	0·9959	0·9972	0·9981	0·9988	0·9993	0·9996
20	0·9823	0·9870	0·9906	0·9933	0·9953	0·9967	0·9978	0·9986	0·9991
21	0·9741	0·9806	0·9856	0·9895	0·9924	0·9946	0·9962	0·9974	0·9983
22	0·9633	0·9720	0·9788	0·9842	0·9883	0·9915	0·9939	0·9957	0·9970
23	0·9495	0·9608	0·9698	0·9770	0·9827	0·9871	0·9905	0·9931	0·9951
24	0·9323	0·9466	0·9582	0·9676	0·9752	0·9812	0·9859	9·9895	0·9923
25	0·9915	0·9291	0·9437	0·9557	0·9655	0·9734	0·9797	0·9846	0·9885
26	0·8868	0·9080	0·9259	0·9408	0·9533	0·9634	0·9716	0·9781	0·9833
27	0·8581	0·8831	0·9045	0·9227	0·9380	0·9507	0·9612	0·9697	0·9765
28	0·8255	0·8543	0·8794	0·9011	0·9196	0·9352	0·9482	0·9589	0·9677
29	0·7893	0·8218	0·8506	0·8759	0·8978	0·9165	0·9324	0·9457	0·9567
30	0·7497	0·7858	0·8182	0·8471	0·8725	0·8945	0·9135	0·9296	0·9432
31	0·7073	0·7466	0·7824	0·8148	0·8437	0·8691	0·8913	0·9105	0·9269
32	0·6626	0·7046	0·7435	0·7792	0·8115	0·8403	0·8658	0·8882	0·9076
33	0·6162	0·6604	0·7020	0·7406	0·7761	0·8082	0·8370	0·8626	0·8851
34	0·5688	0·6146	0·6583	0·6995	0·7378	0·7730	0·8050	0·8338	0·8595
35	0·5212	0·5679	0·6131	0·6563	0·6971	0·7351	0·7700	0·9019	0·8307
36	0·4739	0·5209	0·5670	0·6117	0·6544	0·6948	0·7324	0·7672	0·7989
37	0·4277	0·4743	0·5207	0·5662	0·6103	0·6526	0·6925	0·7299	0·7644
38	0·3831	0·4287	0·4747	0·5205	0·5654	0·6090	0·6508	0·6904	0·7274
39	0·3405	0·3846	0·4297	0·4751	0·5203	0·5647	0·6078	0·6491	0·6883
40	0·3004	0·3425	0·3861	0·4306	0·4755	0·5201	0·5640	0·6066	0·6475

TABLE 2—*continued*

η	ξ 45·0	46·0	47·0	48·0	49·0	50·0	51·0	52·0	53·0
0	1·0	1·0	1·0	1·0	1·0	1·0	1·0	1·0	1·0
1	1·0	1·0	1·0	1·0	1·0	1·0	1·0	1·0	1·0
2	1·0	1·0	1·0	1·0	1·0	1·0	1·0	1·0	1·0
3	1·0	1·0	1·0	1·0	1·0	1·0	1·0	1·0	1·0
4	1·0	1·0	1·0	1·0	1·0	1·0	1·0	1·0	1·0
5	1·0	1·0	1·0	1·0	1·0	1·0	1·0	1·0	1·0
6	1·0	1·0	1·0	1·0	1·0	1·0	1·0	1·0	1·0
7	1·0	1·0	1·0	1·0	1·0	1·0	1·0	1·0	1·0
8	1·0	1·0	1·0	1·0	1·0	1·0	1·0	1·0	1·0
9	1·0	1·0	1·0	1·0	1·0	1·0	1·0	1·0	1·0
10	1·0	1·0	1·0	1·0	1·0	1·0	1·0	1·0	1·0
11	1·0	1·0	1·0	1·0	1·0	1·0	1·0	1·0	1·0
12	1·0	1·0	1·0	1·0	1·0	1·0	1·0	1·0	1·0
13	1·0	1·0	1·0	1·0	1·0	1·0	1·0	1·0	1·0
14	1·0	1·0	1·0	1·0	1·0	1·0	1·0	1·0	1·0
15	1·0	1·0	1·0	1·0	1·0	1·0	1·0	1·0	1·0
16	1·0	1·0	1·0	1·0	1·0	1·0	1·0	1·0	1·0
17	1·0	1·0	1·0	1·0	1·0	1·0	1·0	1·0	1·0
18	1·0	1·0	1·0	1·0	1·0	1·0	1·0	1·0	1·0
19	0·9998	0·9999	1·0	1·0	1·0	1·0	1·0	1·0	1·0
20	0·9995	0·9997	0·9999	1·0	1·0	1·0	1·0	1·0	1·0
21	0·9989	0·9993	0·9996	0·9998	0·9999	1·0	1·0	1·0	1·0
22	0·9979	0·9986	0·9991	0·9995	0·9997	0·9999	1·0	1·0	1·0
23	0·9965	0·9976	0·9984	0·9989	0·9993	0·9996	0·9998	0·9999	1·0
24	0·9944	0·9960	0·9972	0·9981	0·9987	0·9992	0·9995	0·9997	0·9999
25	0·9915	0·9938	0·9955	0·9968	0·9978	0·9985	0·9990	0·9993	0·9996
26	0·9874	0·9906	0·9931	0·9949	0·9964	0·9975	0·9983	0·9988	0·9992
27	0·9819	0·9863	0·9897	0·9923	0·9944	0·9959	0·9971	0·9979	0·9986
28	0·9748	0·9806	0·9852	0·9888	0·9916	0·9938	0·9955	0·9967	0·9977
29	0·9658	0·9732	0·9792	0·9840	0·9878	0·9908	0·9932	0·9949	0·9963
30	0·9545	0·9638	0·9715	0·9778	0·9828	0·9868	0·9900	0·9925	0·9944
31	0·9407	0·9523	0·9619	0·9699	0·9764	0·9816	0·9858	0·9892	0·9918
32	0·9242	0·9383	0·9501	0·9600	0·9682	0·9749	0·9804	0·9848	0·9883
33	0·9047	0·9215	0·9358	0·9479	0·9581	0·9665	0·9735	0·9792	0·9838
34	0·8821	0·9018	0·9188	0·9334	0·9458	0·9562	0·9649	0·9721	0·9779
35	0·8564	0·8791	0·8989	0·9162	0·9310	0·9436	0·9543	0·9632	0·9706
36	0·8277	0·8534	0·8762	0·8962	0·9136	0·9286	0·9415	0·9524	0·9615
37	0·7961	0·8248	0·8505	0·8734	0·8935	0·9111	0·9263	0·9394	0·9505
38	0·7618	0·7933	0·8219	0·8477	0·8706	0·8909	0·9086	0·9240	0·9373
39	0·7251	0·7592	0·7906	0·8192	0·8449	0·8679	0·8883	0·9062	0·9218
40	0·6863	0·7228	0·7567	0·7879	0·8164	0·8422	0·8653	0·8858	0·9038

TABLE 2—*continued*

η	ξ								
	54·0	55·0	56·0	57·0	58·0	59·0	60·0	61·0	62·0
0									
1									
2									
3									
4									
5									
6									
7									
8									
9									
10									
11									
12									
13									
14									
15									
16									
17									
18									
19									
20	1·0	1·0	1·0	1·0	1·0	1·0	1·0	1·0	1·0
21	1·0	1·0	1·0	1·0	1·0	1·0	1·0	1·0	1·0
22	1·0	1·0	1·0	1·0	1·0	1·0	1·0	1·0	1·0
23	1·0	1·0	1·0	1·0	1·0	1·0	1·0	1·0	1·0
24	1·0	1·0	1·0	1·0	1·0	1·0	1·0	1·0	1·0
25	0·9998	0·9999	1·0	1·0	1·0	1·0	1·0	1·0	1·0
26	0·9995	0·9997	0·9999	1·0	1·0	1·0	1·0	1·0	1·0
27	0·9991	0·9994	0·9997	0·9999	1·0	1·0	1·0	1·0	1·0
28	0·9984	0·9989	0·9993	0·9996	0·9998	0·9999	1·0	1·0	1·0
29	0·9974	0·9982	0·9988	0·9992	0·9995	0·9997	0·9999	1·0	1·0
30	0·9959	0·9971	0·9979	0·9986	0·9991	0·9994	0·9997	0·9999	1·0
31	0·9939	0·9955	0·9967	0·9977	0·9984	0·9989	0·9993	0·9996	0·9998
32	0·9911	0·9933	0·9950	0·9964	0·9974	0·9982	0·9988	0·9992	0·9995
33	0·9875	0·9904	0·9927	0·9946	0·9960	0·9971	0·9979	0·9986	0·9991
34	0·9827	0·9866	0·9897	0·9922	0·9941	0·9956	0·9968	0·9977	0·9984
35	0·9767	0·9817	0·9857	0·9889	0·9915	0·9936	0·9952	0·9965	0·9975
36	0·9691	0·9754	0·9806	0·9848	0·9882	0·9909	0·9931	0·9948	0·9962
37	0·9598	0·9676	0·9741	0·9795	0·9839	0·9874	0·9903	0·9926	0·9944
38	0·9486	0·9581	0·9661	0·9728	0·9784	0·9829	0·9866	0·9896	0·9920
39	0·9352	0·9467	0·9564	0·9646	0·9715	0·9772	0·9819	0·9858	0·9889
40	0·9195	0·9331	0·9448	0·9547	0·9631	0·9702	0·9761	0·9809	0·9849

TABLE 2—*continued*

η	ξ								
	63·0	64·0	65·0	66·0	67·0	68·0	69·0	70·0	71·0
0									
1									
2									
3									
4									
5									
6									
7									
8									
9									
10									
11									
12									
13									
14									
15									
16									
17									
18									
19									
20	1·0	1·0	1·0	1·0	1·0	1·0	1·0	1·0	1·0
21	1·0	1·0	1·0	1·0	1·0	1·0	1·0	1·0	1·0
22	1·0	1·0	1·0	1·0	1·0	1·0	1·0	1·0	1·0
23	1·0	1·0	1·0	1·0	1·0	1·0	1·0	1·0	1·0
24	1·0	1·0	1·0	1·0	1·0	1·0	1·0	1·0	1·0
25	1·0	1·0	1·0	1·0	1·0	1·0	1·0	1·0	1·0
26	1·0	1·0	1·0	1·0	1·0	1·0	1·0	1·0	1·0
27	1·0	1·0	1·0	1·0	1·0	1·0	1·0	1·0	1·0
28	1·0	1·0	1·0	1·0	1·0	1·0	1·0	1·0	1·0
29	1·0	1·0	1·0	1·0	1·0	1·0	1·0	1·0	1·0
30	1·0	1·0	1·0	1·0	1·0	1·0	1·0	1·0	1·0
31	0·9999	1·0	1·0	1·0	1·0	1·0	1·0	1·0	1·0
32	0·9997	0·9999	1·0	1·0	1·0	1·0	1·0	1·0	1·0
33	0·9994	0·9996	0·9998	0·9999	1·0	1·0	1·0	1·0	1·0
34	0·9989	0·9993	0·9996	0·9998	0·9999	1·0	1·0	1·0	1·0
35	0·9982	0·9988	0·9992	0·9995	0·9997	0·9999	1·0	1·0	1·0
36	0·9972	0·9980	0·9986	0·9991	0·9994	0·9997	0·9999	1·0	1·0
37	0·9958	0·9969	0·9978	0·9985	0·9989	0·9993	0·9996	0·9998	0·9999
38	0·9939	0·9954	0·9966	0·9976	0·9983	0·9988	0·9992	0·9995	0·9997
39	0·9914	0·9934	0·9950	0·9963	0·9973	0·9981	0·9987	0·9991	0·9994
40	0·9882	0·9908	0·9929	0·9946	0·9959	0·9970	0·9979	0·9985	0·9989

TABLE 2—*continued*

η	ξ								
	72·0	73·0	74·0	75·0	76·0	77·0	78·0	79·0	80·0
0									
1									
2									
3									
4									
5									
6									
7									
8									
9									
10									
11									
12									
13									
14									
15									
16									
17									
18									
19									
20	1·0	1·0	1·0	1·0	1·0	1·0	1·0	1·0	1·0
21	1·0	1·0	1·0	1·0	1·0	1·0	1·0	1·0	1·0
22	1·0	1·0	1·0	1·0	1·0	1·0	1·0	1·0	1·0
23	1·0	1·0	1·0	1·0	1·0	1·0	1·0	1·0	1·0
24	1·0	1·0	1·0	1·0	1·0	1·0	1·0	1·0	1·0
25	1·0	1·0	1·0	1·0	1·0	1·0	1·0	1·0	1·0
26	1·0	1·0	1·0	1·0	1·0	1·0	1·0	1·0	1·0
27	1·0	1·0	1·0	1·0	1·0	1·0	1·0	1·0	1·0
28	1·0	1·0	1·0	1·0	1·0	1·0	1·0	1·0	1·0
29	1·0	1·0	1·0	1·0	1·0	1·0	1·0	1·0	1·0
30	1·0	1·0	1·0	1·0	1·0	1·0	1·0	1·0	1·0
31	1·0	1·0	1·0	1·0	1·0	1·0	1·0	1·0	1·0
32	1·0	1·0	1·0	1·0	1·0	1·0	1·0	1·0	1·0
33	1·0	1·0	1·0	1·0	1·0	1·0	1·0	1·0	1·0
34	1·0	1·0	1·0	1·0	1·0	1·0	1·0	1·0	1·0
35	1·0	1·0	1·0	1·0	1·0	1·0	1·0	1·0	1·0
36	1·0	1·0	1·0	1·0	1·0	1·0	1·0	1·0	1·0
37	1·0	1·0	1·0	1·0	1·0	1·0	1·0	1·0	1·0
38	0·9999	1·0	1·0	1·0	1·0	1·0	1·0	1·0	1·0
39	0·9997	0·9999	1·0	1·0	1·0	1·0	1·0	1·0	1·0
40	0·9993	0·9996	0·9998	0·9999	1·0	1·0	1·0	1·0	1·0

TABLE 2—*continued*

η	ξ								
	16·0	17·0	18·0	19·0	20·0	21·0	22·0	23·0	24·0
40	0·0004	0·0008	0·0015	0·0025	0·0040	0·0061	0·0091	0·0133	0·0190
41	0·0002	0·0005	0·0010	0·0018	0·0029	0·0045	0·0068	0·0101	0·0146
42	0·0001	0·0003	0·0007	0·0013	0·0021	0·0033	0·0051	0·0076	0·0111
43	0	0·0001	0·0004	0·0008	0·0015	0·0024	0·0038	0·0057	0·0084
44	0	0	0·0002	0·0005	0·0010	0·0017	0·0028	0·0043	0·0064
45	0	0	0·0001	0·0003	0·0007	0·0012	0·0020	0·0032	0·0048
46	0	0	0	0·0001	0·0004	0·0008	0·0014	0·0023	0·0036
47	0	0	0	0	0·0002	0·0005	0·0009	0·0016	0·0026
48	0	0	0	0	0·0001	0·0003	0·0006	0·0011	0·0019
49	0	0	0	0	0	0·0001	0·0003	0·0007	0·0013
50	0	0	0	0	0	0	0·0001	0·0004	0·0009
51	0	0	0	0	0	0	0	0·0002	0·0006
52	0	0	0	0	0	0	0	0·0001	0·0004
53	0	0	0	0	0	0	0	0	0·0002
54	0	0	0	0	0	0	0	0	0·0001
55	0	0	0	0	0	0	0	0	0
56	0	0	0	0	0	0	0	0	0
57	0	0	0	0	0	0	0	0	0
58	0	0	0	0	0	0	0	0	0
59	0	0	0	0	0	0	0	0	0
60	0	0	0	0	0	0	0	0	0
61									
62									
63									
64									
65									
66									
67									
68									
69									
70									
71									
72									
73									
74									
75									
76									
77									
78									
79									
80									

TABLE 2—*continued*

η	ξ 25·0	26·0	27·0	28·0	29·0	30·0	31·0	32·0	33·0
40	0·0265	0·0362	0·0484	0·0634	0·0815	0·1030	0·1279	0·1562	0·1878
41	0·0206	0·0284	0·0384	0·0509	0·0662	0·0846	0·1063	0·1313	0·1596
42	0·0159	0·0221	0·0303	0·0406	0·0534	0·0690	0·0877	0·1095	0·1346
43	0·0122	0·1072	0·0238	0·0322	0·0428	0·0559	0·0718	0·0907	0·1127
44	0·0093	0·0132	0·0185	0·0254	0·0341	0·0450	0·0584	0·0746	0·0937
45	0·0071	0·0102	0·0144	0·0199	0·0270	0·0360	0·0472	0·0609	0·0773
46	0·0054	0·0078	0·0111	0·0155	0·0213	0·0287	0·0380	0·0495	0·0634
47	0·0040	0·0059	0·0085	0·0120	0·0167	0·0227	0·0304	0·0400	0·0517
48	0·0029	0·0044	0·0065	0·0093	0·0130	0·0179	0·0242	0·0321	0·0419
49	0·0021	0·0033	0·0049	0·0071	0·0100	0·0140	0·0191	0·0256	0·0338
50	0·0015	0·0024	0·0037	0·0054	0·0077	0·0109	0·0150	0·0203	0·0271
51	0·0011	0·0018	0·0028	0·0041	0·0059	0·0084	0·0117	0·0160	0·0216
52	0·0008	0·0013	0·0021	0·0031	0·0045	0·0065	0·0091	0·0126	0·0171
53	0·0005	0·0009	0·0015	0·0023	0·0034	0·0050	0·0071	0·0099	0·0135
54	0·0003	0·0006	0·0011	0·0017	0·0026	0·0038	0·0055	0·0077	0·0106
55	0·0001	0·0003	0·0007	0·0012	0·0019	0·0029	0·0042	0·0060	0·0083
56	0	0·0001	0·0004	0·0008	0·0014	0·0022	0·0032	0·0046	0·0065
57	0	0	0·0002	0·0005	0·0009	0·0016	0·0024	0·0035	0·0050
58	0	0	0·0001	0·0003	0·0006	0·0011	0·0018	0·0027	0·0039
59	0	0	0	0·0001	0·0004	0·0007	0·0013	0·0020	0·0029
60	0	0	0	0	0·0002	0·0005	0·0009	0·0015	0·0022
61	0	0	0	0	0·0001	0·0003	0·0006	0·0011	0·0017
62	0	0	0	0	0	0·0001	0·0003	0·0007	0·0012
63	0	0	0	0	0	0	0·0002	0·0005	0·0009
64	0	0	0	0	0	0	0·0001	0·0003	0·0006
65	0	0	0	0	0	0	0	0·0001	0·0003
66	0	0	0	0	0	0	0	0	0·0001
67	0	0	0	0	0	0	0	0	0
68	0	0	0	0	0	0	0	0	0
69	0	0	0	0	0	0	0	0	0
70	0	0	0	0	0	0	0	0	0
71	0	0	0	0	0	0	0	0	0
72	0	0	0	0	0	0	0	0	0
73	0	0	0	0	0	0	0	0	0
74	0	0	0	0	0	0	0	0	0
75	0	0	0	0	0	0	0	0	0
76	0	0	0	0	0	0	0	0	0
77	0	0	0	0	0	0	0	0	0
78	0	0	0	0	0	0	0	0	0
79	0	0	0	0	0	0	0	0	0
80	0	0	0	0	0	0	0	0	0

TABLE 2—*continued*

η	ξ								
	34·0	35·0	36·0	37·0	38·0	39·0	40·0	41·0	42·0
40	0·2226	0·2603	0·3004	0·3425	0·3861	0·4306	0·4755	0·5201	0·5640
41	0·1911	0·2257	0·2631	0·3028	0·3445	0·3876	0·4316	0·4759	0·5200
42	0·1629	0·1943	0·2287	0·2658	0·3052	0·3464	0·3890	0·4325	0·4763
43	0·1378	0·1661	0·1974	0·2316	0·2684	0·3074	0·3482	0·3904	0·4333
44	0·1158	0·1410	0·1692	0·2004	0·2344	0·2709	0·3096	0·3500	0·3917
45	0·0966	0·1188	0·1440	0·1722	0·2033	0·2371	0·2734	0·3117	0·3517
46	0·0800	0·0994	0·1217	0·1469	0·1751	0·2061	0·2398	0·2758	0·3138
47	0·0659	0·0827	0·1022	0·1246	0·1499	0·1780	0·2089	0·2424	0·2781
48	0·0539	0·0683	0·0853	0·1049	0·1274	0·1527	0·1808	0·2116	0·2449
49	0·0439	0·0561	0·0707	0·0878	0·1076	0·1302	0·1555	0·1836	0·2143
50	0·0355	0·0458	0·0583	0·0731	0·0904	0·1103	0·1329	0·1583	0·1863
51	0·0286	0·0372	0·0478	0·0605	0·0755	0·0929	0·1129	0·1356	0·1610
52	0·0229	0·0301	0·0389	0·0497	0·0626	0·0778	0·0954	0·1155	0·1383
53	0·1082	0·0242	0·0316	0·0407	0·0517	0·0648	0·0801	0·0978	0·1181
54	0·0144	0·0193	0·0255	0·0331	0·0424	0·0536	0·0669	0·0824	0·1003
55	0·0114	0·0154	0·0205	0·0268	0·0346	0·0441	0·0555	0·0689	0·0846
56	0·0089	0·0122	0·0164	0·0216	0·0281	0·0361	0·0458	0·0574	0·0710
57	0·0069	0·0096	0·0130	0·0173	0·0227	0·0294	0·0376	0·0475	0·0593
58	0·0054	0·0075	0·0103	0·0138	0·0183	0·0239	0·0308	0·0392	0·0493
59	0·0042	0·0059	0·0081	0·0109	0·0146	0·0193	0·0251	0·0322	0·0408
60	0·0032	0·0046	0·0064	0·0087	0·0117	0·0155	0·0203	0·0263	0·0336
61	0·0025	0·0036	0·0050	0·0069	0·0093	0·0124	0·0164	0·0214	0·0275
62	0·0014	0·0025	0·0038	0·0054	0·0074	0·0099	0·0132	0·0173	0·0224
63	0·0012	0·0019	0·0029	0·0042	0·0058	0·0079	0·0106	0·0139	0·0182
64	0·0009	0·0014	0·0022	0·0032	0·0045	0·0062	0·0084	3·0112	0·0147
65	0·0006	0·0010	0·0016	0·0024	0·0035	0·0049	2·0067	0·0089	0·0118
66	0·0003	0·0007	0·0012	0·0018	0·0027	0·0038	0·0053	0·0071	0·0095
67	0·0001	0·0004	0·0008	0·0013	0·0020	0·0029	0·0041	0·0056	0·0076
68	0	0·0002	0·0005	0·0009	0·0015	0·0022	0·0032	0·0044	0·0060
69	0	0	0·0002	0·0005	0·0010	0·0016	0·0024	0·0034	0·0047
70	0	0	0·0001	0·0003	0·0007	0·0012	0·0018	0·0026	0·0037
71	0	0	0	0·0001	0·0004	0·0008	0·0013	0·0019	0·0028
72	0	0	0	0	0·0002	0·0005	0·0009	0·0014	0·0021
73	0	0	0	0	0·0001	0·0003	0·0006	0·0010	0·0016
74	0	0	0	0	0	0·0001	0·0003	0·0006	0·0011
75	0	0	0	0	0	0	0·0001	0·0003	0·0007
76	0	0	0	0	0	0	0	0·0001	0·0004
77	0	0	0	0	0	0	0	0	0·0002
78	0	0	0	0	0	0	0	0	0·0001
79	0	0	0	0	0	0	0	0	0
80	0	0	0	0	0	0	0	0	0

TABLE 2—*continued*

η	ξ								
	43·0	44·0	45·0	46·0	47·0	48·0	49·0	50·0	51·0
40	0·6066	0·6475	0·6863	0·7228	0·7567	0·7879	0·8164	0·8422	0·8653
41	0·5633	0·6054	0·6459	0·6844	0·7206	0·7543	0·7854	0·8138	0·8396
42	0·5198	0·5626	0·6043	0·6444	0·6825	0·7184	0·7519	0·7829	0·8113
43	0·4766	0·5196	0·5619	0·6032	0·6429	0·6807	0·7163	0·7496	0·7805
44	0·4342	0·4769	0·5194	0·5613	0·6021	0·6414	0·6789	0·7143	0·7474
45	0·3929	0·4349	0·4772	0·5193	0·5607	0·6011	0·6400	0·6772	0·7123
46	0·3534	0·3942	0·4357	0·4775	0·5191	0·5601	0·6000	0·6386	0·6755
47	0·3158	0·3550	0·3954	0·4365	0·4778	0·5189	0·5595	0·5991	0·6373
48	0·2804	0·3177	0·3566	0·3966	0·4372	0·4781	0·5188	0·5589	0·5981
49	0·2474	0·2826	0·3196	0·3581	0·3977	0·4379	0·4784	0·5187	0·5584
50	0·2169	0·2498	0·2847	0·3214	0·3596	0·3988	0·4386	0·4787	0·5186
51	0·1889	0·2194	0·2521	0·2868	0·3232	0·3610	0·3998	0·4393	0·4789
52	0·1636	0·1915	0·2218	0·2543	0·2888	0·3249	0·3624	0·4009	0·4399
53	0·1409	0·1662	0·1940	0·2242	0·2565	0·2907	0·3266	0·3638	0·4019
54	0·1206	0·1434	0·1687	0·1965	0·2265	0·2586	0·2926	0·3282	0·3651
55	0·1026	0·1230	0·1459	0·1712	0·1989	0·2288	0·2607	0·2945	0·3298
56	0·0868	0·1049	0·1254	0·1483	0·1736	0·2012	0·2309	0·2627	0·2963
57	0·0731	0·0890	0·1072	0·1278	0·1507	0·1759	0·2034	0·2331	0·2647
58	0·0612	0·0751	0·0912	0·1095	0·1302	0·1532	0·1783	0·2057	0·2352
59	0·0510	0·0631	0·0772	0·0933	0·1118	0·1325	0·1554	0·1806	0·2079
60	0·0423	0·0527	0·0649	0·0791	0·0955	0·1140	0·1347	0·1577	0·1828
61	0·0349	0·0438	0·0544	0·0668	0·0812	0·0976	0·1162	0·1369	0·1599
52	0·0287	0·0363	0·0454	0·0561	0·0687	0·0832	0·0997	0·1183	0·1391
63	0·0235	0·0299	0·0377	0·0469	0·0578	0·0705	0·0851	0·1017	0·1204
64	0·0191	0·0245	0·0311	0·0390	0·0484	0·0595	0·0723	0·0870	0·1037
65	0·0155	0·0200	0·0256	0·0323	0·0404	0·0499	0·0611	0·0741	0·0889
66	0·0125	0·0163	0·0209	0·0266	0·0335	0·0417	0·0514	0·0628	0·0759
67	0·0100	0·0132	0·0171	0·0219	0·0277	0·0347	0·0431	0·0529	0·0644
68	0·0080	0·0106	0·0139	0·0179	0·0228	0·0288	0·0359	0·0444	0·0544
69	0·0064	0·0085	0·0112	0·0146	0·0187	0·0238	0·0299	0·0372	0·0458
70	0·0051	0·0068	0·0090	0·0118	0·0153	0·0196	0·0248	0·0310	0·0384
71	0·0039	0·0054	0·0072	0·0095	0·0124	0·0160	0·0204	0·0257	0·0321
72	0·0030	0·0042	0·0057	0·0076	0·0100	0·0130	0·0167	0·0212	0·0267
73	0·0023	0·0033	0·0045	0·0061	0·0081	0·0106	0·0137	0·0175	0·0221
74	0·0017	0·0025	0·0035	0·0048	0·0065	0·0086	0·0112	0·0144	0·0183
75	0·0012	0·0019	0·0027	0·0038	0·0052	0·0069	0·0091	0·0118	0·0151
76	0·0008	0·0014	0·0021	0·0029	0·0041	0·0055	0·0073	0·0096	0·0123
77	0·0005	0·0009	0·0015	0·0022	0·0032	0·0044	0·0059	0·0078	0·0101
78	0·0003	0·0006	0·0010	0·0018	0·0025	0·0035	0·0047	0·0063	0·0082
79	0·0001	0·0003	0·0007	0·0013	0·0019	0·0027	0·0037	0·0050	0·0066
80	0	0·0001	0·0004	0·0008	0·0014	0·0021	0·0029	0·0039	0·0053

TABLE 2—*continued*

η	ξ 52·0	53·0	54·0	55·0	56·0	57·0	58·0	59·0	60·0
40	0·8858	0·9038	0·9195	0·9331	0·9448	0·9547	0·9631	0·9702	0·9761
41	0·8627	0·8838	0·9014	0·9173	0·9311	0·9429	0·9530	0·9616	9·9689
42	0·8370	0·8602	0·8808	0·8991	0·9151	0·9290	0·9410	0·9513	0·9601
43	0·8088	0·8345	0·8577	0·8784	0·8968	0·9129	0·9269	0·9391	0·9496
44	0·7781	0·8063	0·8320	0·8852	0·8760	0·8945	0·9107	0·9249	0·9373
45	0·7452	0·7758	0·8039	0·8296	0·8528	0·8737	0·8922	0·9086	0·9229
46	0·7104	0·7431	0·7735	0·8016	0·8272	0·8505	0·8714	0·8900	0·9065
47	0·6738	0·7085	0·7410	0·7713	0·7993	0·8249	9·8482	0·8691	0·8878
48	0·5359	0·6722	0·7066	0·7389	0·7691	0·7970	0·8226	0·8458	8·8668
49	0·5972	0·6347	0·6707	0·7048	0·7369	0·7669	0·7948	0·8203	0·8436
50	0·5579	0·5963	0·6335	0·6992	0·7031	0·7350	0·7649	0·7926	0·8181
51	0·5184	0·5574	0·5955	0·6324	0·6678	0·7014	0·7332	0·7629	0·7905
52	0·4792	0·5183	0·5569	0·5947	0·6313	0·6664	0·6998	0·7314	0·7609
53	0·4406	0·4795	0·5182	0·5565	0·5939	0·6302	0·6650	0·6982	0·7296
54	0·4029	0·4412	0·4797	0·5181	0·5560	0·5931	0·6291	0·6637	0·6967
55	0·3664	0·4038	0·4418	0·4799	0·5179	0·5555	0·5023	0·6280	0·6624
56	0·3314	0·3676	0·4047	0·4423	0·4801	0·5178	0·5551	0·5916	0·6270
57	0·2981	0·3328	0·3688	0·4056	0·4429	0·4804	0·5178	0·5547	0·5909
58	0·2667	0·2998	0·3343	0·3699	0·4064	0·4434	0·4806	0·5177	0·5543
59	0·2373	0·2686	0·3015	0·3357	0·3711	0·4073	0·4439	0·4808	0·5176
60	0·2101	0·2393	0·2704	0·3031	0·3371	0·3722	0·4081	0·4444	0·4810
61	0·1850	0·2122	0·2413	0·2722	0·3047	0·3385	0·3733	0·4089	0·4449
62	0·1621	0·1872	0·2142	0·2432	0·2739	0·3062	0·3398	0·3744	0·4097
63	0·1413	0·1643	0·1893	0·2163	0·2451	0·2757	0·3078	0·3411	0·3754
64	0·1225	0·1434	0·1664	0·1914	0·2183	0·2470	0·2774	0·3093	0·3424
65	0·1057	0·1246	0·1455	0·1685	0·1939	0·2205	0·2489	0·2791	0·3108
66	0·0908	0·1077	0·1266	0·1476	0·1708	0·1957	0·2223	0·2507	0·2808
67	0·0776	0·0927	0·1097	0·1287	0·1498	9·1728	0·1976	0·2242	0·2525
68	0·0660	0·0794	0·0946	0·1117	0·1308	0·1518	0·1747	0·1995	0·2260
69	0·0559	0·0677	0·0812	0·0965	0·1137	0·1328	0·1538	0·1767	0·2014
70	0·0472	0·0575	0·0694	0·0829	0·0983	0·1156	0·1347	0·1557	0·1786
71	0·0397	0·0486	0·0590	0·0709	0·0846	0·1001	0·1174	0·1366	0·1576
72	0·0332	0·0409	0·0500	0·0605	0·0726	0·0864	0·1019	0·1193	0·1385
73	0·0277	0·0343	0·0422	0·0514	0·0620	0·0742	0·0881	0·1037	0·1211
74	0·0230	0·0287	0·0355	0·0434	0·0527	0·0635	0·0758	0·0898	0·1055
75	0·0191	0·0239	0·0297	0·0366	0·0447	0·0541	0·0649	0·0774	0·0915
76	0·0157	0·0198	0·0248	0·0307	0·0377	0·0459	0·0554	0·0664	0·0789
77	0·0129	0·0164	0·0206	0·0257	0·0317	0·0388	0·0471	0·0568	0·0679
78	0·0106	0·0135	0·0171	0·0214	0·0266	0·0327	0·0399	0·0484	0·0582
79	0·0086	0·0110	0·0141	0·0178	0·0222	0·0275	0·0337	0·0411	0·0497
80	0·0069	0·0089	0·0115	0·0147	0·0185	0·0230	0·0284	0·0348	0·0423

TABLE 2—*continued*

η	ξ									
	61·0	62·0	63·0	64·0	65·0	66·0	67·0	68·0	69·0	70·0
40	0·9809	0·9849	0·9882	0·9908	0·9929	0·9946	0·9959	0·9970	0·9979	0·9985
41	0·9749	0·9799	0·9841	0·9875	0·9902	0·9924	0·9942	0·9956	0·9968	0·9977
42	0·9675	0·0737	0·9789	0·9832	0·9867	0·9896	0·9919	0·9938	0·9953	0·9965
43	0·9586	0·9662	0·9726	0·9779	0·9823	0·9859	0·9889	0·9914	0·9933	0·9949
44	0·9479	0·9571	0·9649	0·9714	0·9769	0·9814	0·9852	0·9883	0·9908	0·9929
45	0·9354	0·9463	0·9556	0·0635	0·9702	0·9758	0·9805	0·9844	0·9876	0·9903
46	0·9209	0·9336	0·9446	0·9541	0·9622	0·9690	0·9748	0·9796	0·9836	0·9869
47	0·9044	0·9109	0·9381	0·9429	0·9526	9·9608	0·9678	0·9737	0·9787	0·9828
48	0·8856	0·9023	0·9171	0·9300	0·9413	0·9511	0·9595	0·9666	0·9727	0·9778
49	0·8646	0·8835	0·9003	0·9152	0·9283	0·9397	0·9496	0·9581	0·9654	0·9716
50	0·8414	0·8625	0·8814	0·8983	0·9133	0·9265	0·9381	0·9481	0·9568	0·9642
51	0·8159	0·8392	0·8603	0·8793	0·8963	0·9114	0·9248	0·9365	0·9467	0·9555
52	0·7884	0·8138	0·8371	0·8582	0·8773	0·8944	0·9096	0·9231	0·9349	0·9452
53	0·7590	0·7864	0·8118	0·8350	0·8562	0·8753	0·8925	0·9078	0·9214	0·9333
54	0·7279	0·7572	0·7845	0·8098	0·8330	0·8542	0·8734	0·8906	0·9060	0·9197
55	0·6952	0·7262	0·7554	0·7826	0·8078	0·8310	0·8522	0·8714	0·8887	0·9042
56	0·6611	0·6937	0·7246	0·7536	0·7807	0·8059	0·8291	0·8503	0·8695	0·8869
57	0·6260	0·6599	0·6923	0·7229	0·7518	0·7789	0·8040	0·8272	0·8484	0·8677
58	0·5902	0·6251	0·6587	0·6908	0·7213	0·7501	0·7771	0·8022	0·8253	0·8465
59	0·5539	0·5895	0·6241	0·6575	0·6894	0·7198	0·7485	0·7754	0·8004	0·8235
60	0·5175	0·5535	0·5888	0·6232	0·6563	0·6881	0·7183	0·7468	0·7736	0·7986
61	0·4812	0·5174	0·5531	0·5882	0·6223	0·6552	0·6868	0·7168	0·7452	0·7719
62	0·4455	0·4815	0·5173	0·5528	0·5876	0·6214	0·6541	0·6855	0·7154	0·7437
63	0·4105	0·4460	0·4817	0·5173	0·5525	0·5869	0·6205	0·6530	0·6842	0·7139
64	0·3765	0·4113	0·4465	0·4819	0·5172	0·5521	0·5863	0·6197	0·6519	0·6829
65	0·3437	0·3775	0·4120	0·4469	0·4821	0·5171	0·5517	0·5857	0·6188	0·6509
66	0·3123	0·3449	0·3785	0·4127	0·4474	0·4823	0·5170	0·5514	0·5851	0·6180
67	0·2824	0·3137	0·3461	0·3794	0·4134	0·4478	0·4824	0·5169	0·5510	0·5845
68	0·2542	0·2839	0·3150	0·3472	0·3803	0·4141	0·4483	0·4826	0·5168	0·5507
69	0·2278	0·2559	0·2855	0·3164	0·3484	0·3813	0·4148	0·4487	0·4828	0·5168
70	0·2032	0·2296	0·2576	0·2870	0·3177	0·3495	0·3822	0·4155	0·4492	0·4830
71	0·1804	0·2050	0·2313	0·2592	0·2885	0·3195	0·3509	0·3832	0·4162	0·4496
72	0·1595	0·1823	0·2068	0·2330	0·2608	0·2902	0·3206	0·3519	0·3841	0·4169
73	0·1403	0·1613	0·1841	0·2086	0·2347	0·2625	0·2916	0·3218	0·3529	0·3849
74	0·1229	0·1421	0·1631	0·1859	0·2103	0·2364	0·2640	0·2929	0·3229	0·3539
75	0·1072	0·1247	0·1439	0·1649	0·1876	0·2120	0·2380	0·2655	0·2942	0·3241
76	0·0931	0·1089	0·1264	0·1457	0·1667	0·1894	0·2137	0·2396	0·2669	0·2955
77	0·0805	0·0947	0·1106	0·1282	0·1475	0·1685	0·1911	0·2154	0·2412	0·2684
78	0·0694	0·0821	0·0964	0·1123	0·1299	0·1492	0·1702	0·1928	0·2170	0·2427
79	0·0596	0·0709	0·0837	0·0980	0·1139	0·1316	0·1509	0·1719	0·1944	0·2186
80	0·0509	0·0609	0·0723	0·0852	0·0996	0·1156	0·1333	0·1526	0·1735	0·1961

TABLE 2—*continued*

η	ξ									
	71·0	72·0	73·0	74·0	75·0	76·0	77·0	78·0	79·0	80·0
40	0·9989	0·9993	0·9996	0·9998	0·9999	1·0	1·0	1·0	1·0	1·0
41	0·9983	0·9988	0·9992	0·9995	0·9997	0·9999	1·0	1·0	1·0	1·0
42	0·9974	0·9981	0·9987	0·9991	0·9994	0·9997	0·9999	1·0	1·0	1·0
43	0·9962	0·9972	0·9979	0·9985	0·9989	0·9993	0·9996	0·9998	0·9999	1·0
44	0·9946	0·9959	0·9969	0·9977	0·9983	0·9987	0·9992	0·9995	0·9997	0·9999
45	0·9925	0·9942	0·9956	0·9967	0·9975	0·9981	0·9987	0·9991	0·9994	0·9997
46	0·9897	0·9919	0·9938	0·9953	0·9964	0·9973	0·9980	0·9986	0·9990	0·9994
47	0·9863	0·9891	0·9915	0·9934	0·9949	0·9961	0·9971	0·9978	0·9984	0·9989
48	0·9821	0·9856	0·9886	0·9910	0·9929	0·9945	0·9958	0·9968	0·9976	0·9983
49	0·9769	0·9813	0·9849	0·9879	0·9904	0·9925	0·9942	0·9955	0·9966	0·9975
50	0·9706	0·9759	0·9804	0·9842	0·9873	0·9899	0·9921	0·9938	0·9952	0·9964
51	0·9631	0·9695	0·9749	0·9796	0·9835	0·9867	0·9894	0·9916	0·9934	0·9949
52	0·9542	0·9618	0·9684	0·9740	0·9788	0·9828	0·9861	0·9889	0·9912	0·9931
53	0·9438	0·9528	0·9606	0·9673	0·9731	0·9779	0·9820	0·9855	0·9884	0·9908
54	0·9318	0·9423	0·9515	0·9594	0·9663	0·9721	0·9771	0·9813	0·9849	0·9878
55	0·9180	0·9302	0·9409	0·9502	0·9583	0·9652	0·9712	0·9763	0·9806	0·9842
56	0·9025	0·9164	0·9287	0·9395	0·9489	0·9571	0·9642	0·9703	0·9755	0·9799
57	0·8851	0·9008	0·9148	0·9272	0·9381	0·9476	0·9559	0·9631	0·9693	0·9746
58	0·8658	0·8833	0·8991	0·9132	0·9257	0·9367	0·9463	0·9547	0·9620	0·9683
59	0·8447	0·8640	0·8816	0·8974	0·9116	0·9242	0·9353	0·9450	0·9535	0·9609
60	0·8217	0·8429	0·8623	0·8798	0·8957	0·9099	0·9226	0·9338	0·9437	0·9523
61	0·7968	0·8199	0·8411	0·8605	0·8781	0·8940	0·9083	0·9211	0·9324	0·9424
62	0·7703	0·7901	0·8156	0·8381	0·8581	0·8761	0·8922	0·9067	0·9196	0·9310
63	0·7421	0·7661	0·7909	0·8145	0·8363	0·8562	0·8742	0·8905	0·9051	0·9181
64	0·7120	0·7391	0·7650	0·7898	0·8131	0·8347	0·8545	0·9725	0·8888	0·9035
65	0·6815	0·7103	0·7377	0·7638	0·7885	0·8116	0·8331	0·8528	0·8708	0·8872
66	0·6498	0·6800	0·7089	0·7364	0·7625	0·7871	0·8101	0·8315	0·8512	0·8692
67	0·6172	0·6486	0·6788	0·7076	0·7351	0·7611	0·7856	0·8086	0·8299	0·8496
68	0·5839	0·6163	0·6476	0·6776	0·7064	0·7338	0·7597	0·7842	0·8071	0·8284
69	0·5454	0·5809	0·6143	0·6459	0·6762	0·7050	0·7324	0·7583	0·7827	0·8056
70	0·5142	0·5476	0·5809	0·6134	0·6448	0·6749	0·7037	0·7310	0·7568	0·7812
71	0·4819	0·5148	0·5479	0·5807	0·6128	0·6439	0·6738	0·7024	0·7296	0·7554
72	0·4494	0·4821	0·5150	0·5479	0·5803	0·6121	0·6429	0·6727	0·7012	0·7823
73	0·4172	0·4497	0·4823	0·5151	0·5477	0·5799	0·6114	0·6421	0·6717	0·7000
74	0·3856	0·4177	0·4500	0·4826	0·5152	0·5476	0·5795	0·6108	0·6413	0·6707
75	0·3548	0·3863	0·4182	0·4504	0·4828	0·5152	0·5474	0·5791	0·6102	0·6405
76	0·3252	0·3558	0·3870	0·4187	0·4508	0·4830	0·5152	0·5472	0·5787	0·6096
77	0·2968	0·3263	0·3567	0·3877	0·4193	0·4512	0·4832	0·5152	0·5469	0·5783
78	0·2698	0·2981	0·3274	0·3576	0·3885	0·4199	0·4516	0·4834	0·5152	0·5468
79	0·2442	0·2712	0·2993	0·3285	0·3585	0·3892	0·4204	0·4519	0·4836	0·5152
80	0·2202	0·2457	0·2725	0·3005	0·3295	0·3594	0·3899	0·4209	0·4523	0·4838

TABLE 3

Flat Pole Functions. Width 1

η	Δ_{y1}	Δ_{y2}	Δ_{y3}	Δ_{y4}	Δ_{y5}	Δ_{y6}	Δ_{y7}	Δ_{y8}	Δ_{y9}	Δ_{y10}	Δ_{y11}	Δ_{y12}	Δ_{y13}
1·5	0·3746	0·2434	0·1586	0·0976	0·0572	0·0318	0·0175	0·0039	0·0050	0·0025	0·0013	0·0006	0·0003
1·75	0·3178	0·2427	0·1711	0·1108	0·0680	0·0399	0·0226	0·0127	0·0070	0·0035	0·0019	0·0009	0·0005
2·0	0·2674	0·2365	0·1791	0·1231	0·0794	0·0488	0·0288	0·0165	0·0096	0·0050	0·0029	0·0014	0·0008
2·5	0·1898	0·2148	0·1853	0·1413	0·0993	0·0661	0·0420	0·0260	0·0153	0·0089	0·0051	0·0029	0·0015
3·0	0·1342	0·1867	0·1807	0·1516	0·1155	0·0822	0·0558	0·0365	0·0231	0·0142	0·0083	0·0048	0·0028
3·5	0·0942	0·1569	0·1697	0·1549	0·1269	0·0967	0·0693	0·0478	0·0330	0·0182	0·0136	0·0077	0·0047
4·0	0·0659	0·1287	0·1542	0·1521	0·1336	0·1080	0·0820	0·0594	0·0415	0·0275	0·0180	0·0114	0·0071
4·5	0·0460	0·1037	0·1366	0·1454	0·1358	0·1161	0·0927	0·0702	0·0508	0·0356	0·0242	0·0160	0·0103
5·0	0·0320	0·0822	0·1182	0·1350	0·1340	0·1208	0·1014	0·0801	0·0607	0·0441	0·0311	0·0213	0·0142
6·0	0·0154	0·0496	0·0841	0·1095	0·1216	0·1211	0·1111	0·0955	0·0782	0·0612	0·0461	0·0338	0·0240
7·0	0·0073	0·0288	0·0567	0·0831	0·1023	0·1116	0·1113	0·1034	0·0907	0·0759	0·0611	0·0475	0·0357
7·5	0·0050	0·0218	0·0457	0·0710	0·0917	0·1045	0·1082	0·1044	0·0946	0·0819	0·0679	0·0542	0·0419
8·0	0·0034	0·0163	0·0366	0·0599	0·0813	0·0963	0·1037	0·1034	0·0972	0·0865	0·0737	0·0606	0·0483
9·0	0·0016	0·0090	0·0228	0·0415	0·0614	0·0788	0·0913	0·0973	0·0971	0·0919	0·0828	0·0716	0·0600
10·0	0·0007	0·0051	0·0140	0·0277	0·0444	0·0617	0·0761	0·0872	0·0919	0·0918	0·0875	0·0793	0·0697

η	Δ_{y14}	Δ_{y15}	Δ_{y16}	Δ_{y17}	Δ_{y18}	Δ_{y19}	Δ_{y20}	Δ_{y21}	Δ_{y22}	Δ_{y23}	Δ_{y24}	Δ_{y25}
1·5	0·0002	0·0001	0									
1·75	0·0003	0·0002	0·0001	0								
2·0	0·0004	0·0002	0·0001	0·0001	0							
2·5	0·0009	0·0005	0·0002	0·0002	0							
3·0	0·0016	0·0009	0·0005	0·0003	0·0002	0						
3·5	0·0028	0·0016	0·0010	0·0005	0·0002	0·0002	0·0001	0				
4·0	0·0044	0·0026	0·0015	0·0009	0·0005	0·0003	0·0002	0·0001	0·0001	0		
4·5	0·0065	0·0041	0·0025	0·0015	0·0010	0·0005	0·0003	0·0002	0·0001	0·0001	0	
5·0	0·0092	0·0060	0·0037	0·0023	0·0015	0·0009	0·0005	0·0004	0·0002	0·0001	0	
6·0	0·0166	0·0114	0·0075	0·0049	0·0032	0·0020	0·0013	0·0008	0·0006	0·0004	0·0002	0·0001
7·0	0·0262	0·0188	0·0132	0·0090	0·0061	0·0041	0·0027	0·0016	0·0011	0·0008	0·0005	0·0003
7·5	0·0316	0·0232	0·0166	0·0118	0·0081	0·0055	0·0037	0·0023	0·0016	0·0011	0·0007	0·0004
8·0	0·0371	0·0280	0·0206	0·0419	0·0104	0·0073	0·0050	0·0034	0·0022	0·0015	0·0009	0·0006
9·0	0·0486	0·0383	0·0294	0·0222	0·0163	0·0118	0·0085	0·0058	0·0036	0·0025	0·0017	0·0013
10·0	0·0591	0·0487	0·0393	0·0305	0·0235	0·0177	0·0130	0·0093	0·0063	0·0043	0·0028	0·0021

η	Δ_{y26}	Δ_{y27}	Δ_{y28}	Δ_{y29}	Δ_{y30}	Δ_{y31}	Δ_{y32}	Δ_{y33}	Δ_{y34}	Δ_{y35}	Δ_{y36}	Δ_{y37}
1·5												
1·75												
2·0												
2·5												
3·0												
3·5												
4·0												
4·5												
5·0												
6·0												
7·0	0·0002	0·0001	0									
7·5	0·0003	0·0002	0·0001	0·00005	0							
8·0	0·0004	0·0003	0·0002	0·0001	0							
9·0	0·0009	0·0007	0·0005	0·0004	0·0003	0·0001	0·0001	0				
10·0	0·0015	0·0011	0·0009	0·00075	0·0006	0·00045	0·00035	0·00025	0·0002	0·0001	0·0001	0

TABLE 4

Heat Pole Functions. Width 2

η	Δ_{y1}	Δ_{y2}	Δ_{y3}	Δ_{y4}	Δ_{y5}	Δ_{y6}	Δ_{y7}	Δ_{y8}	Δ_{y9}
1·5	0·4963	0·3291	0·1219	0·0381	0·0109	0·0028	0·0007	0·0002	0·0001
1·75	0·4392	0·3478	0·1434	0·0489	0·0150	0·0041	0·0011	0·0004	0
2·0	0·3857	0·3589	0·1653	0·0615	0·0203	0·0061	0·0016	0·0005	0·0001
2·5	0·2972	0·3634	0·2030	0·0880	0·0327	0·0109	0·0034	0·0010	0·0003
3·0	0·2276	0·3498	0·2324	0·1152	0·0484	0·0178	0·0060	0·0020	0·0006
3·5	0·1727	0·3256	0·2526	0·1416	0·0660	0·0266	0·0099	0·0034	0·0011
4·0	0·1303	0·2946	0·2636	0·1657	0·0850	0·0734	0·0150	0·0056	0·0019
4·5	0·0978	0·2612	0·2666	0·1858	0·1037	0·0050	0·0215	0·0086	0·0032
5·0	0·0731	0·2268	0·2620	0·2069	0·1178	0·0612	0·0320	0·0124	0·0050
6·0	0·0402	0·1637	0·2369	0·2194	0·1565	0·0936	0·0492	0·0234	0·0103
7·0	0·0217	0·1127	0·1996	0·2188	0·1804	0·1227	0·0726	0·0385	0·0187
7·5	0·0159	0·0921	0·1795	0·2126	0·1878	0·1359	0·0848	0·0473	0·0241
8·0	0·0116	0·0747	0·1594	0·2035	0·1922	0·1472	0·0972	0·0568	0·0304
9·0	0·0061	0·0481	0·1215	0·1794	0·1917	0·1645	0·1201	0·0773	0·0451
10·0	0·0032	0·0281	0·0891	0·1506	0·1814	0·1731	0·1388	0·1029	0·0570

η	Δ_{y10}	Δ_{y11}	Δ_{y12}	Δ_{y13}	Δ_{y14}	Δ_{y15}	Δ_{y16}	Δ_{y17}	Δ_{y18}	Δ_{y19}
1·5										
1·75										
2·0										
2·5	0·0001	0								
3·0	0·0001	0·00005	0·00001	0						
3·5	0·0004	0·0001	0							
4·0	0·0006	0·0003	0							
4·5	0·0011	0·0004	0·0002	0						
5·0	0·0019	0·0007	0·0002	0						
6·0	0·0042	0·0017	0·0007	0·0002	0					
7·0	0·0085	0·0035	0·0016	0·0006	0·0002	0				
7·5	0·0115	0·0049	0·0023	0·0008	0·0004	0·0001				
8·0	0·0150	0·0070	0·0031	0·0012	0·0006	0·0002	0			
9·0	0·0241	0·0119	0·0051	0·0027	0·0013	0·0008	0·0003	0·00005	0	
10·0	0·0359	0·0190	0·0088	0·0043	0·0023	0·0015	0·00095	0·0005	0·00025	0·00005

TABLE 5

Heat Pole Functions. Width 3

η	Δ_{y1}	Δ_{y2}	Δ_{y3}	Δ_{y4}	Δ_{y5}	Δ_{y6}	Δ_{y7}	Δ_{y8}	Δ_{y9}	Δ_{y10}	Δ_{y11}	Δ_{y12}	Δ_{y13}	Δ_{y14}
1·5	0·5897	0·3332	0·0658	0·0099	0·0012	0·00016	0·00001	0						
1·75	0·5366	0·3644	0·0827	0·01397	0·0020	0·00027	0·00003	0						
2·0	0·4848	0·3905	0·1020	0·0193	0·0029	0·00044	0·00006	0						
2·5	0·3948	0·4246	0·1416	0·0254	0·0125	0·0009	0							
3·0	0·3189	0·4387	0·1181	0·0489	0·0102	0·0019	0·00025	0·00005	0					
3·5	0·2553	0·4372	0·2190	0·0677	0·0168	0·00335	0·00059	0·00001	0					
4·0	0·2031	0·4228	0·2520	0·0908	0·0245	0·0054	0·0011	0·0003	0					
4·5	0·1607	0·4002	0·2791	0·1144	0·0346	0·0087	0·0019	0·00037	0·00003	0				
5·0	0·1262	0·3708	0·3003	0·1375	0·0485	0·0128	0·0032	0·0007	0·00007	0				
6·0	0·0765	0·3035	0·3221	0·1872	0·0768	0·0249	0·0069	0·0018	0·0003	0				
7·0	0·0454	0·2359	0·3190	0·2274	0·1114	0·0425	0·0135	0·0038	0·00098	0·00012	0			
7·5	0·0348	0·2047	0·3095	0·2451	0·1275	0·0532	0·0180	0·0054	0·0014	0·00038	0			
8·0	0·0265	0·1760	0·2963	0·2551	0·1474	0·0650	0·0237	0·0074	0·0020	0·00057	0			
9·0	0·0152	0·1269	0·2615	0·2682	0·1805	0·0913	0·0377	0·0125	0·0041	0·0016	0·00047	0·00003	0	
10·0	0·0088	0·0889	0·2208	0·2669	0·2073	0·1197	0·0553	0·0206	0·0068	0·0028	0·0014	0·00058	0·00010	0

TABLE 6

Heat Pole Functions. Width 4

η	Δ_{y1}	Δ_{y2}	Δ_{y3}	Δ_{y4}	Δ_{y5}	Δ_{y6}	Δ_{y7}	Δ_{y8}	Δ_{y9}	Δ_{y10}	Δ_{y11}
1·5	0·6609	0·3055	0·0313	0·00217	0·00013	0					
1·75	0·6131	0·3417	0·0416	0·00336	0·00023	0					
2·0	0·5651	0·3755	0·0541	0·0049	0·00038	0·00002	0				
2·5	0·4789	0·4287	0·0822	0·0093	0·00085	0·00005	0				
3·0	0·4025	0·4649	0·1149	0·0159	0·00167	0·00013	0				
3·5	0·3355	0·4682	0·1501	0·0249	0·00298	0·00032	0				
4·0	0·2776	0·4938	0·1865	0·0365	0·0050	0·00057	0·00003	0			
4·5	0·2284	0·4901	0·2216	0·0508	0·0080	0·00103	0·00007	0			
5·0	0·1865	0·4789	0·2518	0·0688	0·0122	0·00167	0·00013	0			
6·0	0·1220	0·4285	0·3130	0·1077	0·0241	0·0042	0·0005	0			
7·0	0·0780	0·3654	0·3512	0·1519	0·0434	0·00855	0·00145	0·0001	0		
7·5	0·0620	0·3318	0·3620	0·1765	0·0535	0·0117	0·0022	0·0003	0		
8·0	0·0489	0·2985	0·3676	0·1992	0·0663	0·0160	0·0030	0·0005	0		
9·0	0·0301	0·2353	0·3636	0·2411	0·0958	0·0265	0·0065	0·00108	0·00002	0	
10·0	0·0184	0·1676	0·3532	0·2768	0·1265	0·0413	0·0098	0·00313	0·0011	0·0017	0

TABLE 7

Heat Pole Functions. Width 5

η	Δ_{y1}	Δ_{y2}	Δ_{y3}	Δ_{y4}	Δ_{y5}	Δ_{y6}	Δ_{y7}	Δ_{y8}	Δ_{y9}
1·5	0·7150	0·2703	0·0142	0·00045	0·00001	0			
1·75	0·6725	0·3070	0·0197	0·00079	0				
2·0	0·6292	0·3429	0·0267	0·00117	0·00003	0			
2·5	0·5492	0·4045	0·0437	0·0025	0·0001	0			
3·0	0·4757	0·4518	0·0676	0·00468	0·00022	0			
3·5	0·4089	0·4914	0·0913	0·0079	0·00049	0			
4·0	0·3489	0·5169	0·1208	0·0125	0·00088	0			
4·5	0·2962	0·5311	0·1522	0·0189	0·00154	0·00006	0		
5·0	0·2495	0·5351	0·1855	0·0272	0·00259	0·00011	0		
6·0	0·1737	0·5173	0·2528	0·0498	0·0060	0·0004	0		
7·0	0·1181	0·4742	0·3136	0·0807	0·0121	0·00128	0		
7·5	0·0966	0·4465	0·3394	0·0989	0·0165	0·0020	0·0001	0	
8·0	0·0786	0·4164	0·3612	0·1188	0·0220	0·0028	0·0002	0	
9·0	0·0514	0·3523	0·3922	0·1615	0·0359	0·00575	0·00093	0·00002	0
10·0	0·0331	0·2888	0·4048	0·2057	0·0550	0·0096	0·0025	0·00047	0

TABLE 8

Efficiency of a Balanced Regenerator

Results obtained from solutions by Mallock machine

Non-Dim. Time Π	Non-dimensional length Λ															
	5		6		8		10		12		16		20		32	
	η_{reg}	$\eta_{rec}-\eta_{reg}$	η_{reg}	$\eta_{rec}-\eta_{reg}$	η_{reg}	$\eta_{rec}-\eta_{reg}$	η_{reg}	$\eta_{rec}-\eta_{reg}$	η_{reg}	$\eta_{rec}-\eta_{reg}$	η_{reg}	$\eta_{rec}-\eta_{reg}$	η_{reg}	$\eta_{rec}-\eta_{reg}$	η_{reg}	$\eta_{rec}-\eta_{reg}$
1·0	0·690	0·024	0·716	0·034	0·774	0·026	0·752	0·081	0·752	0·105	—	—	—	—	—	—
1·5	0·691	0·023	0·728	0·022	—	—	—	—	—	—	—	—	—	—	—	—
2·0	0·690	0·024	0·728	0·022	0·783	0·017	0·792	0·041	0·810	0·047	—	—	0·768	0·141	—	—
3·0	0·680	0·034	0·723	0·027	—	—	0·807	0·026	—	—	0·867	0·022	—	—	—	—
4·0	0·662	0·052	0·708	0·042	0·773	0·027	0·809	0·024	0·838	0·019	0·874	0·015	0·870	0·039	0·878	0·063
5·0	0·638	0·076	0·689	0·061	—	—	0·803	0·030	0·832	0·025	0·873	0·016	—	—	—	—
6·0	0·609	0·105	0·665	0·085	0·746	0·054	0·795	0·038	0·828	0·029	0·871	0·018	0·890	0·019	0·924	0·017
7·0	—	—	0·639	0·111	—	—	0·786	0·047	0·821	0·036	0·869	0·020	—	—	—	—
7·5	—	—	0·625	0·125	—	—	—	—	—	—	—	—	—	—	—	—
8·0	0·540	0·174	0·618	0·132	0·707	0·093	0·769	0·064	0·813	0·044	0·864	0·025	0·890	0·019	0·929	0·012
9·0	—	—	0·576	0·174	—	—	0·757	0·076	0·798	0·059	0·859	0·030	—	—	—	—
10·0	0·469	0·0245	0·542	0·208	0·657	0·143	0·739	0·094	0·790	0·067	0·851	0·038	0·882	0·027	0·928	0·013
.0	0·7143		0·7500		0·8000		0·8333		0·8571		0·8889		0·9091		0·9412	

TABLE 9

Efficiency of a Balanced Regenerator

Results obtained from solution of five equations

Heat pole width	Non-dim. Length Λ	Non-dim. Time Π	Regenerator Efficiency η_{reg}	Difference $\eta_{rec}-\eta_{reg}$	Error from curves
		1·5	0·6997	0·0146	−0·0003
1	5	5	0·6366	0·0777	+0·0006
		7	0·5741	0·1402	−0·0030
		9	0·5037	0·2106	+0·0037
2	10	5	0·7996	0·0337	−0·0044
		10	0·7379	0·0954	+0·0019
		5	0·8566	0·0257	−0·0104
		6	0·8544	0·0279	−0·0076
		7	0·8511	0·0312	−0·0060
3	15	8	0·8647	0·0356	−0·0043
		9	0·8411	0·0412	−0·0029
		10	0·8343	0·0480	−0·0027
		7	0·8826	0·0265	−0·0104
4	20	9	0·8790	0·0301	−0·0080
		10	0·8835	0·0256	+0·0050
		8	0·8993	0·0266	−0·0147
5	25	9	0·8991	0·0268	−0·0119
		10	0·8984	0·0275	−0·0106

TABLE 10

Recommended Values of Efficiency of Balanced Regenerators

Non-dim. Length Λ	Non-dimensional blow Time Π										
	0	1	2	3	4	5	6	7	8	9	10
5	0·714	0·705	0·694	0·680	0·660	0·636	0·509	0·577	0·540	0·500	0·458
6	0·750	0·743	0·734	0·723	0·707	0·688	0·666	0·641	0·613	0·579	0·541
7	0·778	0·773	0·765	0·755	0·743	0·727	0·709	0·690	0·668	0·643	0·618
8	0·800	0·796	0·789	0·781	0·771	0·759	0·744	0·728	0·710	0·688	0·664
9	0·818	0·815	0·809	0·802	0·793	0·783	0·771	0·758	0·743	0·724	0·701
10	0·833	0·831	0·826	0·820	0·812	0·804	0·794	0·783	0·770	0·755	0·736
11	0·846	0·844	0·840	0·835	0·829	0·821	0·813	0·804	0·793	0·779	0·765
12	0·857	0·856	0·852	0·848	0·842	0·836	0·828	0·821	0·811	0·800	0·788
13	0·867	0·866	0·863	0·859	0·854	0·849	0·842	0·835	0·827	0·188	0·808
14	0·875	0·874	0·872	0·868	0·864	0·859	0·853	0·847	0·840	0·832	0·824
15	0·882	0·882	0·879	0·876	0·872	0·867	0·862	0·857	0·851	0·844	0·837
16	0·889	0·889	0·887	0·884	0·880	0·876	0·872	0·867	0·862	0·855	0·849
17	0·895	0·895	0·893	0·890	0·887	0·883	0·879	0·874	0·870	0·865	0·859
18	0·900	0·900	0·898	0·896	0·893	0·889	0·886	0·882	0·877	0·873	0·868
19	0·905	0·905	0·903	0·901	0·899	0·896	0·892	0·888	0·885	0·880	0·876
20	0·909	0·909	0·907	0·906	0·903	0·901	0·897	0·894	0·891	0·887	0·883
22	0·917	0·917	0·916	0·914	0·912	0·910	0·907	0·905	0·902	0·899	0·895
24	0·923	0·923	0·922	0·921	0·919	0·917	0·915	0·913	0·910	0·907	0·904
26	0·929	0·929	0·929	0·928	0·926	0·924	0·922	0·920	0·918	0·915	0·913
28	0·933	0·933	0·933	0·932	0·931	0·929	0·928	0·926	0·924	0·921	0·919
30	0·938	0·938	0·938	0·938	0·936	0·936	0·934	0·932	0·930	0·928	0·926
35	0·946	0·946	0·946	0·946	0·945	0·944	0·943	0·942	0·941	0·939	0·937
40	0·952	0·952	0·952	0·952	0·952	0·951	0·951	0·950	0·949	0·947	0·946

TABLE 11

Efficiency of Unbalanced Regenerators

Ratio	Non-dim. Length	Non-dim. Blow Time	Regenerator Efficiencies							
			Air side	Gas side	Mean	Calc. from heat poles	Estimated True value	Corr. factor	By Hausen Method	Corr. factor
$\frac{\Lambda_g}{\Lambda_a}$	Λ_a	Π_a	η_a	η_g	η_m	$\eta_{calc.}$	η_T	$\eta_m - \eta_T$	η_H	$\eta_H - \eta_T$
2	5	1·5	0·700	0·820	0·760	0·750	0·753	0·007	0·775	0·022
		1·75	0·697	0·916	0·756	0·747	0·750	0·006	0·772	0·022
		2·0	0·694	0·812	0·753	0·747	0·749	0·004	0·762	0·013
		2·5	0·687	0·804	0·746	0·740	0·742	0·004	0·760	0·018
		3	0·680	0·794	0·737	0·732	0·734	0·003	0·751	0·017
		4	0·660	0·770	0·715	0·711	0·7115	0·0035	0·727	0·0155
		5	0·636	0·736	0·686	0·682	0·681	0·005	0·700	0·019
2	10	3	0·820	0·897	0·858	0·845	0·853	0·005	0·870	0·017
		4	0·812	0·891	0·852	0·843	0·851	0·001	0·862	0·011
		5	0·804	0·883	0·844	0·839	0·841	0·003	0·854	0·013
3	5	1·5	0·700	0·870	0·785	0·770	0·776	0·009	0·820	0·044
		2·0	0·694	0·862	0·778	0·766	0·770	0·008	0·812	0·042
		2·5	0·687	0·854	0·770	0·760	0·762	0·008	0·804	0·042
		3·0	0·680	0·844	0·762	0·752	0·753	0·009	0·794	0·041
4	5	1·5	0·700	0·897	0·799	0·780	0·786	0·013	0·849	0·063
		1·75	0·697	0·894	0·796	0·777	0·782	0·014	0·846	0·064
		2·0	0·694	0·891	0·793	0·776	0·781	0·012	0·842	0·061
		2·5	0·687	0·883	0·785	0·773	0·773	0·012	0·834	0·061
5	5	1·5	0·700	0·915	0·808	0·787	0·795	0·013	0·870	0·075
		2·0	0·694	0·909	0·802	0·783	0·788	0·014	0·862	0·074

TABLE 13

Experimental Results

Matrix Type	Expt. No.	Mass flow W lb/sec	Mass Velocity $G = \frac{W}{A}$	Mass Velocity $G_{\max} = \frac{W}{A_t}$	Reynolds No. (Hydraulic) $R = \frac{G_{\max} d}{\mu}$	Reynolds No. (diameter) $R_d = \frac{G_{\max} D}{\mu}$	Reynolds No. (perimeter) $R_p = \frac{G_{\max} \pi D}{\mu}$	Heat Transfer Coefficient α CHU/sec/ft^2 °C	Heat Transfer Coefficient $k_h = \frac{\alpha}{G_{\max} c_p}$	Nusselt No. $N_u = \frac{\alpha D}{k}$	Press drop Δp in. H_2O	Half friction $\frac{c_f}{2}$	Heat transfer efficiency $k_H/(c_f/2)$
100 × 30 × 0·0105	52	0·0127	0·248	0·528	43·5	24·7	77·6	0·00884	0·0691	1·228	3·10	0·192	0·360
	53	0·0165	0·322	0·687	56·3	32·0	100·5	0·01160	0·0699	1·601	4·37	0·171	0·408
	54	0·0195	0·381	0·812	65·0	36·9	116·2	0·01118	0·0569	1·508	5·61	0·162	0·351
	55	0·0220	0·430	0·916	74·0	42·0	132·2	0·01313	0·0592	1·777	6·76	0·150	0·395
98 × 40 × 0·0045	62	0·0103	0·200	0·298	33·3	6·01	18·9	0·0105	0·1474	0·625	1·31	0·623	0·237
	66	0·0240	0·468	0·697	76·1	13·7	43·1	0·0155	0·0925	0·894	3·93	0·326	0·284
	63	0·0335	0·654	0·974	104·3	18·8	59·0	0·0183	0·0784	1·035	6·45	0·270	0·290
	67	0·0462	0·902	1·343	144·1	26·0	81·6	0·0192	0·0595	1·091	10·6	0·231	0·257
	68	0·0739	1·443	2·149	237·1	42·8	134·3	0·0264	0·0512	1·525	21·5	0·195	0·262
	65	0·0911	1·779	2·648	302·0	49·3	155·0	0·0305	0·0480	1·658	27·1	0·153	0·315
150 × 30 × 0·0105	69	0·0191	0·373	0·796	64·9	36·8	116·0	0·0115	0·0602	1·613	5·05	0·0876	0·687
	70	0·0217	0·424	0·904	71·8	40·8	128·2	0·0108	0·0495	1·470	9·4	0·1205	0·411
	71	0·0299	0·584	1·246	96·2	54·6	171·8	0·0145	0·0485	1·917	14·3	0·0923	0·526
	72	0·0400	0·781	1·666	132·7	75·3	237·0	0·0164	0·0410	2·242	21·5	0·0827	0·496
	73	0·0582	1·137	2·425	182·0	103·3	325·0	0·0225	0·0387	2·887	46·6	0·0815	0·475
	74	0·1108	2·164	4·617	326·9	185·8	584·0	0·0372	0·0336	4·459	148·5	0·0810	0·415
100 × 20 × 0·009	109	0·00819	0·160	0·238	44·2	10·0	31·5	0·0072	0·1267	0·905	0·59	0·452	0·280
	110	0·0139	0·272	0·404	71·8	16·3	51·1	0·0111	0·1148	1·325	1·42	0·286	0·402
	111	0·0208	0·406	0·605	104·6	23·7	74·5	0·0136	0·0940	1·574	2·54	0·284	0·331
	112	0·0204	0·398	0·593	102·9	23·3	73·3	0·0114	0·0801	1·319	2·45	0·278	0·288
	113	0·0310	0·606	0·901	152·7	34·6	108·7	0·0171	0·0792	1·935	3·85	0·182	0·435
	114	0·0418	0·816	1·215	203·4	46·1	144·8	0·0209	0·0717	2·326	6·91	0·176	0·407
2-Element Flame Trap	81	0·0100	0·195	0·233	25·4	—	—	0·00189	0·0339	0·582	0·50	0·249	0·136
	82	0·0128	0·259	0·298	32·1	—	—	0·00258	0·0361	0·808	0·77	0·230	0·157
	83	0·0186	0·363	0·433	45·1	—	—	0·00380	0·0366	1·230	1·26	0·169	0·217
	75	0·0196	0·383	0·456	48·2	—	—	0·00394	0·0360	1·234	0·79	0·097	0·373
	76	0·0267	0·521	0·621	63·7	—	—	0·00510	0·0342	1·544	1·47	0·091	0·374
	77	0·0376	0·734	0·874	89·3	—	—	0·00629	0·0030	1·890	2·20	0·069	0·432
	78	0·0454	0·887	1·056	102·8	—	—	0·00658	0·0260	1·880	3·34	0·067	0·388
	79	0·0553	1·080	1·286	125·4	—	—	0·00692	0·0224	1·980	4·81	0·065	0·345
	80	0·0762	1·488	1·772	170·4	—	—	0·00655	0·0154	1·847	6·32	0·0445	0·346
4-Element Flame Trap	91	0·0273	0·533	0·635	66·0	—	—	0·00429	0·0282	1·313	3·18	0·097	0·289
	92	0·0438	0·856	1·019	101·7	—	—	0·00480	0·0196	1·402	5·82	0·065	0·301
	95	0·0622	1·215	1·447	144·7	—	—	0·00554	0·0160	1·613	7·67	0·042	0·376
	93	0·0706	1·379	1·642	159·7	—	—	0·00559	0·0142	1·697	8·51	0·035	0·405
	90	0·0725	1·416	1·686	160·1	—	—	0·00665	0·0164	1·834	9·71	0·039	0·417
	94	0·0900	1·758	2·093	198·8	—	—	0·00592	0·0118	1·633	14·4	0·037	0·322
1-Element Flame Trap	100	0·0068	0·144	0·172	18·5	—	—	0·00150	0·0364	0·483	0·13	0·230	0·158
	96	0·0116	0·246	0·293	30·4	—	—	0·00308	0·0438	0·946	0·28	0·162	0·271
	97	0·0152	0·322	0·384	39·2	—	—	0·00386	0·0419	1·158	0·40	0·131	0·319
	98	0·0179	0·379	0·452	45·5	—	—	0·00448	0·0413	1·346	0·53	0·123	0·334
	99	0·0208	0·441	0·525	52·9	—	—	0·00503	0·0399	1·498	0·52	0·090	0·446
1-Element Flame Trap (slitted)	101	0·0083	0·179	0·213	23·2	—	—	0·00226	0·0443	0·734	0·15	0·174	0·255
	102	0·0117	0·252	0·300	31·9	—	—	0·00334	0·0464	1·051	0·25	0·141	0·329
	103	0·0157	0·338	0·403	41·4	—	—	0·00423	0·0438	1·287	0·46	0·137	0·321
	104	0·0211	0·454	0·541	53·9	—	—	0·00480	0·0370	1·408	0·56	0·089	0·416
1-Element Flame Trap (small)	105	0·0086	0·182	0·228	16·7	—	—	0·00154	0·0281	0·334	0·47	0·310	0·091
	106	0·0118	0·250	0·313	22·4	—	—	0·00242	0·0322	0·513	0·64	0·230	0·140
	107	0·0165	0·350	0·438	30·0	—	—	0·00345	0·9328	0·697	1·11	0·189	0·173
	108	0·0214	0·453	0·568	38·3	—	—	0·00440	0·0322	0·876	1·59	0·157	0·205
4-Element Flame Trap	120	0·0191	0·405	0·507	34·4	—	—	0·00517	0·0238	0·580	6·0	0·186	0·128
	121	0·0277	0·587	0·735	49·0	—	—	0·00429	0·0243	0·842	8·3	0·119	0·205
	122	0·0367	0·778	0·974	66·0	—	—	0·00476	0·0204	0·955	10·6	0·089	0·230
	123	0·0456	0·966	1·210	80·3	—	—	0·00520	0·0182	1·028	15·2	0·081	0·225
	124	0·0611	1·294	1·621	106·2	—	—	0·00643	0·0165	1·234	22·5	0·067	0·247
	128	0·1145	2·426	3·037	192·6	—	—	0·00836	0·0115	1·548	43·9	0·039	0·298
	129	0·0840	1·780	2·228	142·9	—	—	0·00792	0·0148	1·487	30·8	0·049	0·304
100 × 20 × 0·009	113	0·0525	1·025	1·526	249·3	56·5	177·5	0·0244	0·0666	2·652	10·6	0·167	0·399
	116	0·0648	1·266	1·884	307·4	69·7	218·9	0·0246	0·0544	2·662	14·2	0·148	0·367
	117	0·0775	1·514	2·253	364·0	82·6	259·2	0·0277	0·0512	2·968	21·2	0·156	0·329
	118	0·0959	1·873	2·788	446·0	101·2	317·6	0·0308	0·0460	3·253	27·7	0·135	0·342
	119	0·1145	2·236	3·329	520·0	117·9	370·2	0·0365	0·0457	3·75	44·9	0·156	0·294

TABLE 12

Particulars of Matrices

Matrix Type	Mesh wires/in. or crimp	Wire diameter D in.	No. of Layers N	Material	Container	Frontal Area A sq ft	Minimum Throughway Area A_t sq ft	Surface Area A_a sq ft	Length L ft	Volume V_L cu ft	Weight of Matrix M lb	Effective Weight of Container M_c lb	$\frac{A_t}{A}$	$\frac{A_a}{A}$	$\frac{A_a}{A_t}$	Hydr. dia. d ft	$\frac{L}{d}$	$\frac{A_a}{V_L \text{ or } NA}$	$\frac{A_a}{A_tL \text{ or } A_tN}$	$\frac{M}{V_L \text{ or } NA}$
Flame trap	0·03	—	4	Cu Ni	square	0·0373	0·0313	18·44	0·292	0·0109	1·02	0·872	0·839	494·4	589	0·00198	147·4	1693	2017	93·6
,, ,,	0·03	—	6	,, ,,	,,	0·0373	0·0313	27·65	0·438	0·0163	1·53	1·258	0·839	742	883	0·00198	221·1	1693	2017	93·6
,, ,,	0·03	—	2	,, ,,	round	0·0512	0·043	12·66	0·146	0·00747	0·668	0·013	0·839	247	294	0·00198	73·7	1693	2017	89·4*
,, ,,	0·03	—	4	,, ,,	,,	0·0512	0·043	25·3	0·292	0·0149	1·336	0·026	0·839	494	589	0·00198	147·4	1693	2017	89·6*
,, ,,	0·03	—	1	,, ,,	,,	0·0472	0·0396	5·82	0·0729	0·00344	0·280	0·007	0·839	123·6	147·3	0·00198	36·8	1693	2017	81·4*
,, ,, (slitted)	0·03	—	1	,, ,,	,,	0·0465	0·0390	5·75	0·0729	0·00339	0·273	0·007	0·839	123·6	147·3	0·00198	36·8	1693	2017	80·6*
Flame trap (small)	0·02	—	1	,, ,,	,,	0·0472	0·0377	8·3	0·0729	0·00344	0·429	0·007	0·800	176	220	0·001324	55·0	2416	3020	124·6*
Gauze	30	0·0105	51	Brass	square	0·0384	0·0183	4·23	0·0833	0·0032	0·542	0·230	0·477	110·2	231	0·00144	57·8	2·16	4·53	0·277
,,	50	0·004	100	Copper	,,	0·0384	0·0244	5·95	0·0833	0·0032	0·318	0·230	0·635	154·9	244	0·00137	61·0	1·549	2·44	0·0828
,,	24	0·0132	71	Steel	round	0·0491	0·0230	7·63	0·1625	0·00798	1·113	0·0150	0·468	155·3	332	0·00196	82·8	2·19	4·68	0·3195
,,	30	0·0105	100	Brass	,,	0·0512	0·0240	11·16	0·175	0·00895	1·23	0·0155	0·469	218	465	0·00151	114	2·18	4·65	0·240*
,,	30	0·0105	150	,,	,,	0·0512	0·0240	16·73	0·262	0·0134	1·86	0·0230	0·469	327	697	0·00150	175	2·18	4·65	0·240*
,,	20	0·009	100	Staybrite	,,	0·0512	0·0344	6·22	0·150	0·00768	0·573	0·0130	0·672	121·3	180·5	0·00332	45·3	1·213	1·805	0·112*
,,	40	0·0045	98	,,	,,	0·0512	0·0344	8·20	0·094	0·00480	0·278	0·008	0·672	121·0	180·0	0·00208	45·0	1·234	1·836	0·0554*
Wool	loose pack	—	—	Steel	—	1·00	0·9375	0·200	0·100	0·100	3·04	—	0·9375	200	213	0·00188	53·25	2000	2130	30·4
,,	tight pack	—	—	,,	—	1·00	0·8125	0·600	0·100	0·100	9·12	—	0·8125	600	738	0·000626	159·8	6000	7380	91·2

* Indicates matrices from which useful results were obtained.

D

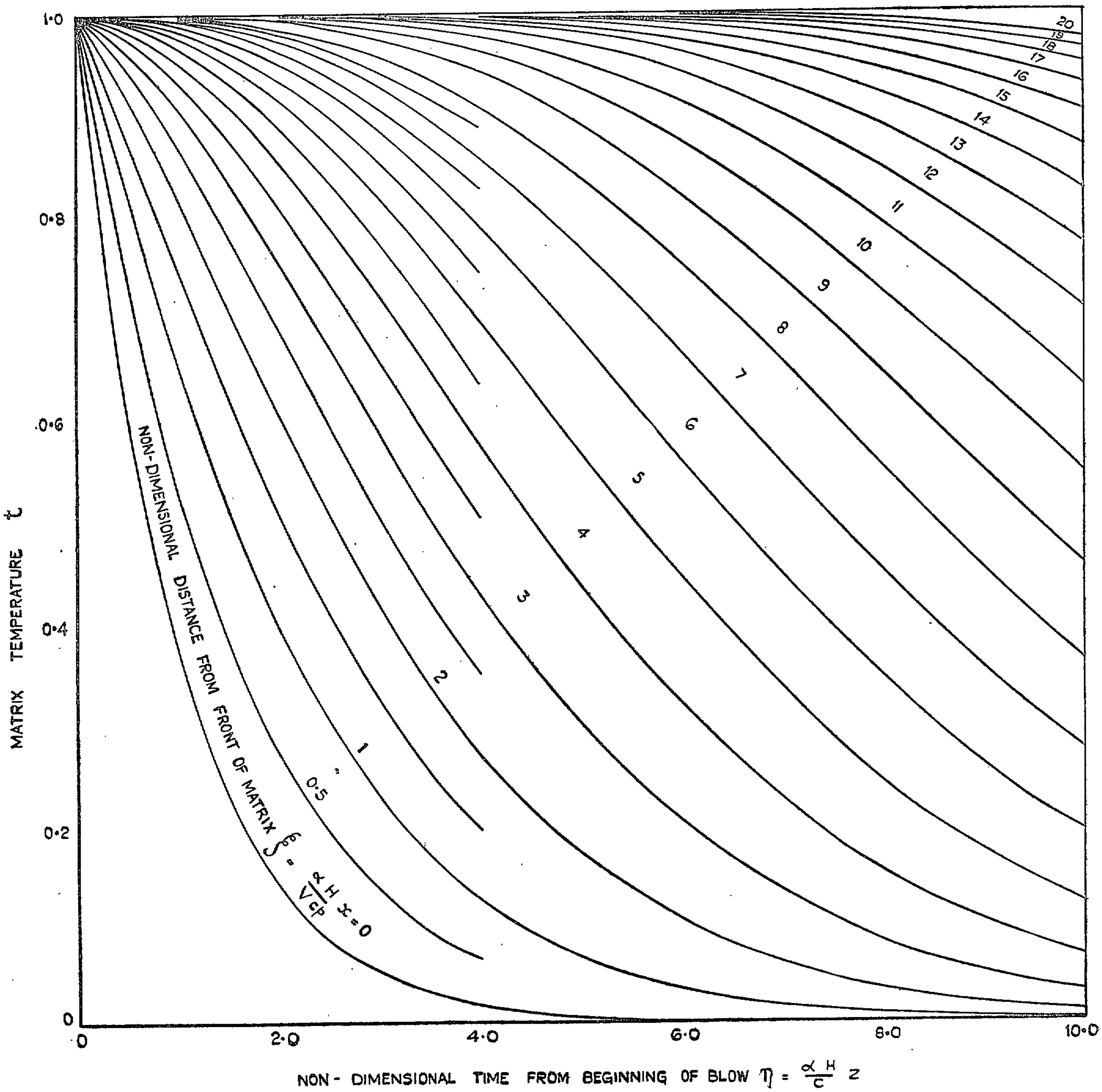

FIG. 1. Matrix temperature during initial cooling.

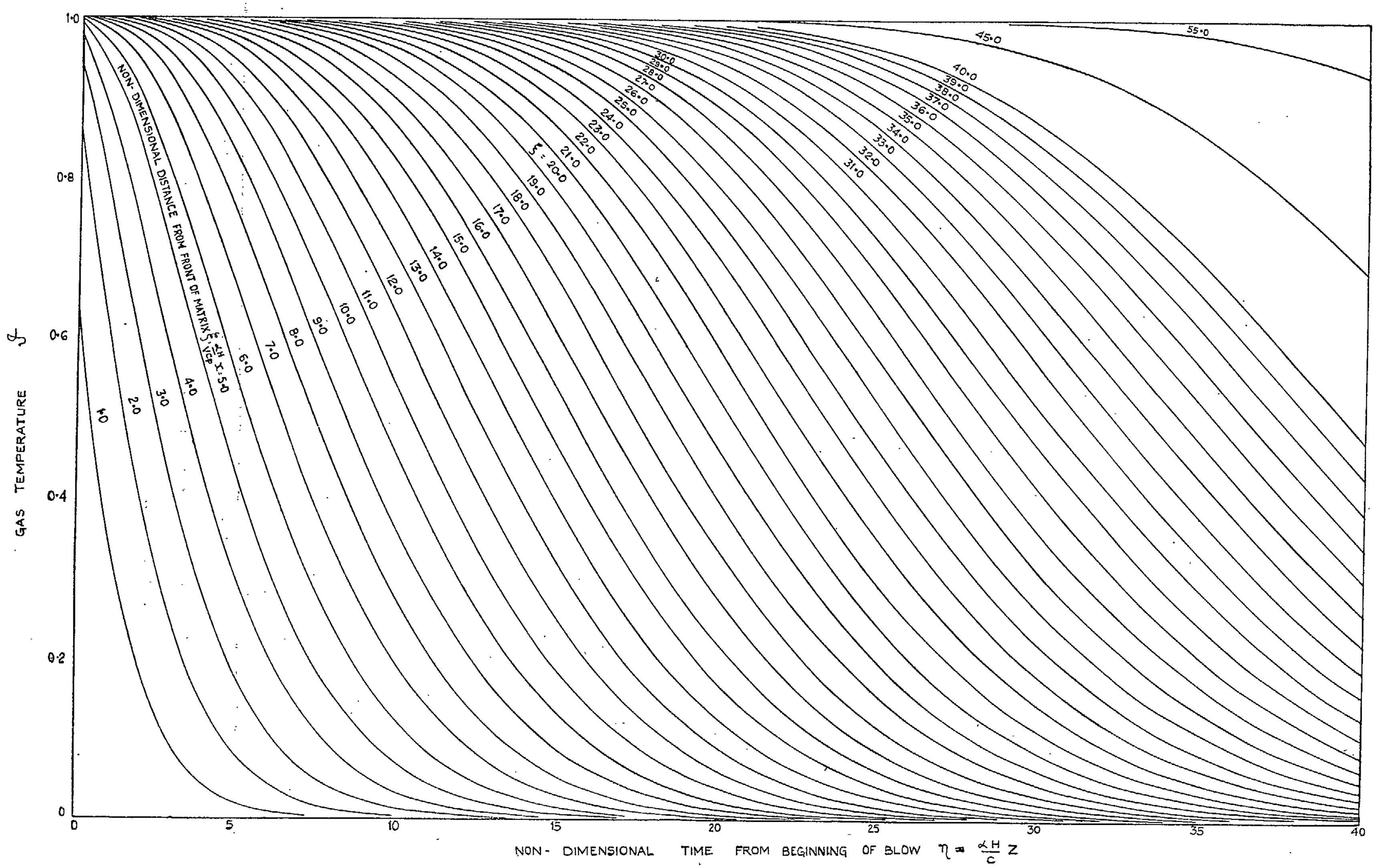

FIG. 2. Gas temperature during initial cooling.

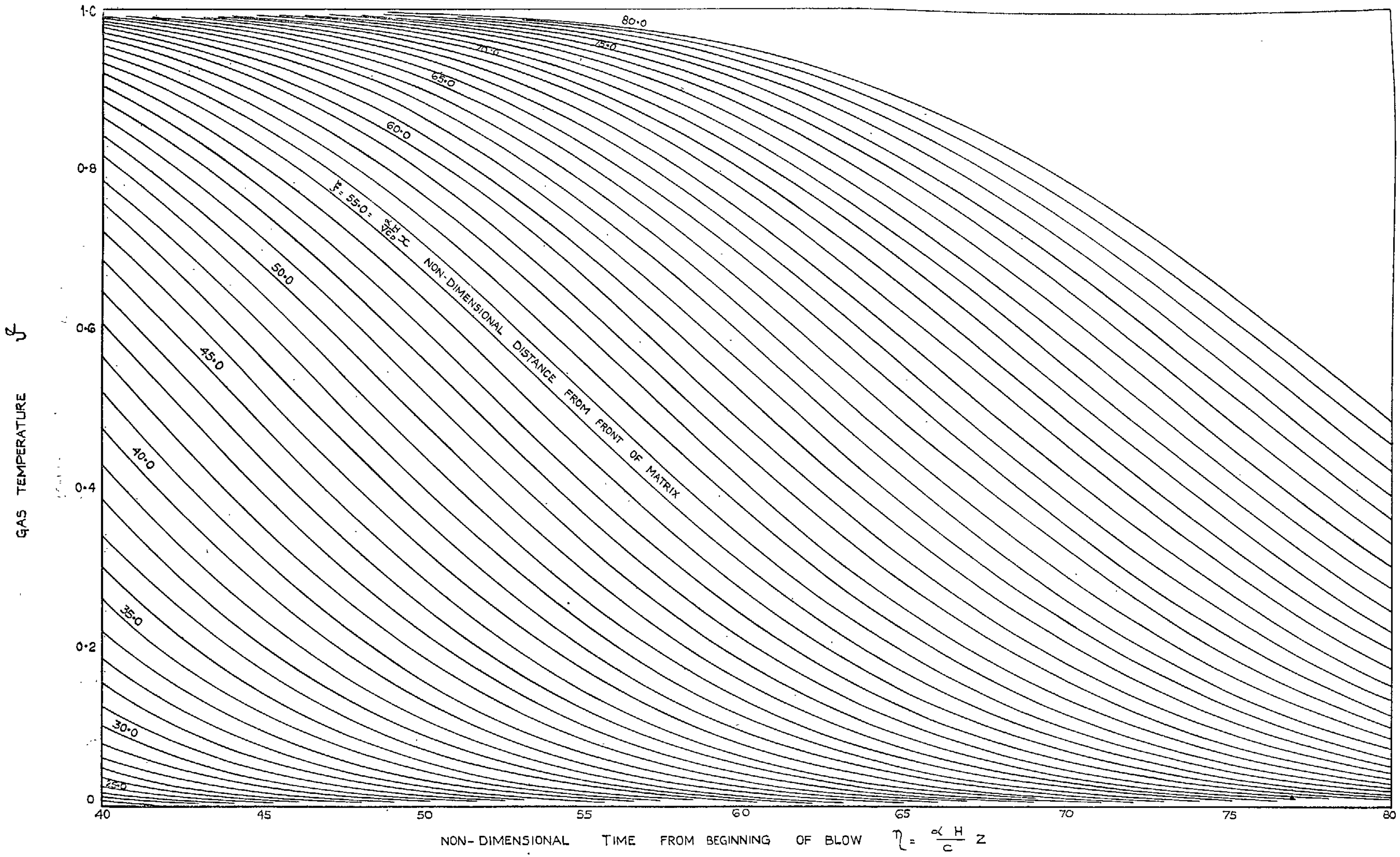

FIG. 3. Gas temperature during initial cooling.

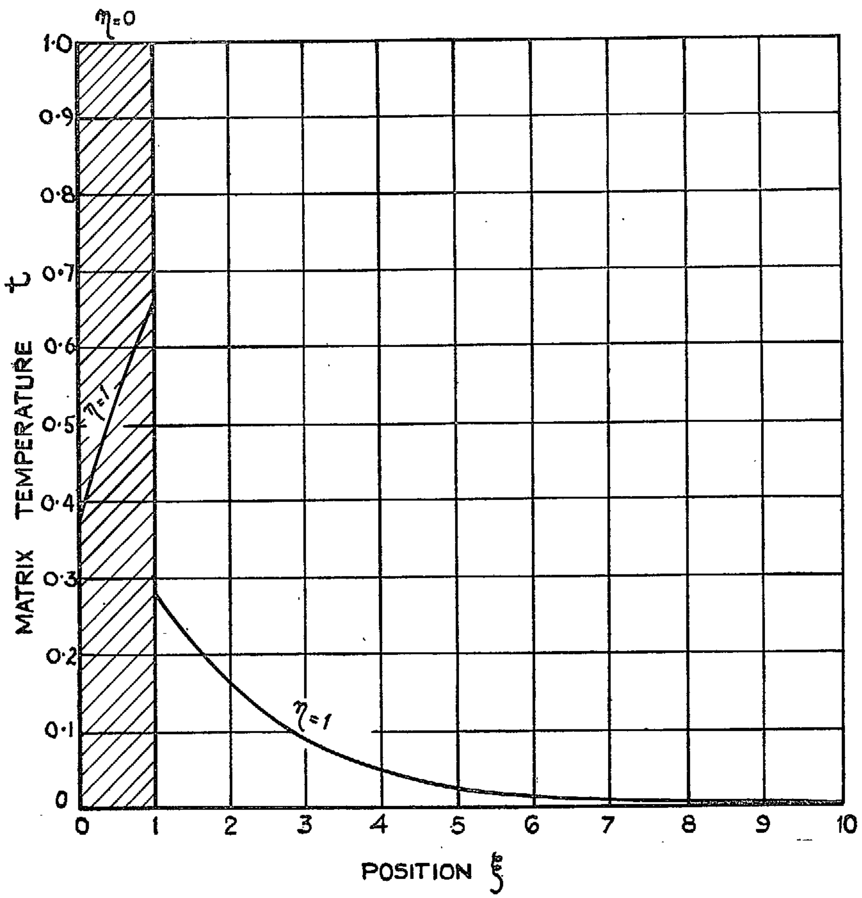

FIG. 4. Heat pole function Δy for a heat pole of width 1.

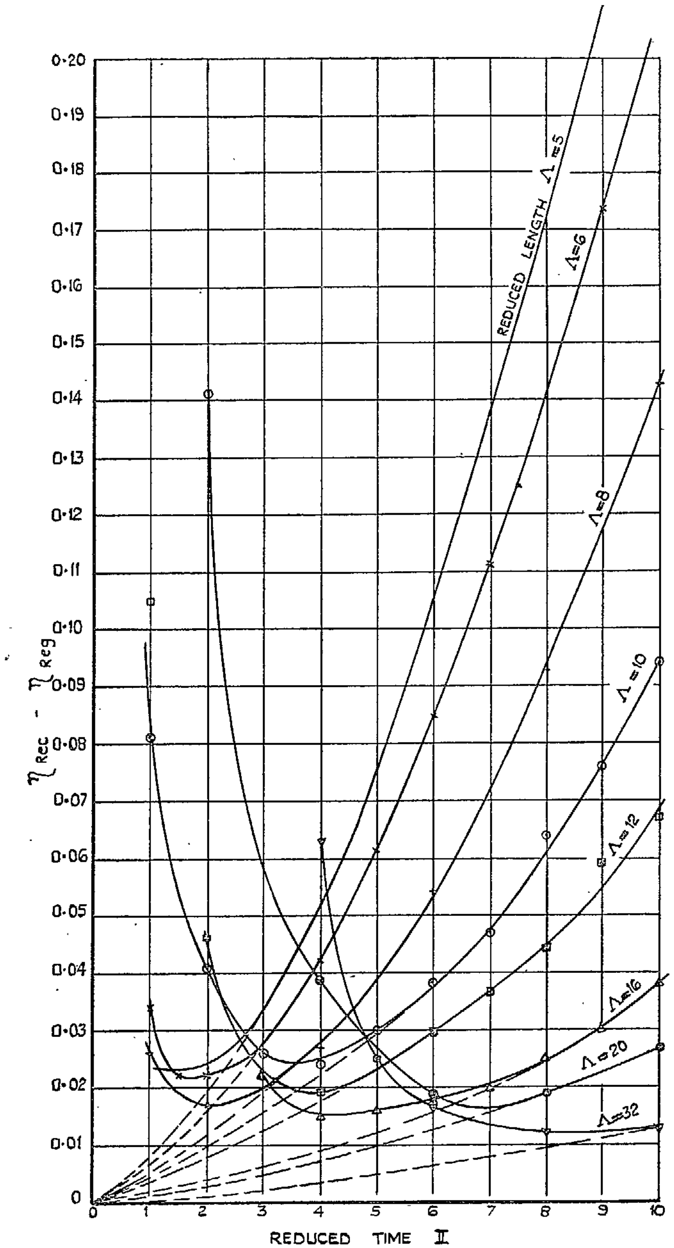

FIG. 5. Efficiency of balanced regenerators calculated by heat pole method on Mallock machine.

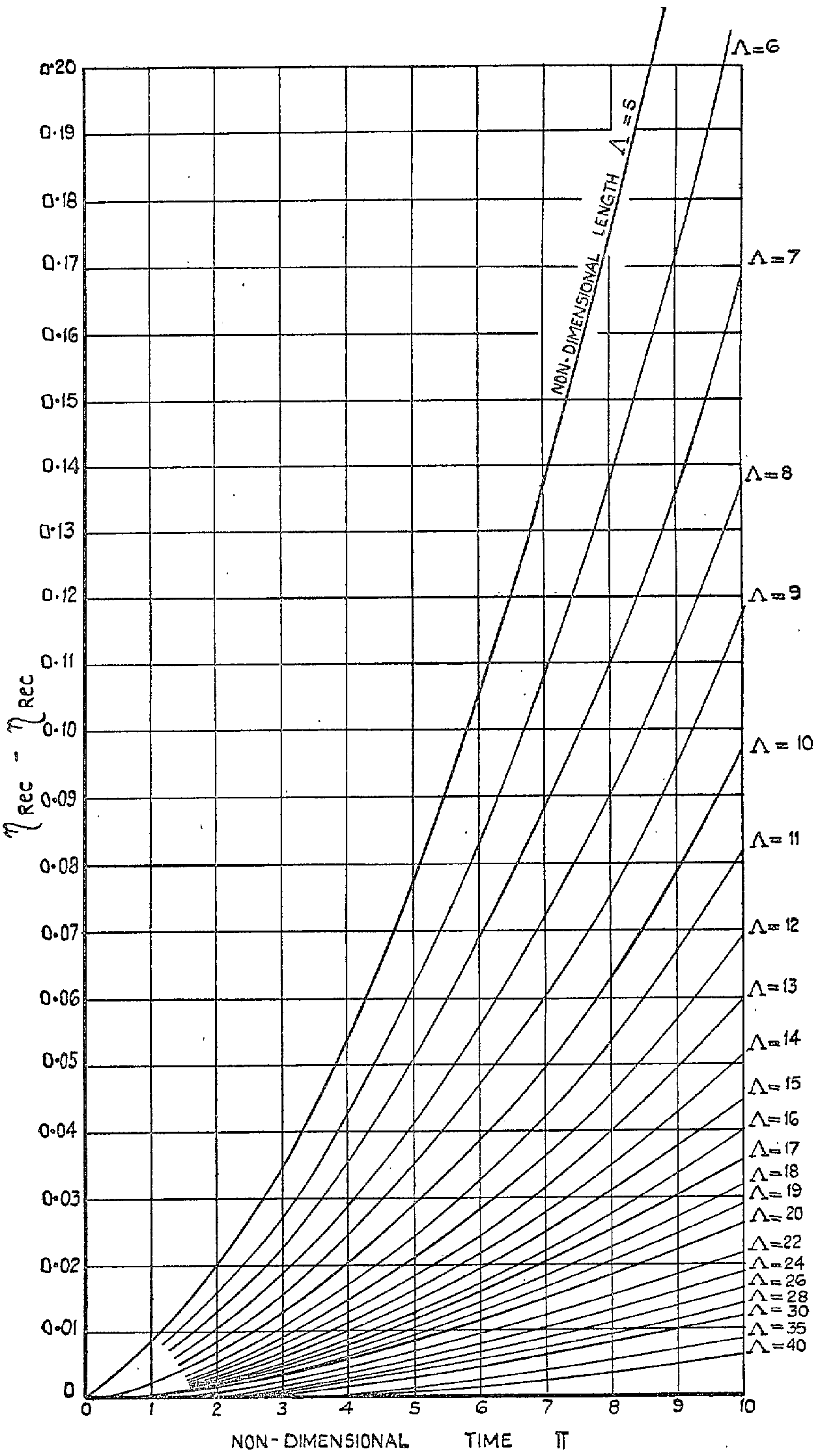

FIG. 6. Efficiency of balanced regenerator.

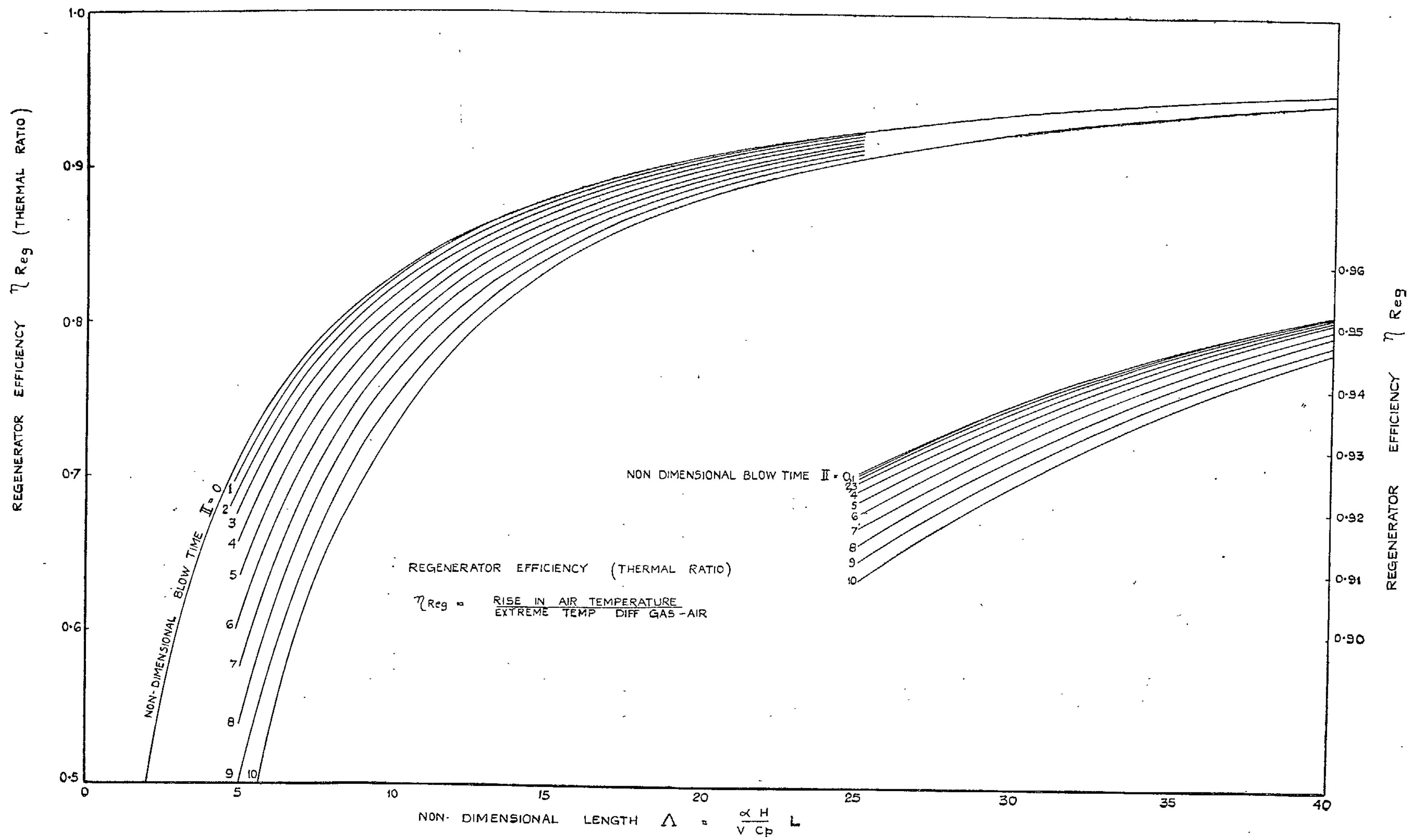

FIG. 7. Effect of length on efficiency of balanced regenerators.

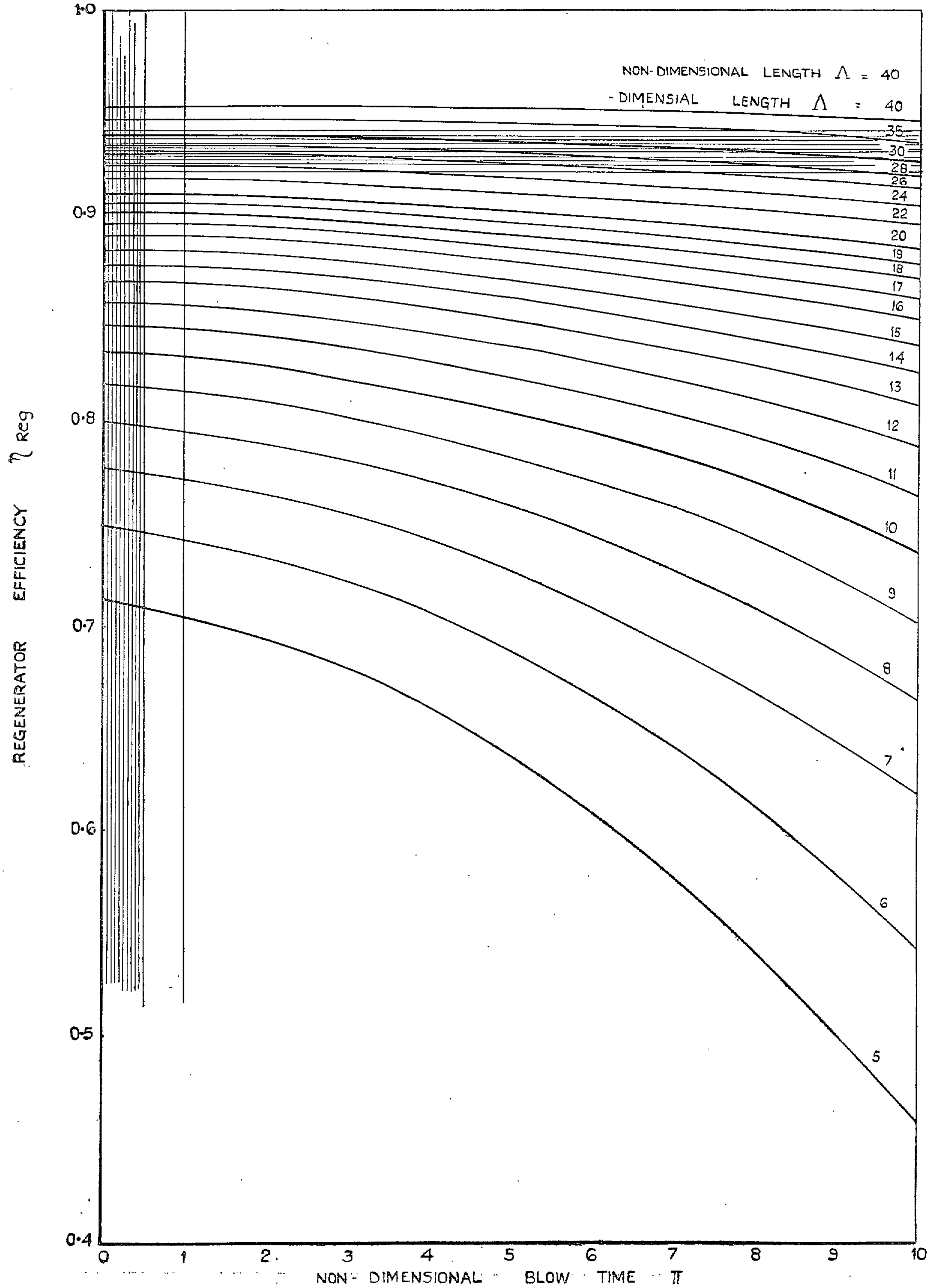

FIG. 8. Effect of blow time on efficiency of balanced regenerators.

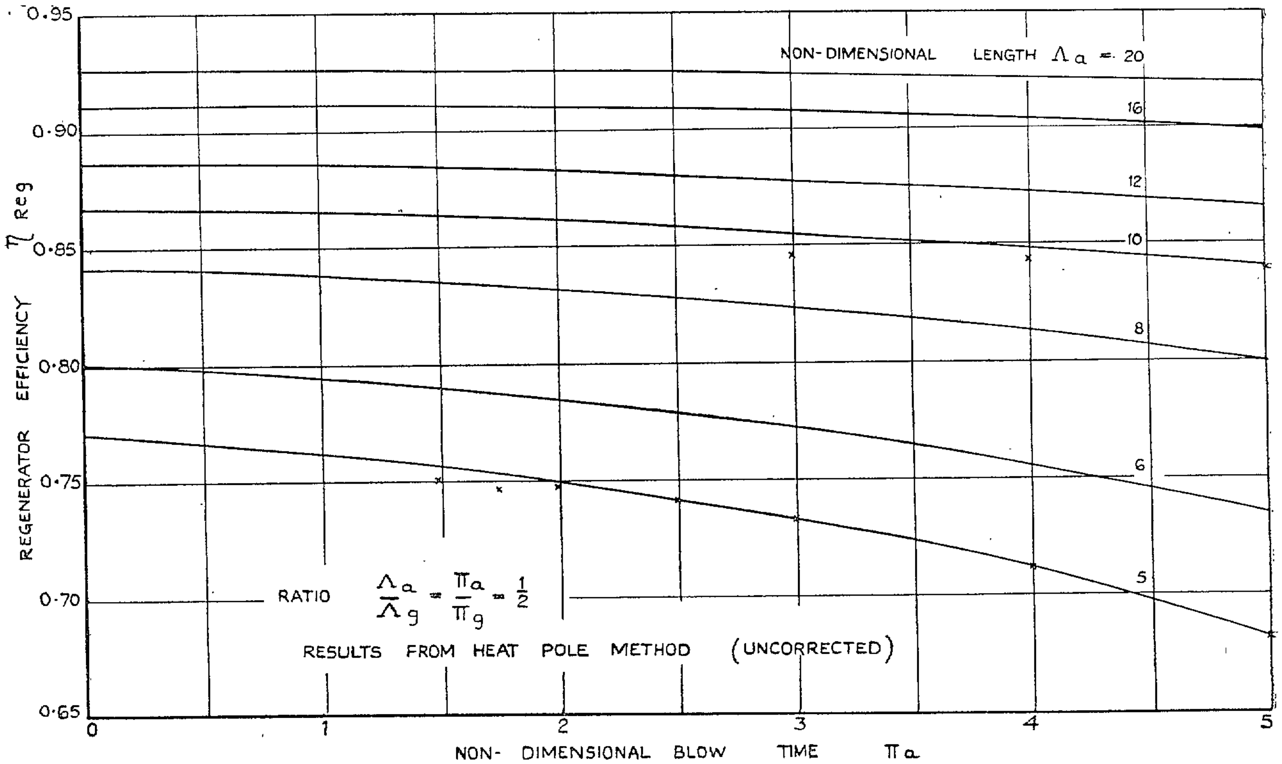

FIG. 9. Effect of blow time on efficiency of unbalanced regenerator. Ratio 1/2.

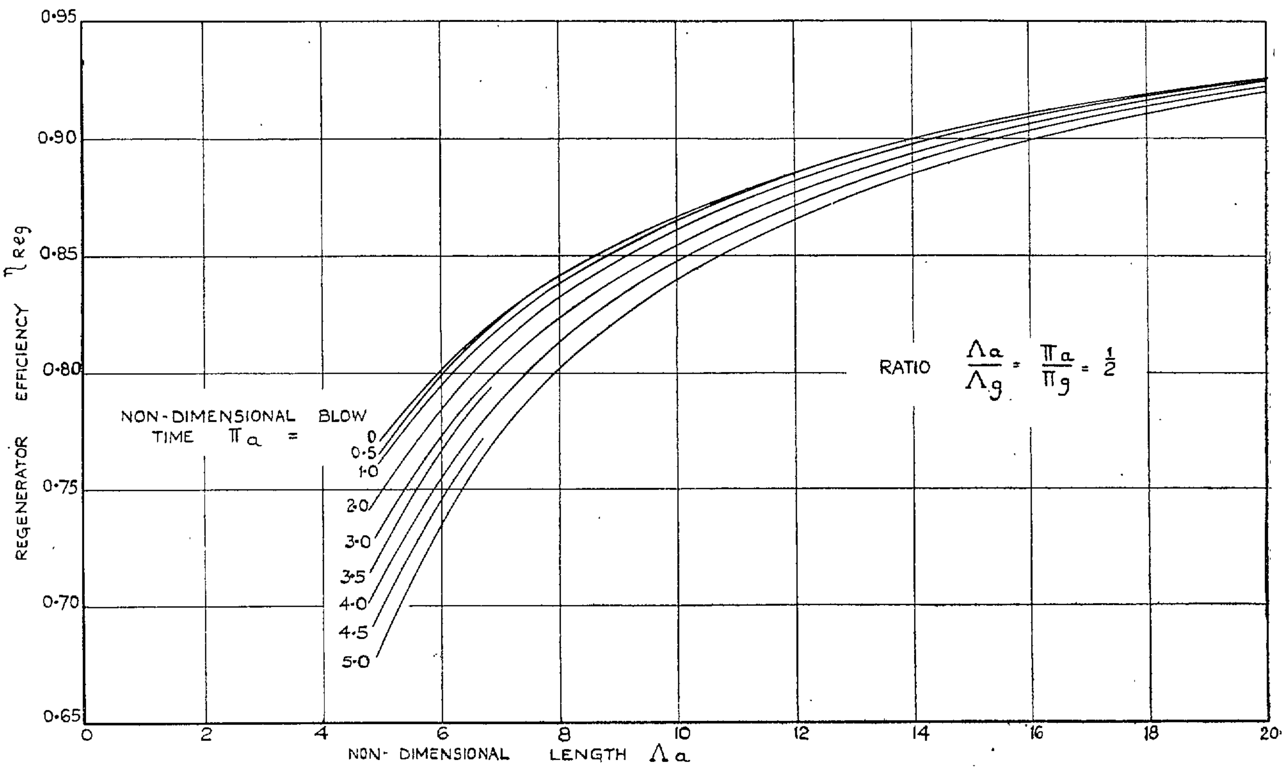

FIG. 10. Effect of length on efficiency of unbalanced regenerator. Ratio 1/2.

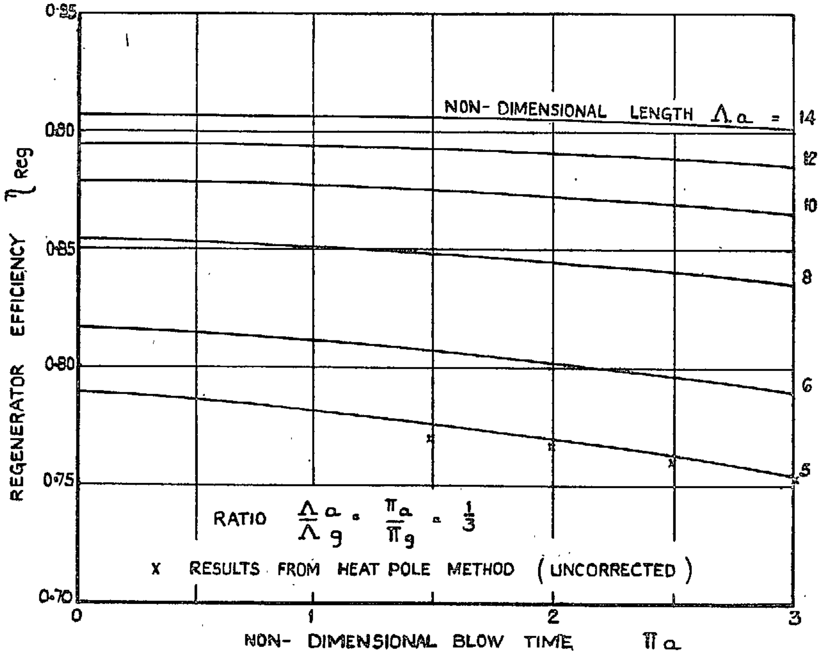

FIG. 11. Effect of blow time on efficiency of unbalanced regenerator. Ratio 1/3.

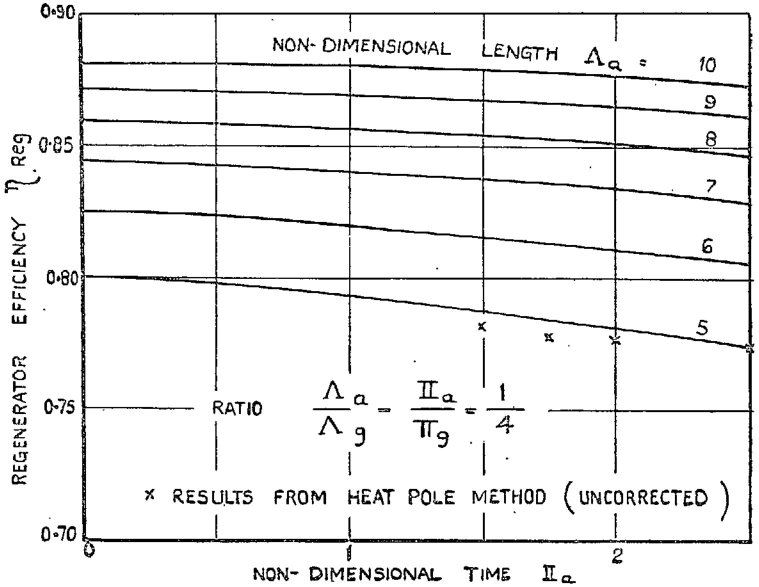

FIG. 13. Effect of blow time on efficiency on unbalanced regenerator. Ratio 1/4.

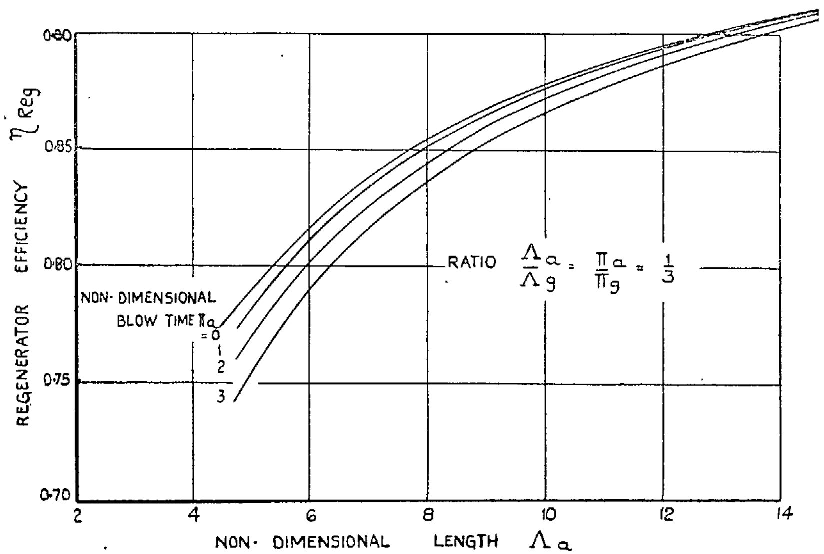

FIG. 12. Effect of length on efficiency of unbalanced regenerator. Ratio 1/3.

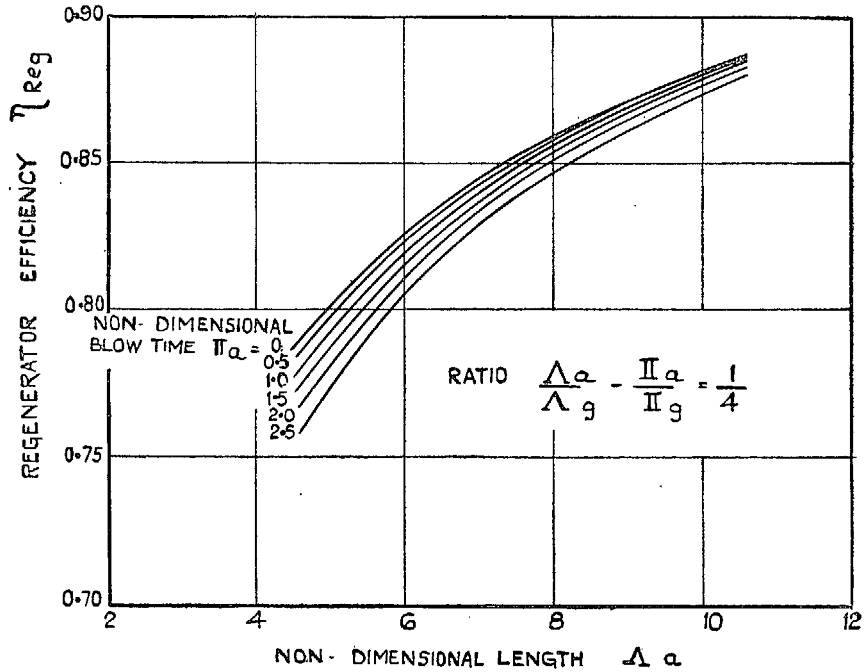

FIG. 14. Effect of length on efficiency of unbalanced regenerator. Ratio 1/4.

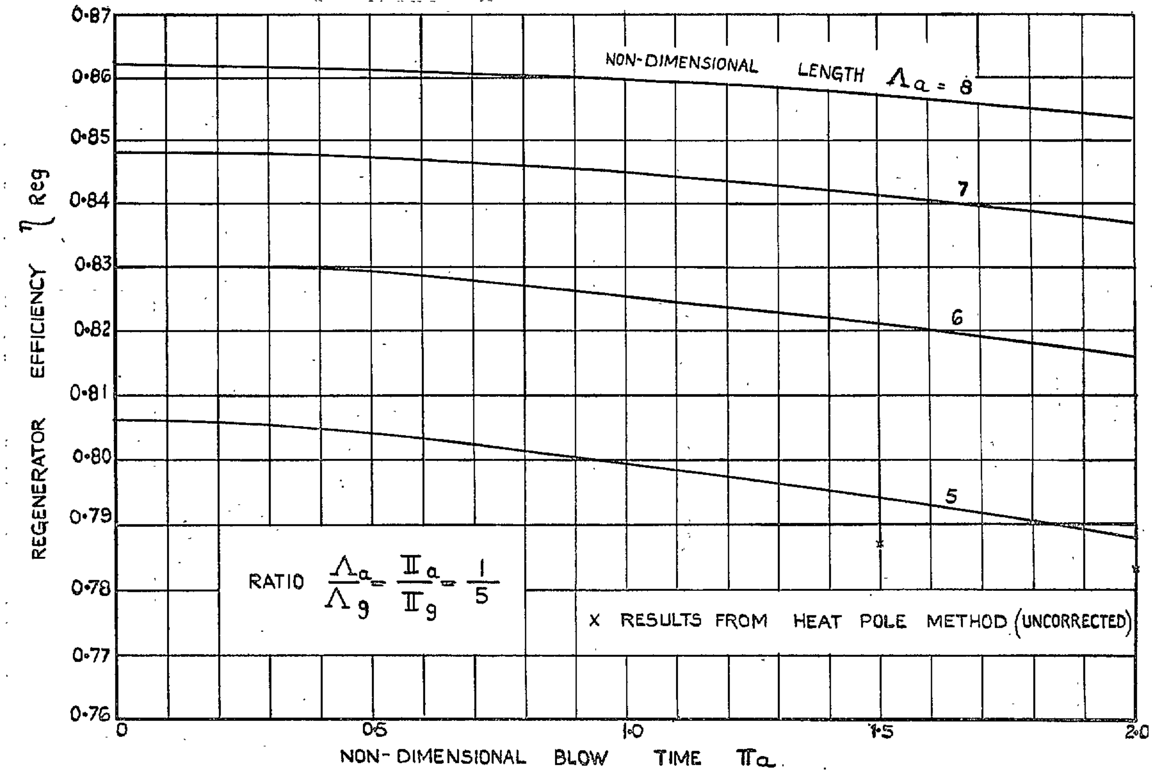

FIG. 15. Effect of blow time on efficiency of unbalanced regenerator. Ratio 1/5.

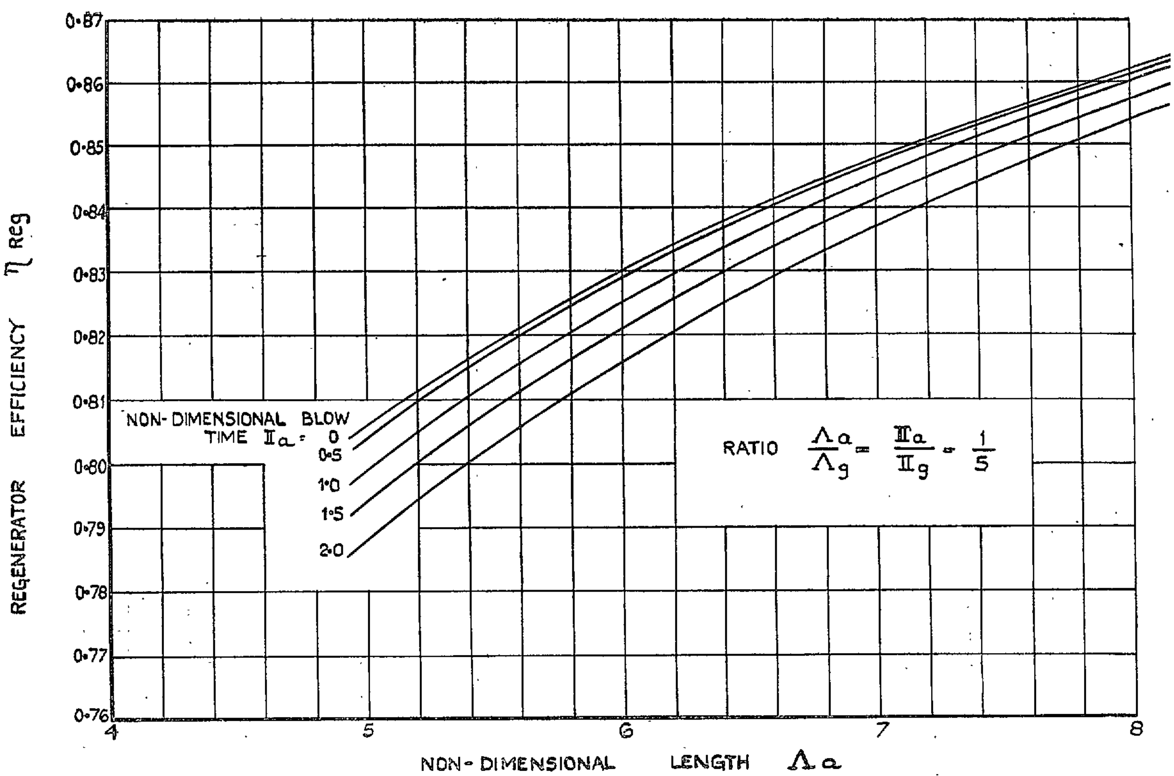

FIG. 16. Effect of length on efficiency of unbalanced regenerator. Ratio 1/5.

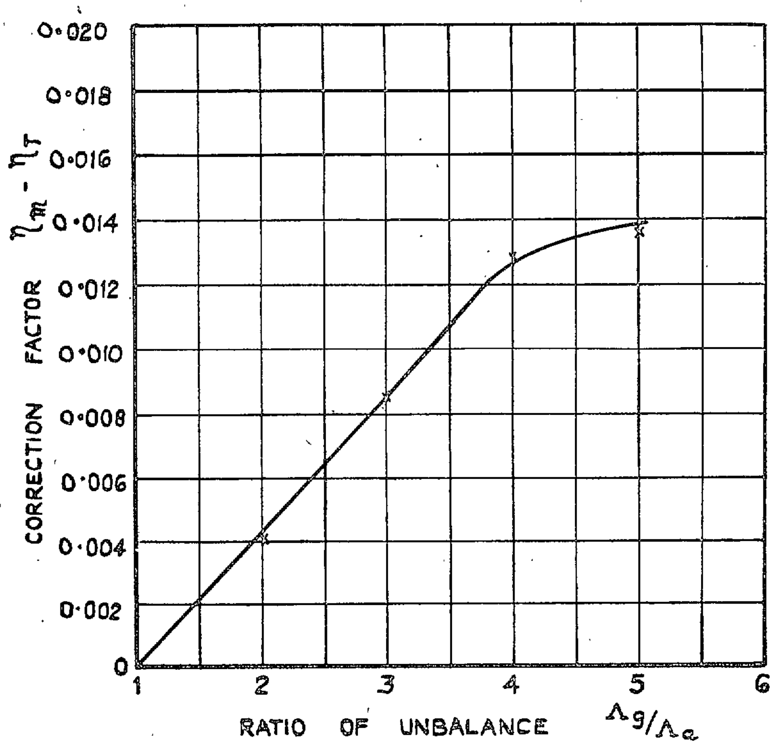

FIG. 17. Correction factor for obtaining efficiency of unbalanced regenerator from mean efficiency.

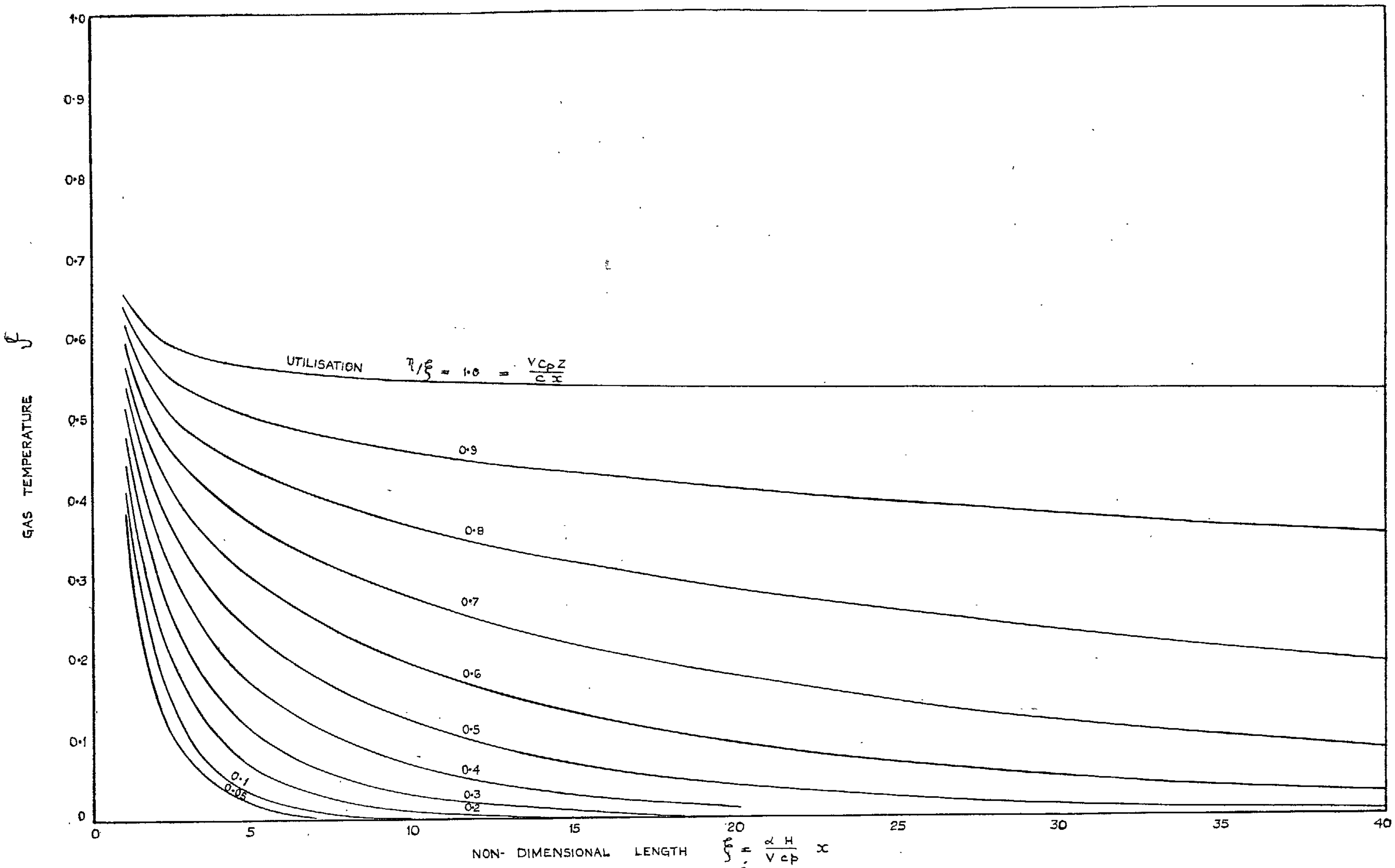

FIG. 18. Gas temperature during initial heating.

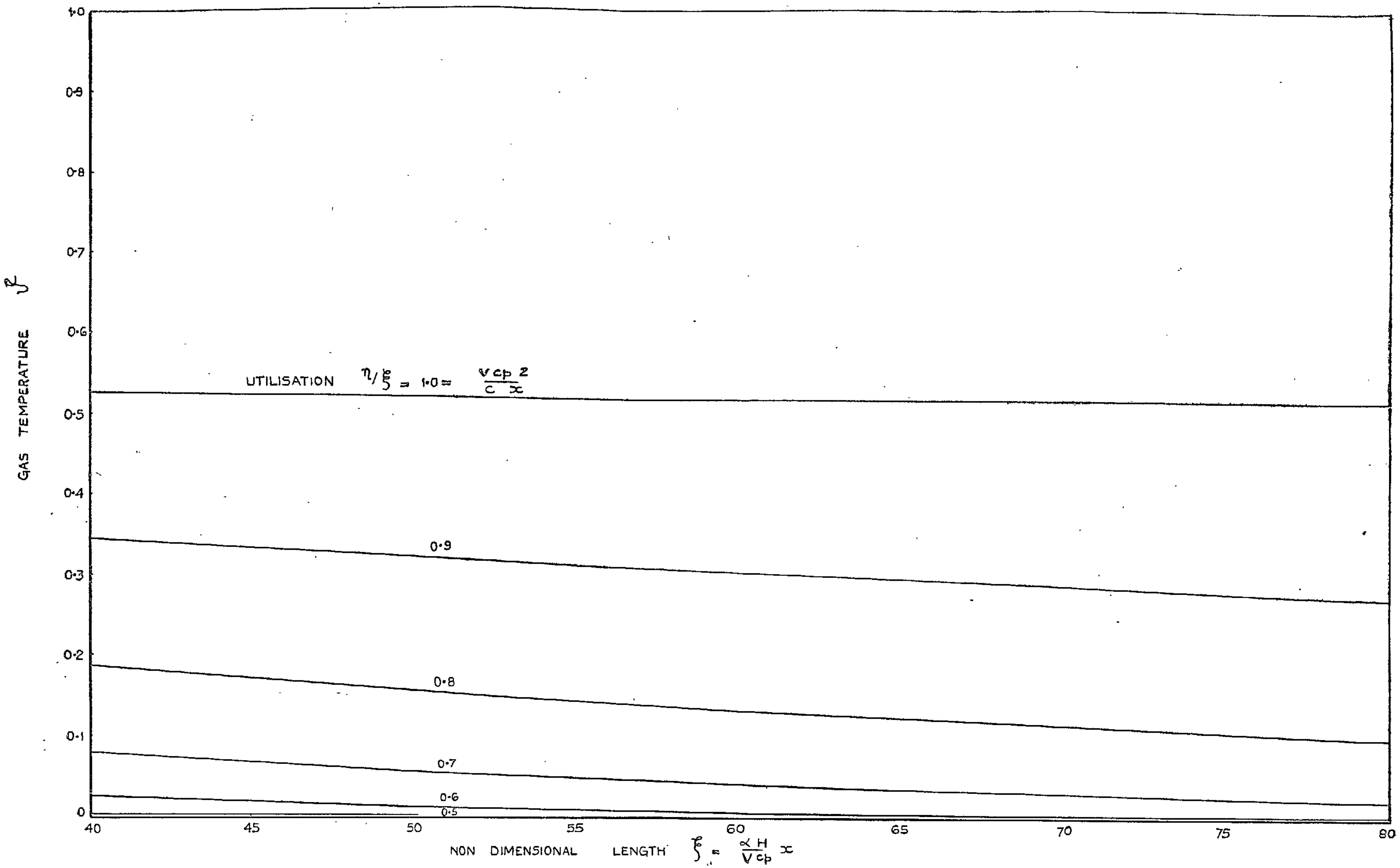

FIG. 19. Gas temperature during initial heating.

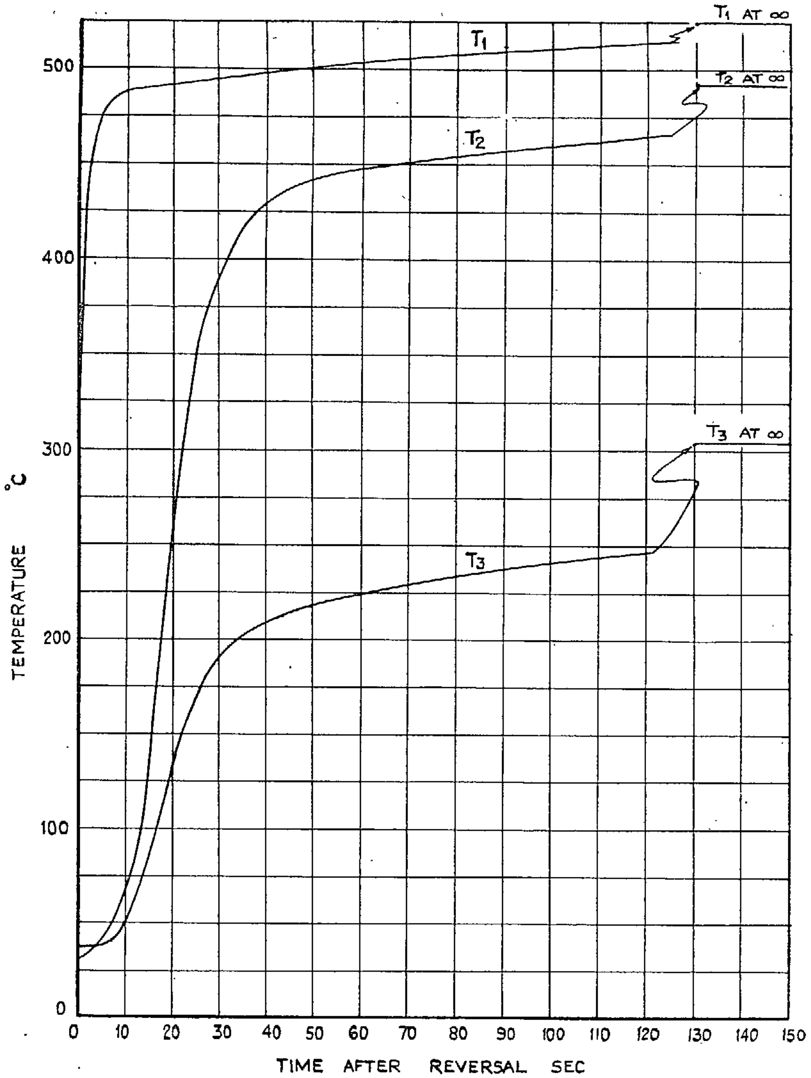

FIG. 22. Heating curve for 4-element flame trap matrix (without lagging or flow compensation).

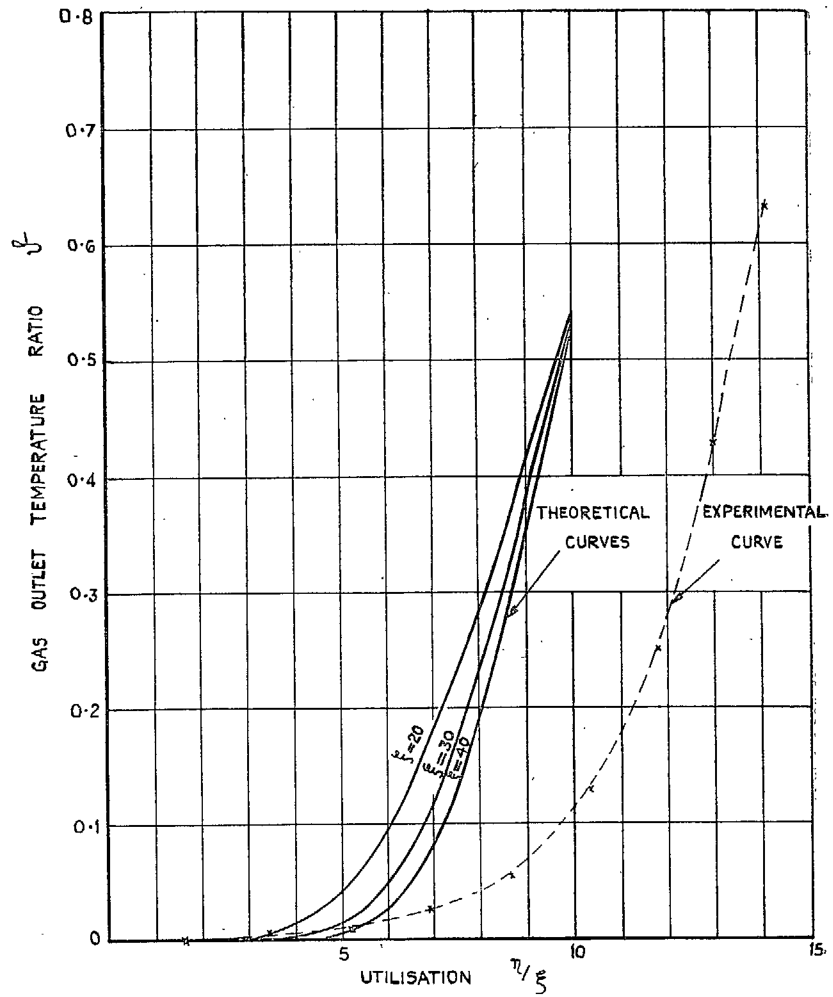

FIG. 23. Comparison between theoretical and experimental curves. Copper gauze matrix in heavy square container.

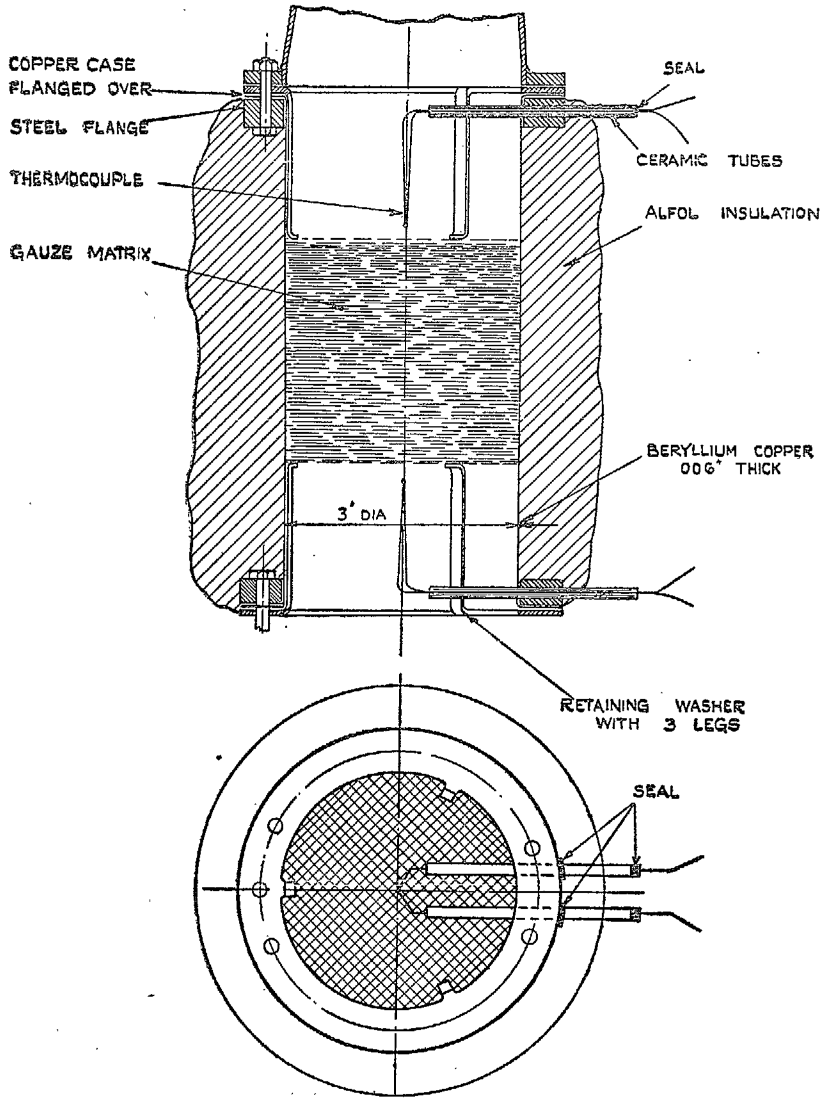

FIG. 24. Details of matrix container. Regenerator matrix test rig.

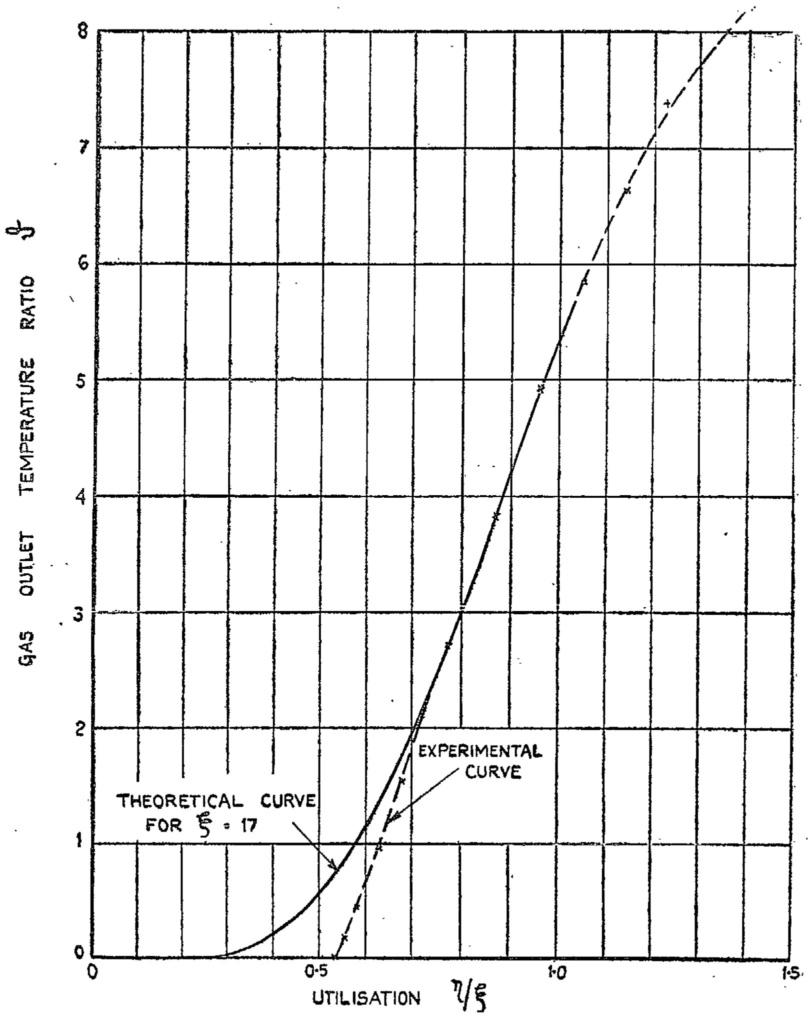

FIG. 25. Comparison between theoretical and experimental curves. 24-mesh steel-gauze matrix in light round container.

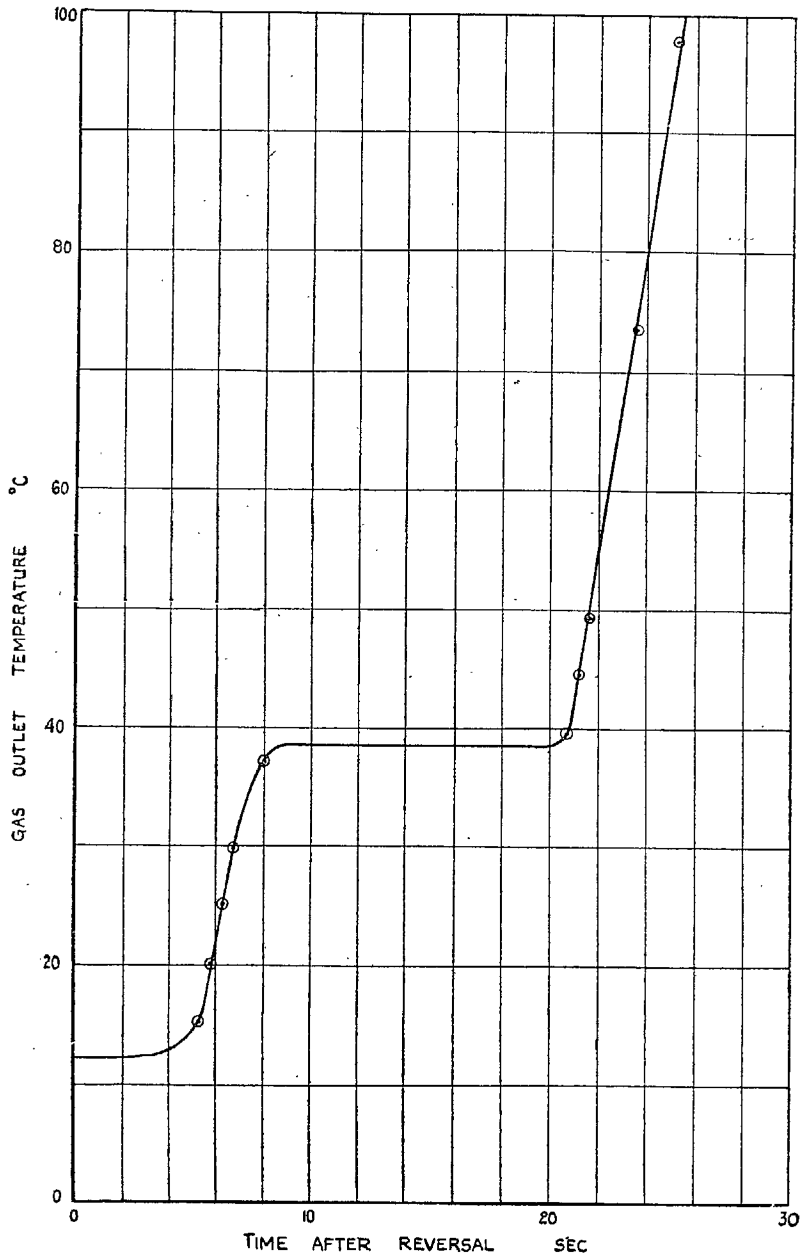

FIG. 26. Temperature jump caused by condensation on matrix.

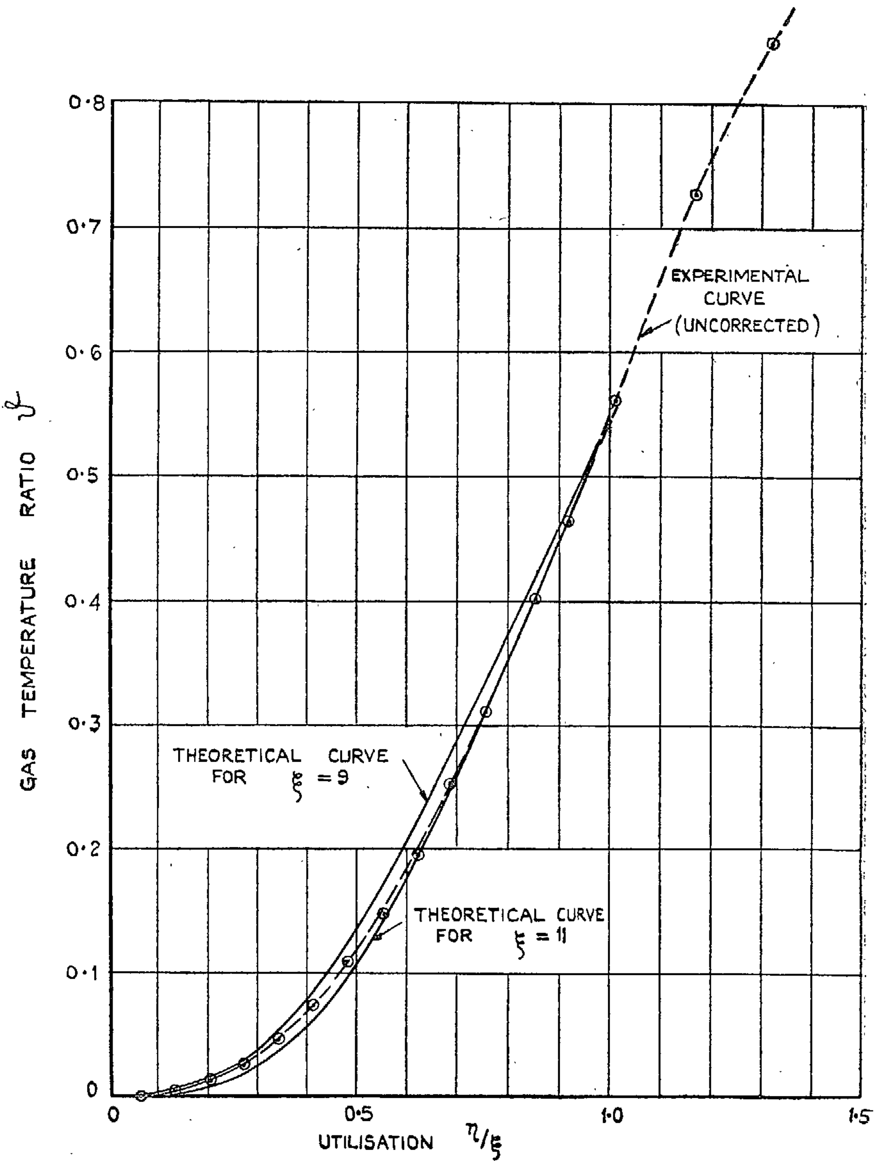

FIG. 27. Comparison between theoretical and experimental curves. 40-mesh stainless steel gauze matrix in light round container. Condensation eliminated.

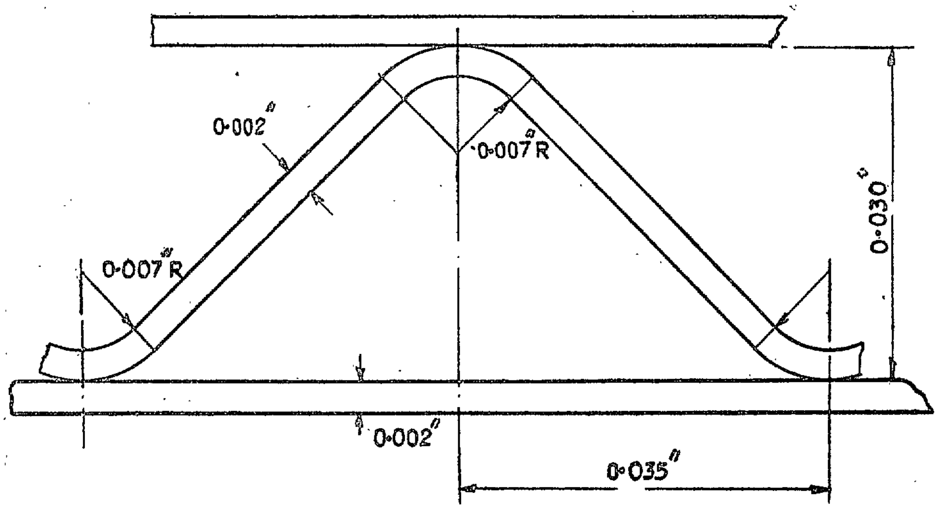

FOR ONE ELEMENT WITH PASSAGE LENGTH OF 0·875″

THROUGHWAY AREA / FRONTAL AREA = 0·839 = $\frac{At}{A}$

SURFACE AREA / FRONTAL AREA = 123·6 = $\frac{Aa}{A}$

SURFACE AREA / THROUGHWAY AREA = 147·3 = $\frac{Aa}{At}$

HYDRAULIC DIAMETER = $4L\frac{At}{Aa}$ = 0·00198 FT = d

MATERIAL 80/20 CUPRO NICKEL 0·002″ x 0·875″

FIG. 28. Dimensions of flame trap material (large).

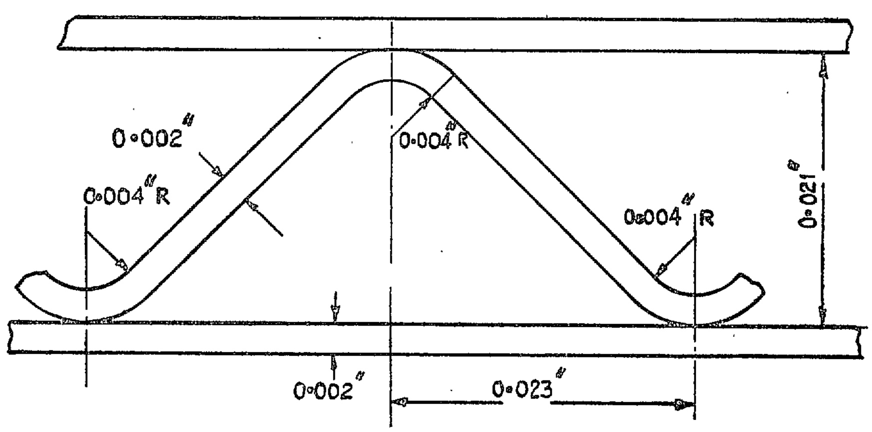

FOR ONE ELEMENT WITH PASSAGE LENGTH OF 0·875″

THROUGHWAY AREA / FRONTAL AREA = 0·800 = $\frac{At}{A}$

SURFACE AREA / FRONTAL AREA = 176 = $\frac{Aa}{A}$

SURFACE AREA / THROUGHWAY AREA = 220 = $\frac{Aa}{At}$

HYDRAULIC DIAMETER = $\frac{4LAt}{Aa}$ = 0·001324 ft = d

MATERIAL 80/20 CUPRO NICKEL 0·002″ x 0·875″

FIG. 29. Dimensions of flame trap material (small).

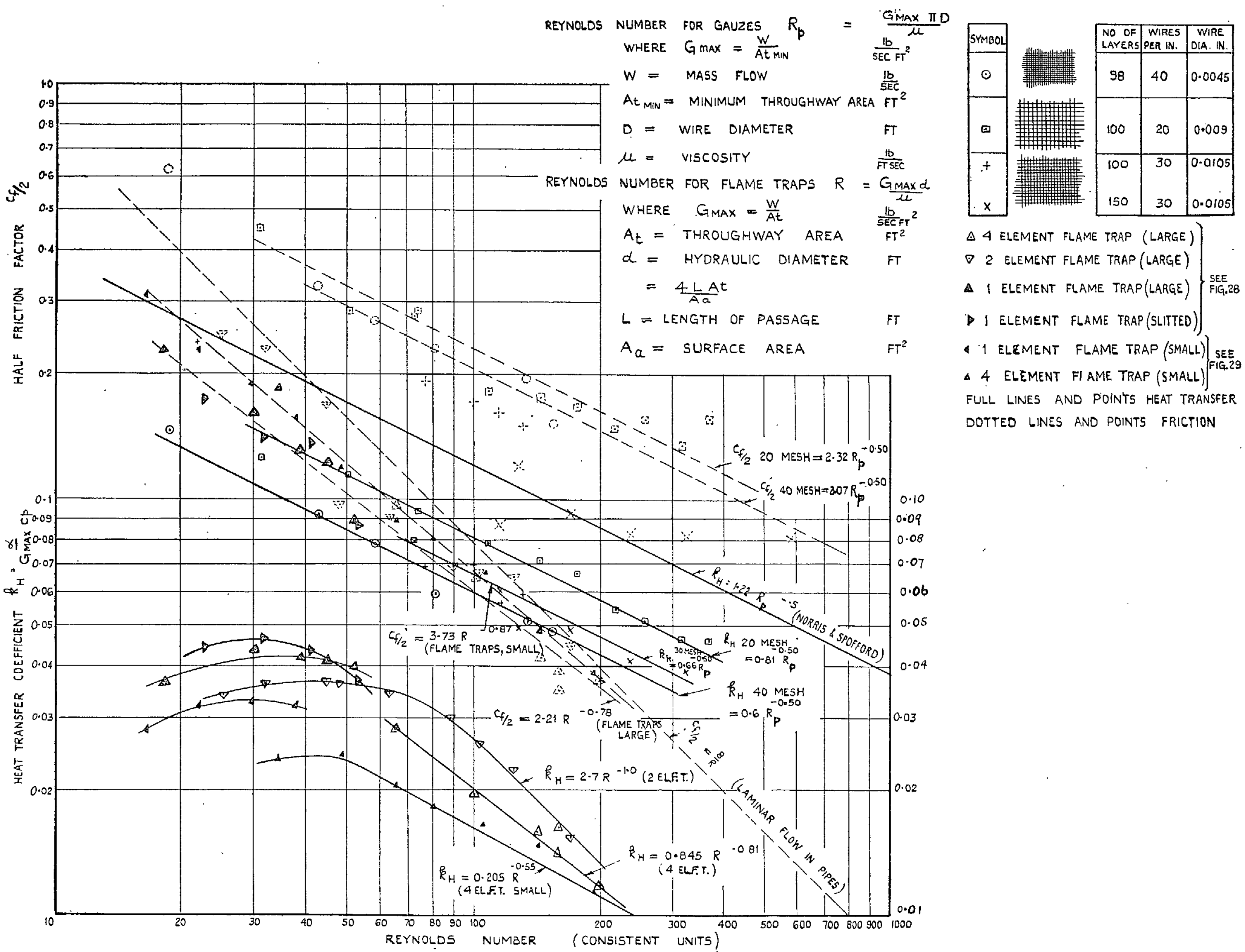

Fɪɢ. 30. Experimental results. Heat transfer coefficients and friction factors.

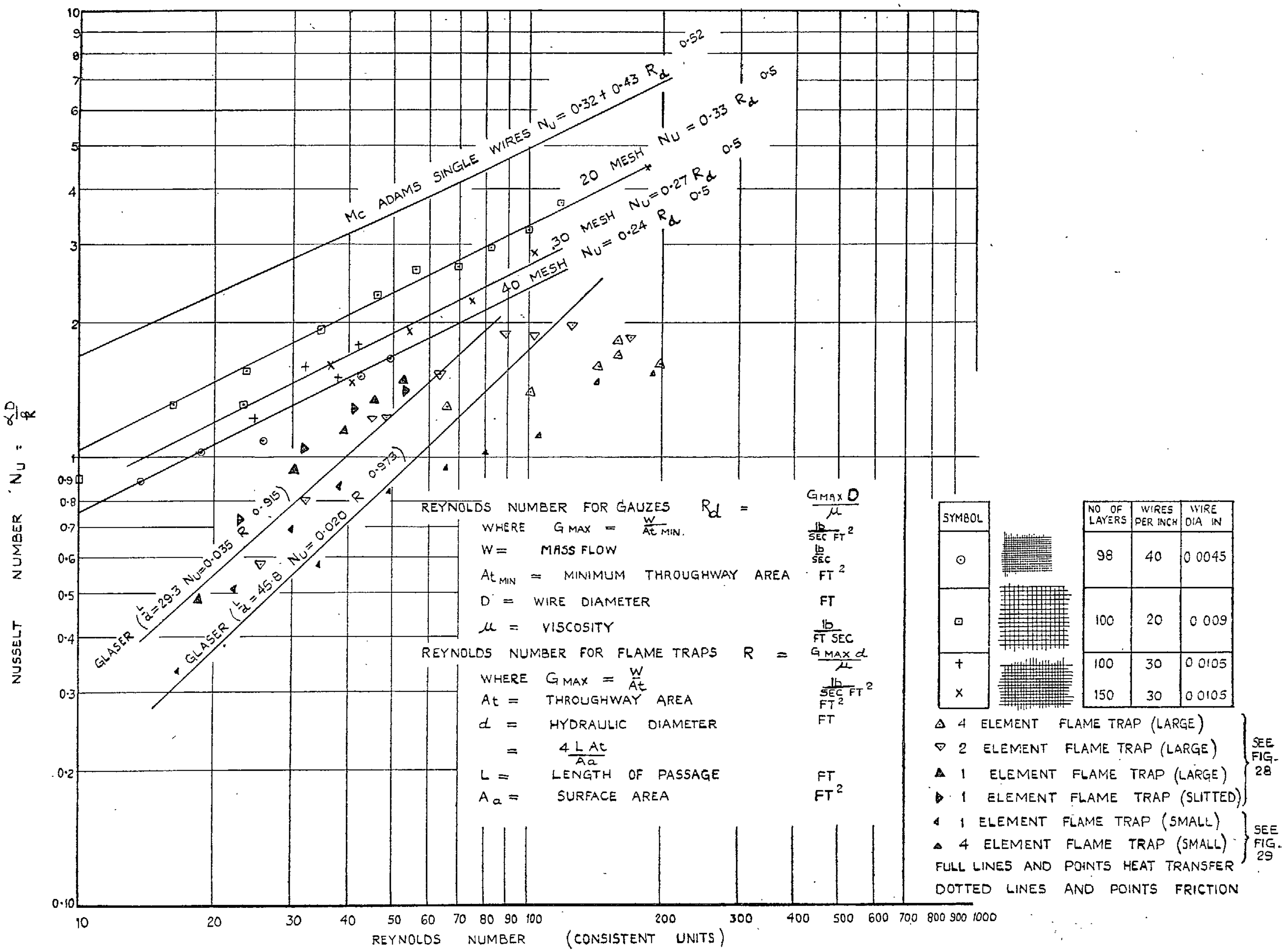

FIG. 31. Experimental results :. Variation of Nusselt number with Reynolds number.

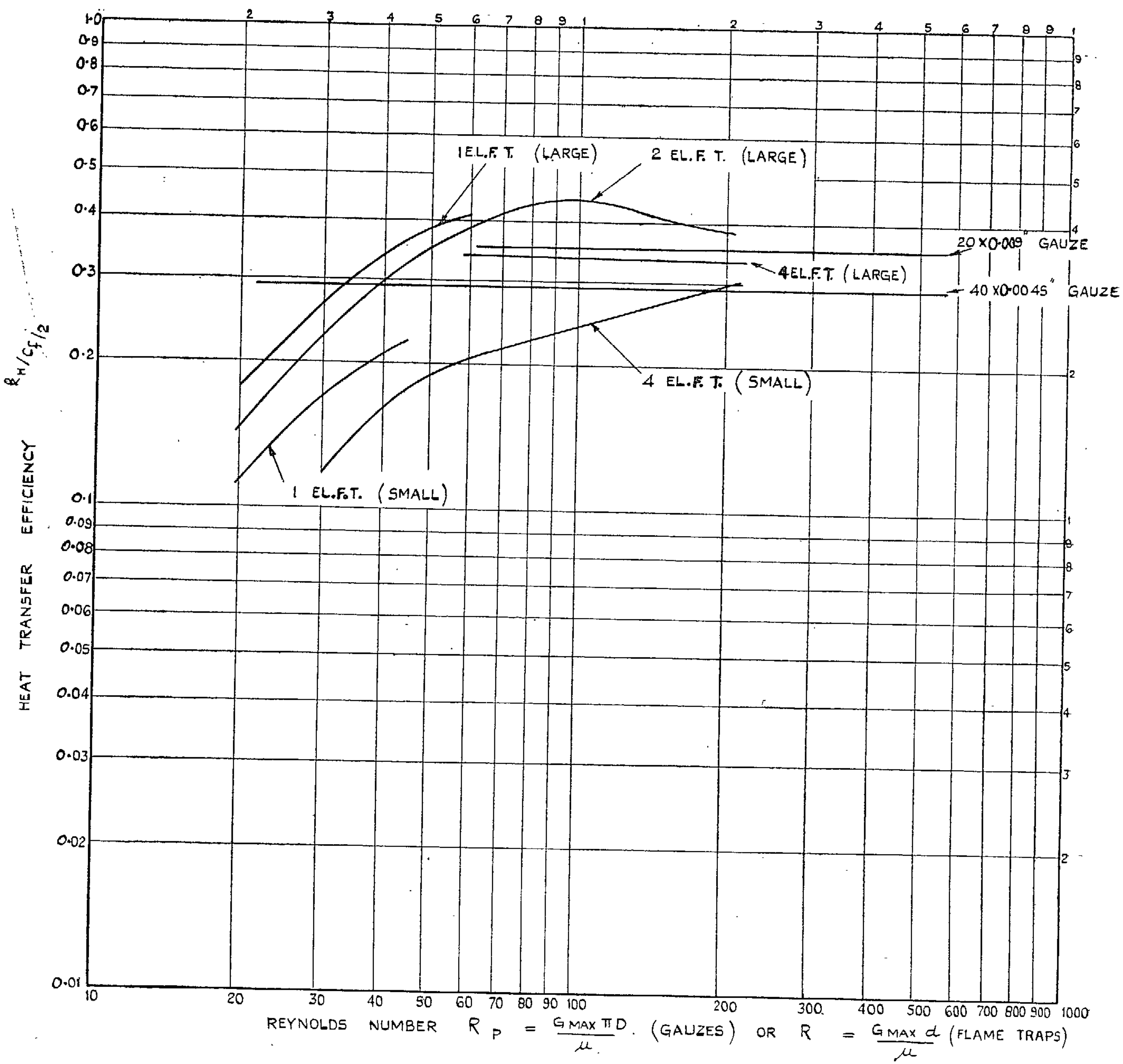

FIG. 32. Experimental results. Heat transfer efficiency.

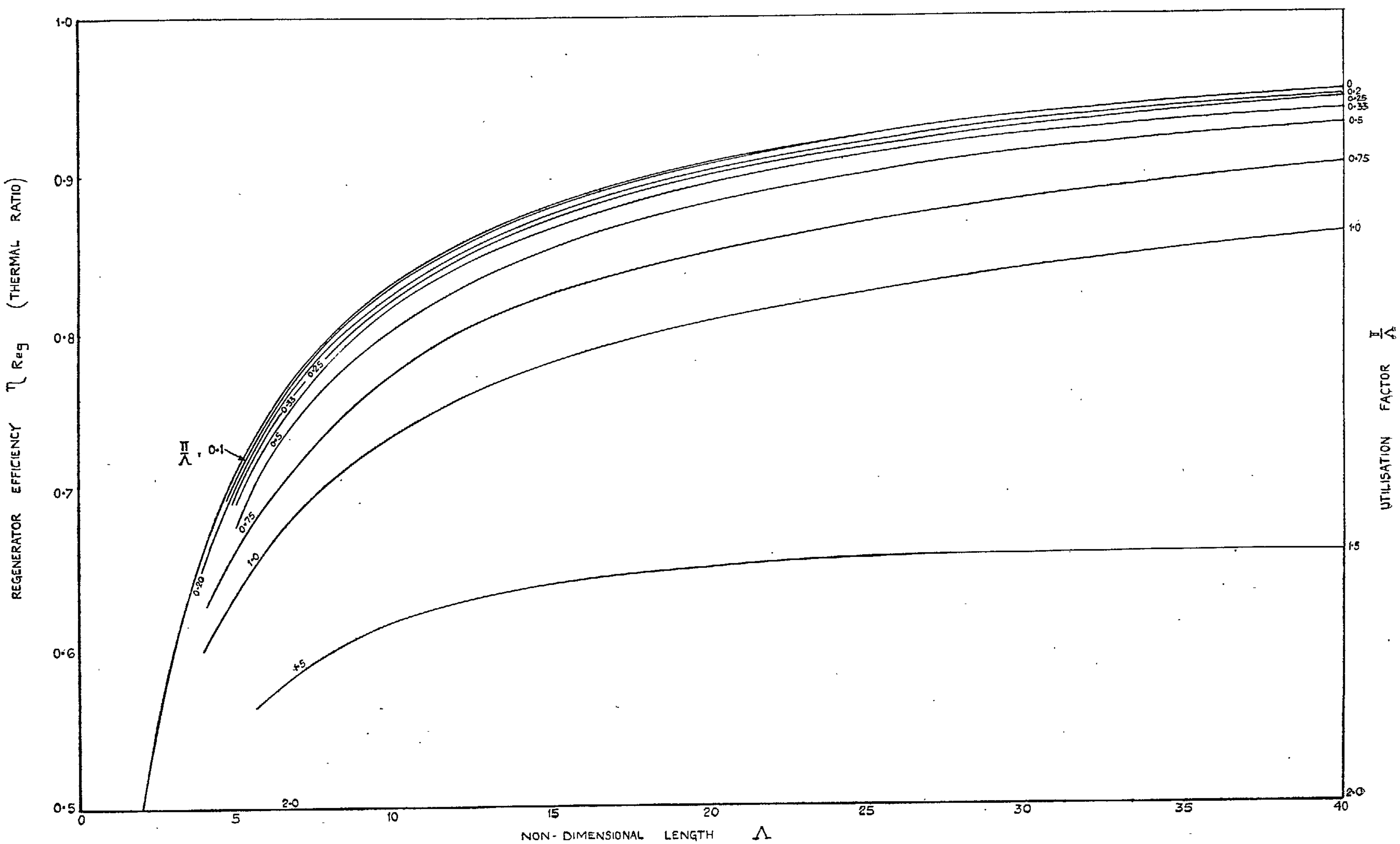

FIG. 33. Effect of length and utilisation factor on efficiency of a balanced regenerator.

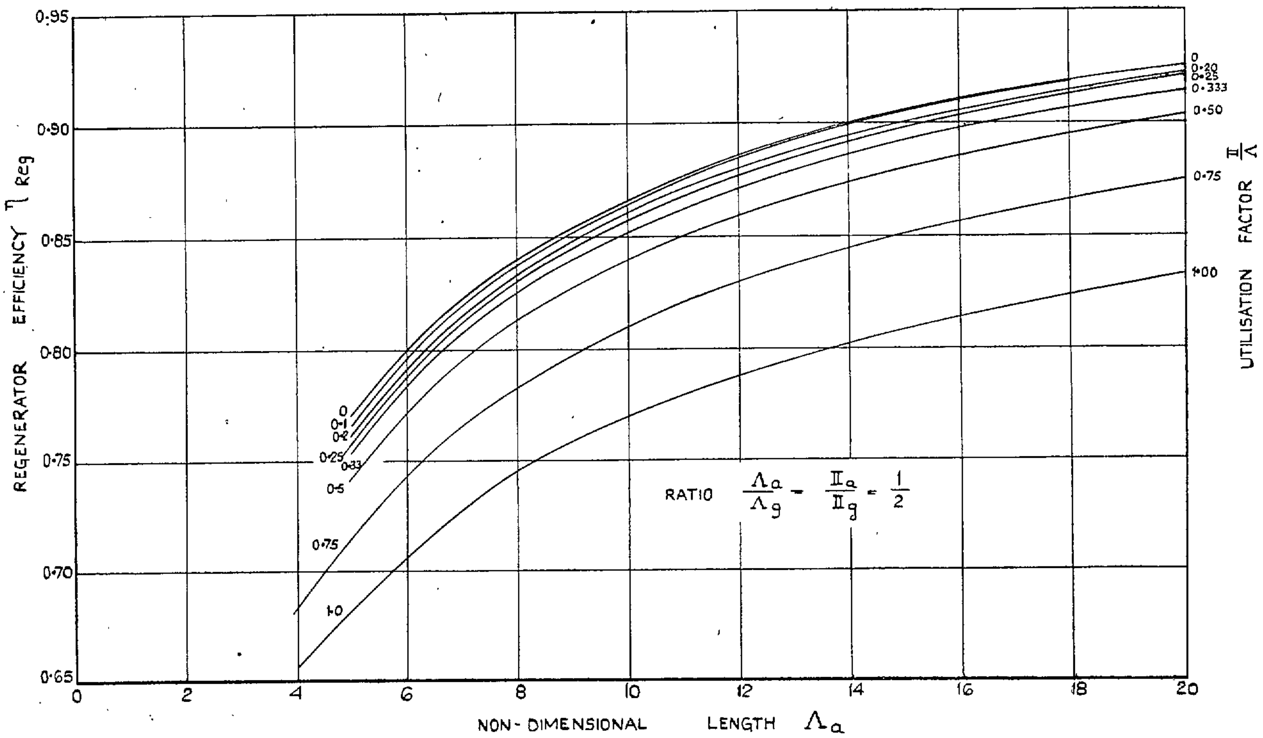

Fig. 34. Effect of length and utilisation factor on efficiency of an unbalanced regenerator. Ratio 1/2.

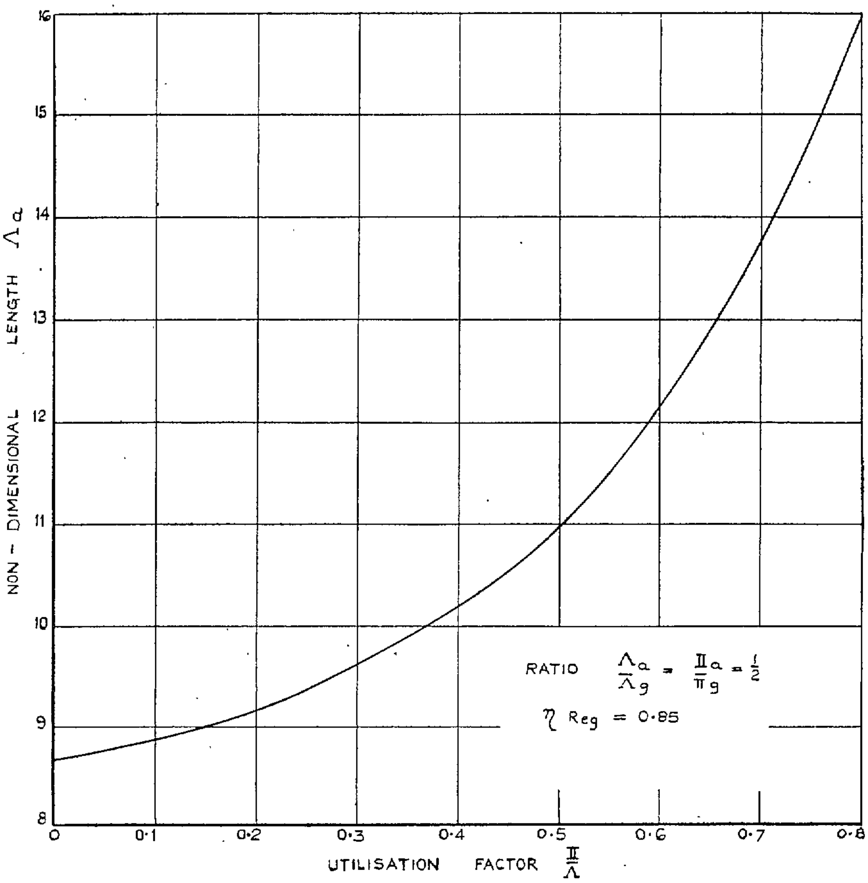

Fig. 35. Length and utilisation factor for an unbalanced regenerator. Ratio 1/2. Efficiency 0·85.

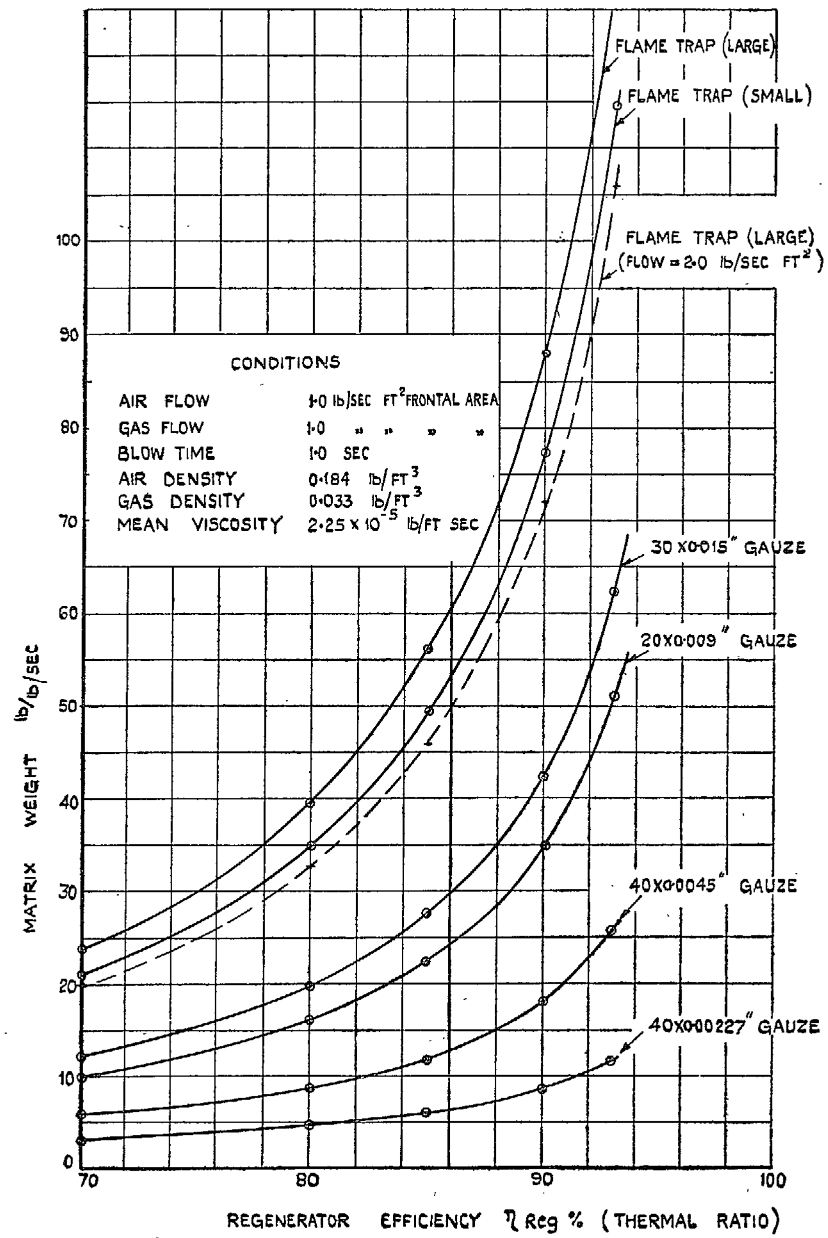

FIG. 36. Weight of gauze and flame trap matrices for a balanced regenerator.

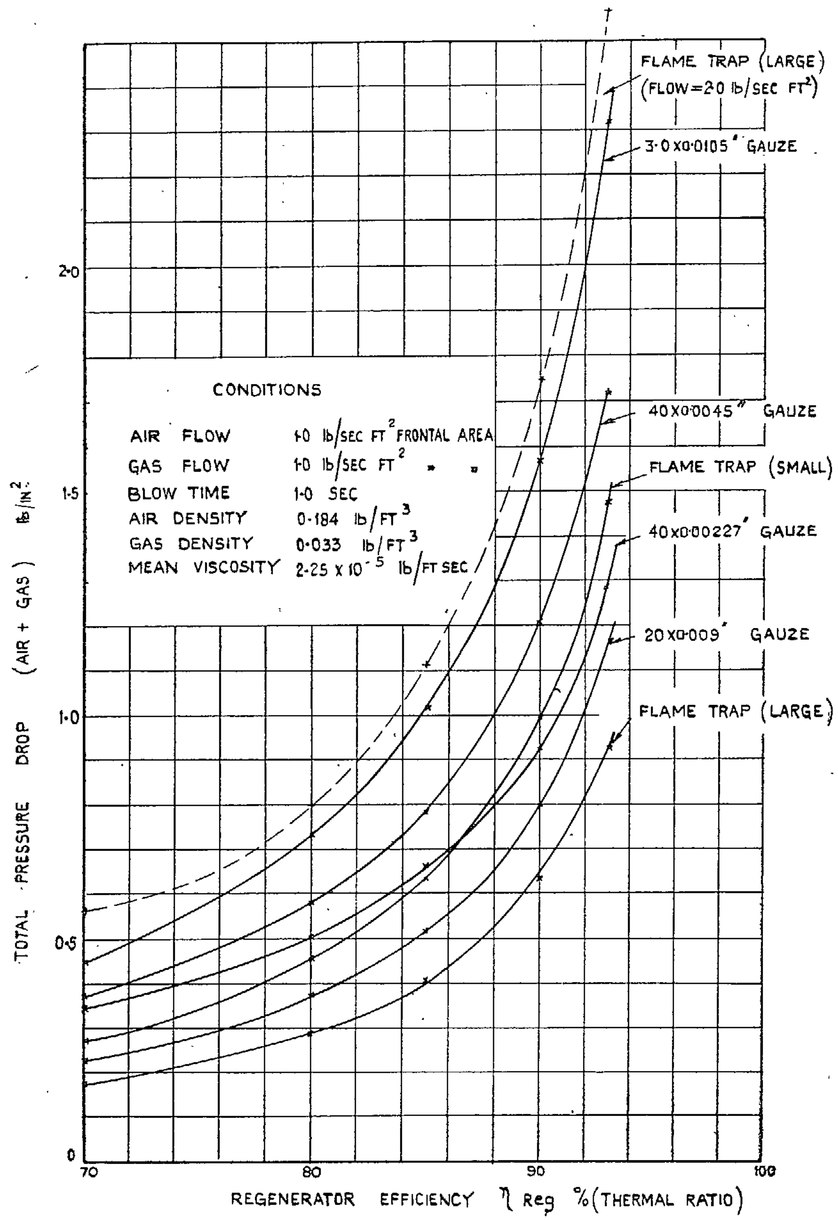

FIG. 37. Pressure drop of gauze and flame trap matrices for a balanced regenerator.

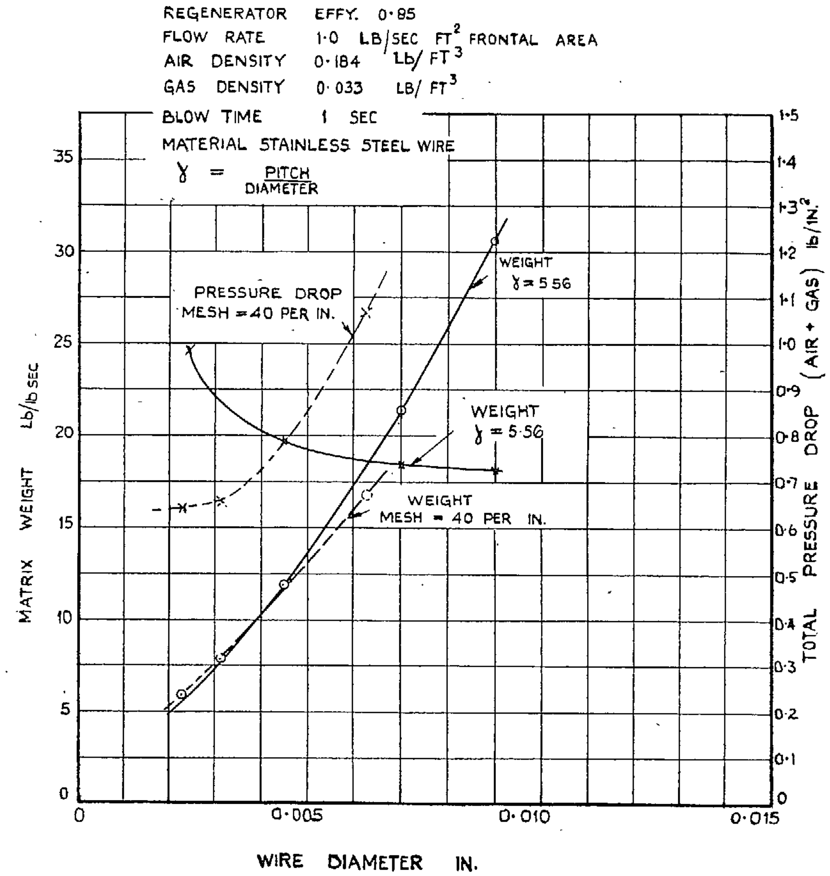

FIG. 38. Effect of wire diameter on weight and pressure drop of a gauze matrix for a balanced regenerator.

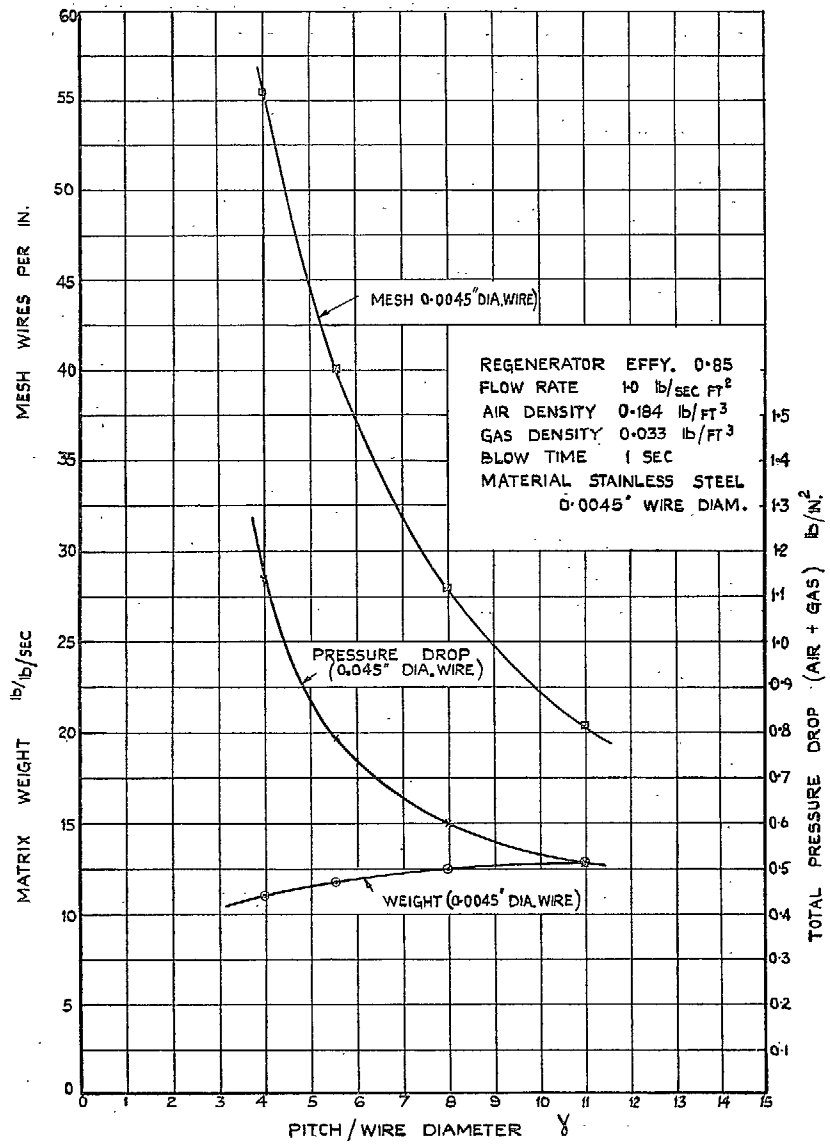

FIG. 39. Effect of wire pitch on weight and pressure drop of a gauze matrix for a balanced regenerator.

J4273 Wt.13/806 K.9 1/52 D&Co. 34-263

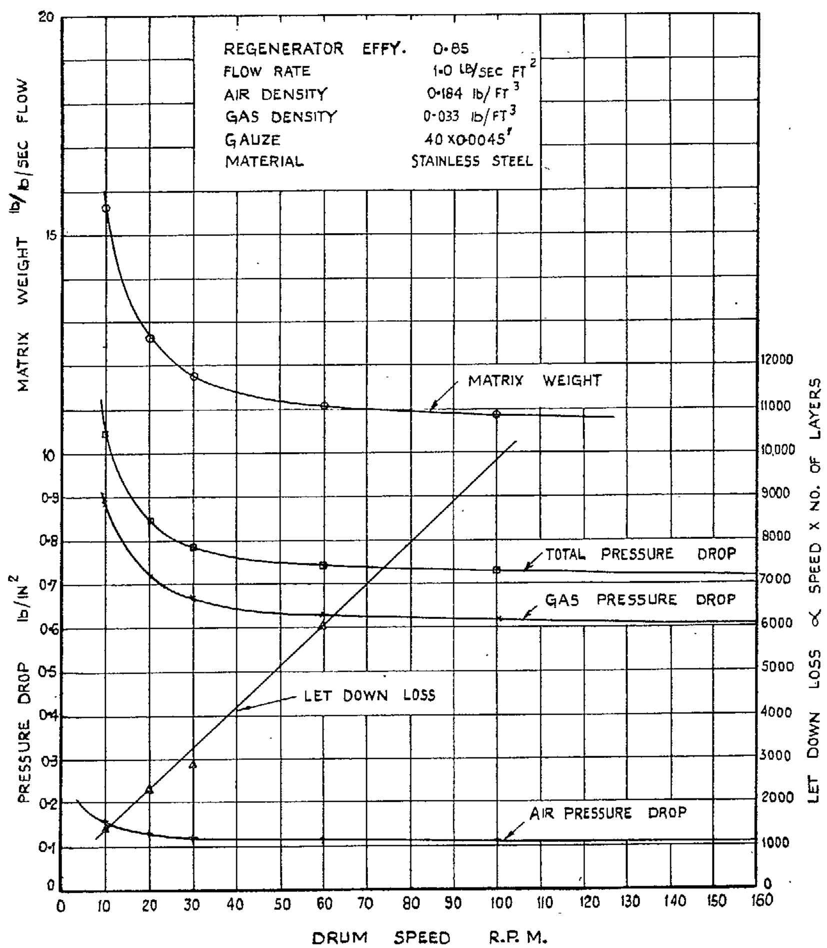

FIG. 40. Effect of drum speed on weight, pressure drop and let-down loss of a balanced regenerator.

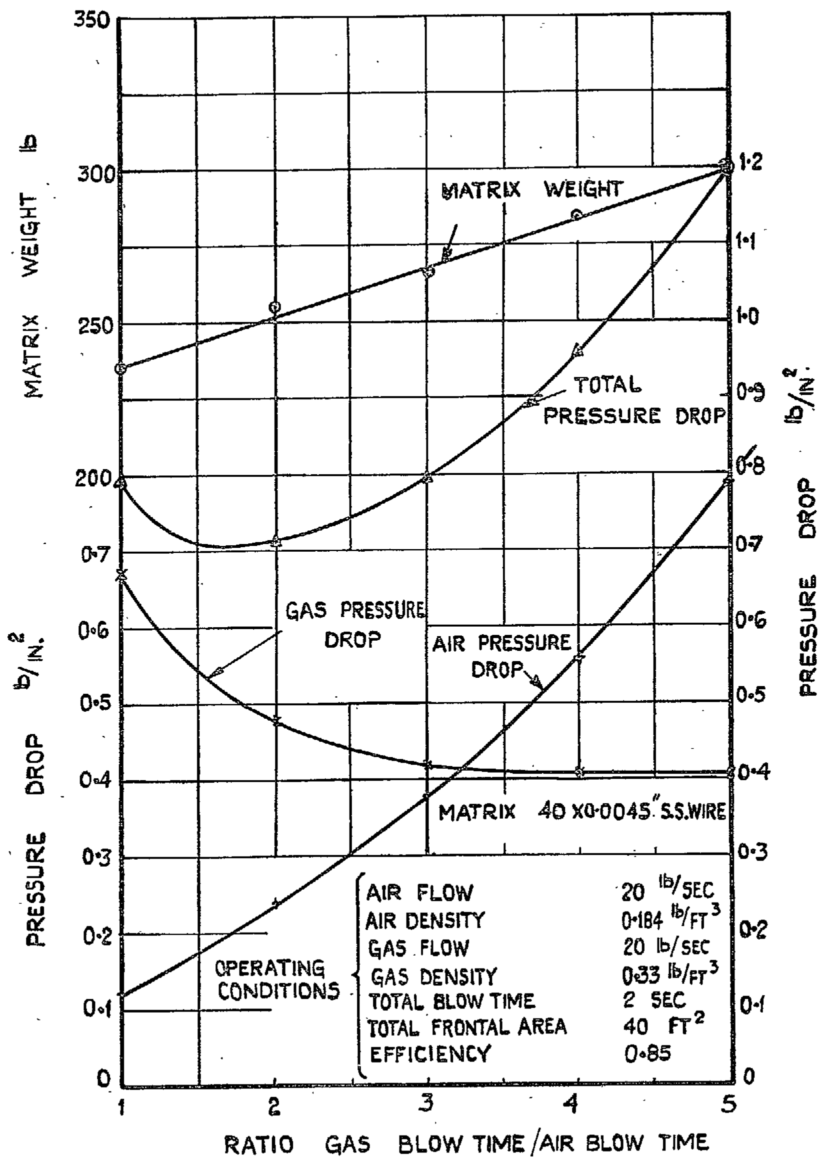

FIG. 41. Effect of ratio of gas blow time to air blow time on the weight and pressure drop of a particular regenerator.

PRINTED IN GREAT BRITAIN

R. & M. No. 2630
(11,770)
A.R.C. Technical Report

Publications of the Aeronautical Research Council

S.O. Code No. 23-2630